

NORTHWESTERN UNIVERSITY

Epstein-Barr Virus Glycoprotein 42: the Dynamic Trigger of B-cell Membrane Fusion

A DISSERTATION

SUBMITTED TO THE GRADUATE SCHOOL
IN PARTIAL FULFILLMENT OF THE REQUIREMENTS

for the degree

DOCTOR OF PHILOSOPHY

Integrated Graduate Program in the Life Sciences

by

Amanda Renée Kim Eun-Ja Silva Lowrey

Evanston, Illinois

December 2008

© Copyright by Amanda R. Lowrey 2008
All Rights Reserved

ABSTRACT**Epstein-Barr Virus Glycoprotein 42: the Dynamic Trigger of B-Cell Membrane Fusion****Amanda R. Lowrey**

Epstein-Barr virus (EBV) is a human herpesvirus that is able to infect both epithelial cells as well as B lymphocytes, where the virus establishes life-long latency in the host. Five glycoproteins are involved in infection of B cells: gp350/220 for initial tethering of the virus to the cell via CD21, followed by gB, gH/gL, and gp42 for membrane fusion. Epithelial cell fusion and infection is inhibited by gp42, thus virion surface expression levels of the protein determine which cell type the virus will infect most efficiently i.e., high gp42 levels facilitate B-cell infection and low gp42 levels facilitate epithelial cell infection. The class II human leukocyte antigen (HLA class II) is a co-receptor for the virus on B cells, binding gp42 to trigger membrane fusion. Although the role of gp42 in fusion and infection of both cell types had been established, functional domains remained relatively uncharacterized. Based on the crystal structure of soluble gp42 bound to the HLA-DR1 allele, gp42 mutants were created and assayed for their ability to bind receptor, other glycoproteins, and mediate membrane fusion. Our data determined the three critical interactions required for receptor binding, leading to the discovery that a hydrophobic pocket on the surface of the protein is not involved in HLA class II engagement, but is required for fusion. Our mutants also revealed that two separate regions of the gp42 amino-terminal ectodomain are required for binding of gH/gL and to mediate membrane fusion. This led to the identification of a gp42 peptide that competitively bound gH/gL and potently inhibited B-cell membrane fusion, as well as epithelial cell fusion and infection. Our results have more clearly defined three separate domains of gp42 that are required

for membrane fusion, providing a model for the mechanisms by which gp42 is able to trigger fusion with B cells, in addition to targets for development of anti-viral therapeutics.

ACKNOWLEDGEMENTS

It is here that I wish to acknowledge all the important people who have helped me to attain this goal. I am most grateful to Dr. Richard Longnecker, who believed in me and supported me unwaveringly, even when he had every reason not to. I never would have finished if you hadn't kept the faith. Many thanks also to my wonderful committee members, Dr. Ted Jardetzky, Dr. Kathy Rundell, Dr. Hank Seifert, and Dr. Pat Spear. You all challenged me and supported me to become a better scientist and a better person. I also am grateful for my previous mentors, Dr. Sui Huang, Dr. Warren Tourtellotte, Dr. Mike Mlynarek, Dr. Anne Luebke, and especially Dr. Stan Lipkowitz, my very first mentor. Thank you all for the excellent advice and guidance in the early parts of my career. Your love for science and research was truly inspiring.

I am also extremely grateful for the many members of the Longnecker lab who helped me along from the beginning to the very end, with words of encouragement, reagents, protocols, advice, coffee and humor. I was there for so long that there are many, many people, but in particular I am especially grateful to Dr. Keith Haan, Dr. Marisa McShane, and Dr. Jasmina Omerovic. I received help with creating my mutants from Dr. Gant Luxton, George Stanton, and Asheera Alvarez. Other members of the lab who cheered me on along the way include: Dr. Rachel Swart, Dr. Mark Merchant, Dr. Rebecca Katzman, Dr. Neeta Shanoy, Dr. Makoto Fukuda, Akiko Ikeda, Lori Lev, Dr. Ana Chee, Dr. Caroline Jackson, Patrick Dennis, Dr. Charu Deshpande, Dr. Toni Portis, Nick Ghosh Roy, Dr. Brett Brinker and Semira Yaseen. I am especially grateful for the labbies who bid me farewell and cheered me on from afar to help me finish: Rebecca Bultema, Dr. Michelle Swanson-Mungerson, Dr. Leah Anderson, Jessica Reimer, Dr. Mark Rovedo, Dr. Masato Ikeda, Kathryn Bieging, Jessica Sorem, Aileen Baldwin,

Rhoda Chang, Alexandra Amick, Dr. Osman Cen, Nicholas Garcia, Dr. Heather Hensler, Dr. Julia Jackson MacKenzie, and Omar Perez.

All great work is a team effort, and I am extremely grateful to the Jardetzky lab for our collaborations, especially Dr. Austin Kirschner, who was and shall always remain a good friend and true inspiration for me, and also Dr. Maureen Mullen and Dr. Marija Backovic. I am also indebted to the Spear lab, especially Nanette Susmarski, who gave me the best cells and technical advice ever. Thanks also to Dr. Cheryl Jogger, Dr. Anna Zago, Dr. Nancy Ruel, Craig Steffel, Dr. Erick Lin, the Lovely Jamaican Vonia Thompson, Dr. Sharmilla Manoj, Dr. Frank Struyf and Melissa McNealy.

I also want to thank Dr. Steve Anderson, whose gentle patience and kind words were a reassuring and delightful presence from even before the first interview weekend all the way to the very end. Many thanks also to Judy Brown, Cynthia Naugles, Dr. Roberta Baer, and Marva Golden, who all made sure that I was able to finish.

Last but not least, I want to thank the many people away from school who helped me along the way. There was a definite overlap, and there are so many I cannot possibly name you all, but you know who you are! Thanks to my family & friends, my fellow classmates, KADS and TRADS, KRCC, I2I, Hawaii Peeps, KAHI, Dr. Strange, and the Hawaii Department of Agriculture-Aquaculture Development Program, especially Dr. Leonard Young & Dr. Allen Riggs who took a chance on hiring and supporting me to make sure that I finished. You all are very special to me and I am grateful to have you in my life to help me get through this.

Herzlichen Dank, Khop chai lai lai, 감사합니다

Mahalo nui loa and THANK YOU!!

DEDICATION

I dedicate this thesis to my parents Dr. Austin Lowrey III and Elizabeth Barr Brown Lowrey. There was never a doubt who my “real” parents were. I never would have been able to complete this without all your love and support. My father the nuclear physicist was a particular inspiration all these years for me to obtain my doctorate.

I also dedicate this to the first person in my life, Omma. Although I don’t know your name, I do remember you. The difficult decisions you made forever altered my life course and set me down the path I now tread. Although we may never see each other again in this lifetime, I will never forget you. Thank you for giving me life and for giving me a new life by erasing my past. Though you were not physically by my side, you taught me so much about life and about myself, particularly my strength. I have carried you in my heart all these years, and now I can see your eyes looking back at me in the mirror. I miss you and think of you often. I hope some day you are able to find peace in your heart and know that I have done well.

TABLE OF CONTENTS

	<i>Page</i>
ABSTRACT	3
ACKNOWLEDGEMENTS	5
DEDICATION.....	7
LIST OF FIGURES	9
LIST OF TABLES.....	11
CHAPTER ONE—INTRODUCTION.....	12
CHAPTER TWO—MUTATIONAL ANALYSES OF EPSTEIN-BARR VIRUS GLYCOPROTEIN 42 REVEAL FUNCTIONAL DOMAINS NOT INVOLVED IN RECEPTOR BINDING BUT REQUIRED FOR MEMBRANE FUSION.....	32
CHAPTER THREE—BINDING-SITE INTERACTIONS BETWEEN EPSTEIN-BARR VIRUS FUSION PROTEINS GP42 AND GH/GL REVEAL A PEPTIDE THAT INHIBITS BOTH EPITHELIAL AND B-CELL MEMBRANE FUSION	66
CHAPTER FOUR—CONCLUSIONS AND FUTURE DIRECTIONS.....	110
REFERENCES	121

LIST OF FIGURES

<i>Number</i>	<i>Page</i>
Figure 1.1. Epstein-Barr virus life cycle.....	21
Figure 1.2. Model of EBV infection of B cells.	25
Figure 2.1. Important Structural Features of EBV gp42 and Residue Sequence Mapping Location of Mutations.....	44
Figure 2.2. Verification of mutant gp42 surface expression by CELISA and whole-cell expression by Western blotting.....	47
Figure 2.3. Mutant gp42s Vary in Ability to Mediate Cell-Cell Fusion.....	49
Figure 2.4. FACS analysis reveals differences among mutants in binding to HLA class II and mediating fusion.....	54
Figure 2.5. Ribbon models identifying locations of all gp42 mutants based on classes identified from Table 2.2.....	58
Figure 3.1. Schematic of gp42 mutants, fusion assay, and CELISA data	80
Figure 3.2. Binding of gp42 mutants with transfected gH/gL in coimmunoprecipitations and soluble gH/gL in CELISA	83
Figure 3.3. Equilibrium binding of gp42 peptides to soluble gH/gL measured by fluorescence polarization	87
Figure 3.4. Kinetics of FITC-labeled gp42 peptide 36-81 binding soluble gH/gL as determined by fluorescence polarization.....	91
Figure 3.5. Peptide from gp42 residues 36 to 81 inhibits epithelial and B-cell membrane fusion.	94
Figure 3.6. Shorter gp42-derived peptides tested in epithelial and B-cell fusion assays.....	97

	10
Figure 3.7. Peptide 36-81 inhibits EBV entry into epithelial cells.....	99
Figure 3.8. Model of peptide inhibition of EBV membrane fusion apparatus.....	108
Figure 4.1. Proposed model of Epstein-Barr virus glycoprotein 42-induced B-cell membrane fusion.....	118

LIST OF TABLES

<i>Number</i>	<i>Page</i>
Table 1.1. Epstein-Barr Virus Glycoproteins.....	24
Table 2.1. Plasmids utilized for present studies.	40
Table 2.2. Summary of assays reveals four classes of gp42 mutations.....	51
Table 3.1. Activity summary of gp42 deletion mutants.....	77
Table 3.2. Activity summary of gp42-derived peptides.....	89

CHAPTER ONE—INTRODUCTION

Membrane Fusion: A Common Biological Process

Membrane fusion is an essential biological process between cells in yeast mating, *C. elegans* epidermal cell fusion, myoblast fusion, mammalian fertilization, placenta trophoblast fusion, stem cell fusion, macrophage fusion, and muscle cell syncytia, as well as for intracellular vesicle transport and infection by enveloped viruses [For review see (21)]. X-ray diffraction patterns at various humidity levels demonstrated that when the two membranes fuse, they form an hourglass-shaped intermediate structure called a stalk, which confirmed basic theoretical predictions that had never been previously observed (148). When the stalk stretches further, it creates a connecting bridge between the membranes. This connection then enlarges, and the two membranes ultimately become one single membrane. It is not unreasonable to assume that the widely different processes mentioned have evolved to follow the same mechanistic steps. In the case of vesicle transport, the Soluble N-Ethylmaleimide-sensitive (NSF) Attachment protein REceptor (SNARE) family of proteins has been conserved through evolution, performing similar functions even in primitive organisms such as yeast and fruit flies. Some of the fusion proteins are embedded in the vesicle and the cell wall membranes, while others float freely (12). Enveloped viruses have lipid bilayers, which fuse with host-cell membranes as an integral event of infection, where strict spatial and temporal protein-protein requirements maintain a tight control for maximal efficiency. Accumulated evidence suggests that viral fusion proteins lower the various kinetic barriers and therefore catalyze the membrane fusion process [For review see (50)]. Many viral fusion proteins, including those of influenza and the human immunodeficiency virus (HIV), form hairpin-like structures similar to the SNAREs during fusion of viral and cellular membranes. A family of bacterial membrane proteins that mediate cell-adherence and entry resembles the structural architecture of both viral fusion proteins and eukaryotic SNAREs,

and it has been proposed that they share similar, but distinct, mechanisms of cell membrane translocation [For review see (9)]. SNARE mediates fusion involving cytoplasmic faces of membrane fusion, whereas cell fusion and viral entry involve external faces. The two types of fusion could be fundamentally different, or possibly evolution has resulted in many viruses and bacteria sharing a common mechanistic principle with SNAREs in how they fuse membranes.

Viral Fusion Proteins and Antiviral Therapeutics

Enveloped viruses are able to enter cells either by fusing their lipid membranes at the plasma surface or by endocytosis in a low pH environment (50). Most viruses utilize one surface protein, which undergoes a pH-induced conformational change in the endocytic vesicle or binds the cellular receptor to mediate membrane fusion at the surface, although herpesviruses use multiple glycoproteins for infection [For review see (52, 107)]. The proteins that mediate membrane fusion for enveloped virus infection have been categorized as Class I or Class II based on their characteristics [For review see (25, 63)]. Of the two classes of fusion proteins that have been identified, Class I includes influenza virus hemagglutinin and paramyxovirus F protein, which undergo proteolytic cleavage and form trimers both before and after fusion; and Class II includes flavivirus E and alphavirus E1 proteins, which form pre-fusion dimers and post-fusion trimers [For review see (65)].

Class I fusion proteins are usually synthesized as single-chain polypeptide precursors cleaved by host proteases, which then assemble into metastable trimers, usually coiled-coil bundles of α -helices. This is exemplified by hemagglutinin (HA) of the influenza virus and HIV glycoprotein 120/glycoprotein 41 (gp120/gp41) [For review see (35)]. These proteins contain a “fusion peptide”, the part of the protein that becomes associated with the target membrane by

penetrating the interior of the target bilipid membrane. Typically the peptide is found at or near the amino-terminus of an internal cleavage point. This hydrophobic and glycine-rich segment is initially buried in the cleaved and primed trimer, but emerges after a large-scale conformational rearrangement that is triggered by events such as low endosomal pH for HA, receptor binding for gp120/41, or other cell-entry related signal. Such changes allow the fusion peptide to be presented at the tips of the coiled-coil bundles. The fusion peptide is inserted into the target membrane, creating a structure known as the pre-hairpin extended intermediate due to its elongated shape. This is followed by collapse of the pre-hairpin intermediate when the protein folds back at the base of the helix-bundle, usually forming additional α -helices that can eventually bind to the outside grooves of the trimer as the membrane stalk is formed. When collapse of the intermediate has proceeded far enough to bring the two bilayers into contact, the apposed, proximal leaflets merge into the hemifusion stalk. This creates an inversely bent structure in the fusion proteins, where the transmembrane domains are at the same end as the fusion peptides, followed by elongation of the stalk. Fusion is completed by the formation of the fusion proteins into symmetric trimer hairpins, which open the fusion pore irreversibly. The structures of the pre- and post-fusion conformations, as well as the uncleaved precursor of HA have all been demonstrated, leading the way in our understanding of Class I fusion proteins (16, 22, 144, 145).

The Class II fusion proteins, which have not been studied as extensively as the Class I proteins, are exemplified by flaviviruses (M) and alphaviruses (E2) and have evolved a structurally different, but mechanistically related fusion architecture. There is proteolytic cleavage as in Class I proteins, but cleavage yields mature virions with the fusion protein in an already metastable conformation, primed for fusion. Thus, the fusion proteins are not themselves

proteolytically activated. Also different from Class I proteins, the fusion peptide is internal, generally a loop at the tip of an elongated subdomain of the protein, which is buried at a protein interface and becomes exposed upon conformational change initiated by exposure to low pH (2, 15, 54, 141). Unlike Class I proteins, the E-glycoproteins are composed of β -strands that hold the fusion peptide in place and coiled-coils apparently do not play a role in the conformational changes upon activation. Instead, it appears that the glycoproteins form icosahedral scaffolds on the virus surface and most likely interact in a concerted fashion during activation (45, 93, 111). The conformational change causes the fusion peptides to become exposed and then reoriented toward the viral membrane. Insertion into target membranes may be mediated by β -barrels, rather than the amphiphilic α -helices seen with Class I proteins. Most impressive, studies indicate that the different classes of viral fusion proteins have no common ancestor and have evolved independently.

Recently a third class of fusion proteins has been proposed based on structural homology that includes vesicular stomatitis virus (VSV) G, herpes simplex type 1 glycoprotein B (HSV-1 gB), and baculovirus gp64 (67). These proteins are particularly interesting because they are all able to mediate fusion in cells of various species (73, 151). The VSV-G protein forms a trimeric complex and binds to its cellular receptor. Fusion typically occurs in an endocytic vesicle following a drop in pH (113, 114). HSV-1 gB, which can mediate fusion at the plasma membrane after initial tethering of the virus to the cell, has domains similar to VSV-G, but in a more stretched out structure (53). It is interesting to surmise whether the startling similarities between a DNA virus and a negative strand RNA virus evolved divergently or convergently. It has been postulated that because all three classes of fusion proteins are actually more related structurally than had been previously suggested, Class III might not be another independent

class, but rather a link between Class I and Class II (67). Herpesviruses are still distinct from other members of the proposed class because of the requirement for multiple glycoproteins for complete membrane fusion (110).

Membrane fusion is a critical step of both viral infection and egress, and provides a prime target for therapeutic strategies. Monoclonal antibodies (mAb) have been successfully used as chemotherapeutic agents against various cancers. They are excellent tools of modern science because they are easy to produce in both great quantity and variety, which can then be carefully screened for high specificity and affinity. Chimeric drugs can be created by fusing a toxin to a mAb that binds a specific protein, allowing for targeted destruction of cancerous growths. The humanized monoclonal antibody palivizumab (Synagis) was the first monoclonal antibody approved by the FDA to provide passive immunity for an infectious disease by binding to the fusion glycoprotein of human respiratory syncytial virus (RSV) (1). The HIV envelope (ENV) protein gp41/gp120 complex that binds CD4 and a co-receptor was the target of the antiviral T-20 also known as Fuzeon (Roche & Trimeris) and Enfuvirtide (ENF), the first anti-viral compound developed that targeted membrane fusion, which is the initial step of viral infection (77). ENF is a 36 amino acid peptide (T-20 C-peptide) derived from the HR2 coiled-coil domain of the C-terminus to competitively bind the HR1 coiled-coil N-terminal domain of gp41 after ENV has bound CD4, preventing necessary conformational changes required for membrane fusion to proceed (142, 143). Typically HIV in patients would rapidly mutate to become resistant to drugs, necessitating careful combinations of anti-viral therapies (84). ENF was given in combination with other anti-viral drugs that targeted later steps of the viral cycle, but only after other protocols had failed to help the patient. Analysis of strains isolated from patients receiving ENF revealed various mutations, some more common than others. Two single amino

acid changes, GIV to GIA in the HR1 domain, which led to a 45-fold increased T20 resistance, and SNY to SKY in the HR2 domain, leading to loss of a glycosylation site, created a strain that dominated the viral population after 32 weeks and was both resistant to and dependent on the drug for replication. The double mutation would cause a premature switch of the hairpin leading to spontaneous shedding of gp120 and a dead virus, but the presence of a high concentration of ENF would reverse this phenotype, allowing ENF to transiently bind and act as a safety pin to prevent premature switching, but also easily fall off the complex, allowing the correct hairpin conformational change to occur and membrane fusion to proceed (8, 106). Although DNA viruses do not mutate at anywhere near the rate of HIV, such unexpected side effects must be taken into consideration when strategically designing effective drugs.

Herpesviruses: All in the Family

Due to the requirement of multiple surface proteins for membrane fusion and the infection of host cells, the herpesviruses are the most unique among the enveloped viruses. Herpesviruses constitute a large family (*Herpesviridae*) of over 200 identified viruses, which can infect a variety of vertebrate species (115). The viruses have glycoprotein-studded membranous envelopes surrounding an icosahedral capsid, which contains a large, linear double-stranded DNA genome, usually between 150 and 200 kb. A hallmark characteristic of herpesviruses is the ability to establish a lifelong latent infection in the host. The cycle of latent and lytic infections in the host ensures sporadic shedding of the virus, which can spread to new hosts. Thus far eight human herpesviruses have been discovered, which are classified into three subfamilies based on the cell type in which they establish latency. The alpha-herpesviruses latently infect neurons and include Herpes Simplex Virus type 1 and 2 (HSV-1 and HSV-2), and varicella zoster virus

(VZV). The beta-herpesviruses include human cytomegalovirus (HCMV), and human herpes virus type 6 and 7 (HHV-6 and HHV-7). The latency host of HCMV is likely macrophages, while for HHV-6 and HHV-7 it is T cells. The gamma-herpesviruses Epstein-Barr virus (EBV) and Kaposi's sarcoma herpesvirus (KSHV) are able to latently infect B cells and are considered oncogenic viruses because of their strong association with various cancers.

Much work on HSV-1 has helped to provide a detailed model of herpesvirus membrane fusion and has revealed differences in entry compared to egress, which involves envelopment, de-envelopment and re-envelopment of the maturing virus as it exits the nucleus and passes through Golgi-derived vesicles on its way through the cytoplasm to the plasma membrane for release (38, 90, 107). There is a clear sequential involvement of HSV-1 gD for attachment, followed by gH/gL for hemifusion and gB to complete fusion at the plasma membrane for infection (3, 87, 124, 129). Studies of gB have helped reveal important structural determinants for fusion, as well as identifying the paired immunoglobulin-like type 2 receptor (PILR) α that associates with gB and acts as a co-receptor for infection (11, 53, 83, 119). The HSV-1 gB crystal structure revealed characteristics resembling both Class I and Class II viral fusion proteins, such as residues positioned as possible fusion loops and coiled-coil helices in a trimeric form, which unfolds like an umbrella (53, 110). It has also been determined that gB is important for both entry and egress of the virus, and some regions of gB have roles in both (10, 116).

There is mounting evidence for a role of gH/gL in both binding and as a fusogen as well. Receptors for HSV-1, HCMV, and HHV-6 have been identified (68, 102, 117, 118, 136). Three lines of evidence suggest that EBV infection of epithelial cells requires the interaction of gH/gL with a specific receptor. First, EBV virions lacking gH are unable to attach to epithelial cells (98). Second, gH/gL has been shown to bind to epithelial cells permissive in membrane fusion

and infection (94, 138). Third, viruses using gH/gL for both adhesion and fusion are compromised in infection (14). Despite all the data, this putative epithelial cell receptor remains elusive, although preliminary evidence from Dr. Hutt-Fletcher's lab indicates it may be an integrin. The fact that HSV-1 and HCMV gH binds $\alpha V\beta 3$ integrin adds weight to the possibility of EBV gH/gL binding an integrin receptor on non-CD21-expressing epithelial cells [(134); Chesnokova and Hutt-Fletcher, IHW 2007]. Although early studies of HSV-1 heptad repeats (HR) that formed coiled coils and their role in fusion and infection were questioned, a later study by Galdiero *et al.* demonstrated that gH HR1 and HR2 interact with each other and were important for fusion and infection (41-44). VZV, HCMV and KSHV gH/gL are all able to mediate some levels of fusion alone (24, 69, 104). It is clear that the requirement of gD, gH/gL and gB for membrane fusion indicates that the herpesvirus membrane fusion mechanism is different from the known single-component systems in which trimeric fusion proteins assemble into hairpin-like conformations that bring the viral and cellular membranes together (110, 127).

Epstein-Barr Virus Life Cycle and Disease

Epstein-Barr virus (EBV) is a ubiquitous member of the human γ -herpes subfamily, which establishes life-long latency in B cells [(37); for review see (85, 123)]. EBV was identified by electron micrograph as the fourth human herpes virus by the presence of surface glycoproteins and its ability to establish latency, but in a new cell class: lymphoid (37). Virus in saliva of infected hosts is passed to naïve individuals, where it can infect epithelial cells of the oropharynx or circulating B cells (Figure 1.1). Infection of B cells leads to massive proliferation, which is controlled by a strong cytotoxic T lymphocyte (CTL) response. Approximately one in one million mature memory B cells that evades immune detection has an established latent

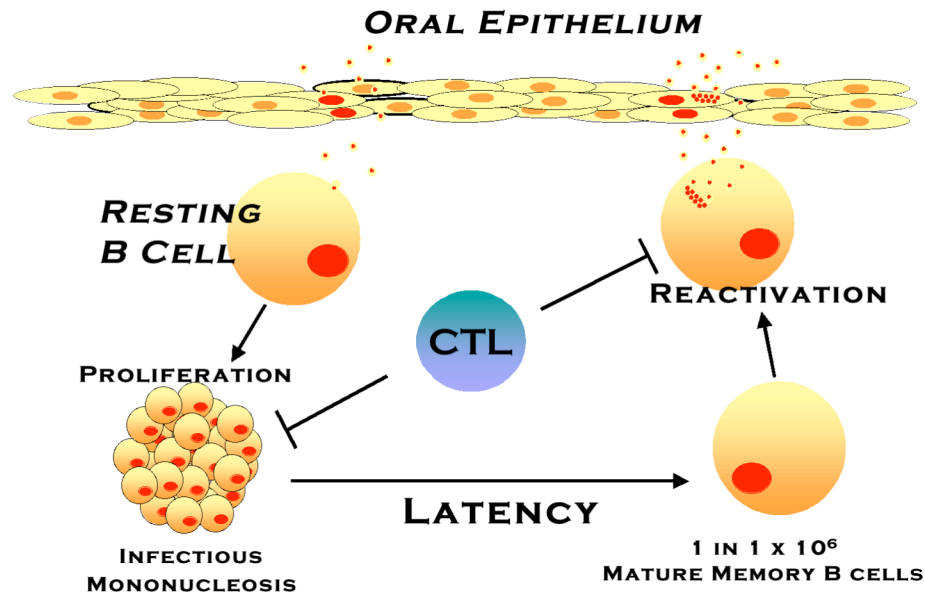


Figure 1.1. Epstein-Barr virus life cycle.

The virus primarily infects epithelial and B cells, and is passed through saliva to naïve individuals, where it can infect the oral epithelium. After replication, virus is released from the basolateral side, where it can infect trafficking, resting B cells. Alternately it can reach the B cell compartment if there are any wounds or cuts in the oropharynx, resulting in proliferation, which is controlled mainly by the host cytotoxic T cell response (CTL). Such infection in adolescence or adulthood can manifest as infectious mononucleosis. Some B cells are able to escape immune detection and a latent infection is established in approximately 1 in 1 X 10⁶ mature memory B cells, whereby the viral genome is maintained in circular episomes attached to the host DNA. Periodic reactivation leads to shedding of the virus, which can then infect epithelial cells and pass on through saliva to new hosts. Lytic infection is also controlled by the CTL response.

infection, which uses the host cell machinery to replicate the viral genome. There are three types of latent infection based on which viral proteins are expressed. Periodic reactivation of lytic infection occurs, which leads to viral shedding and the opportunity for infection of new individuals.

More than 90% of the adult population is seropositive for EBV, which efficiently infects both epithelial and B cells [For review see (112); (13)]. It is therefore no surprise that the virus has been associated with diseases of both lymphoid and epithelial origin, including its initial discovery to be the causative agent of a lymphoma endemic to central and western Africa where malaria was prevalent (17, 18). This was the first time a virus was directly implicated in a cancerous growth. Although infection in infancy is generally asymptomatic, acute EBV infection acquired in adolescence or adulthood can cause infectious mononucleosis (IM), accompanied by a proliferation of B cells (55). It was serendipitously discovered to be the causative agent of IM by the technician who had been using her blood as a negative control while characterizing the virus. Because they are both susceptible to EBV infection, epithelial and B cells can develop tumors that are directly linked to EBV, such as gastric carcinoma, nasopharyngeal carcinoma and Hodgkin's disease (57, 58, 130, 139). Other disorders also connected to EBV include post-transplant lymphoproliferative disorder as well as oral hairy leukoplakia and B cell lymphomas of the central nervous system prevalent in AIDS and immunosuppressed individuals (56, 135). Although a link to breast cancer has been proposed, evidence of EBV as a causative agent is not conclusive (33). EBV has also been proposed to have a role in the etiology of multiple sclerosis and lupus, but it remains unclear if the virus is actually the cause of such autoimmune diseases, or if active lytic EBV replication is exacerbating disease progression. As EBV is linked with so

many different diseases, it is an important subject of study, especially understanding the mechanism by which the virus enters its two target cell types.

The Role of EBV Glycoproteins in Membrane Fusion and Entry

As previously mentioned, herpesviruses do not neatly fit in to Class I or II models. It is unclear if there is a single protein that presents the fusion peptide, as the concerted action of multiple glycoproteins is required for efficient membrane fusion. EBV has a huge double-stranded linear genome (over 170 kb) and the ability to latently infect B lymphocytes, which can lead to the transformation and outgrowth of both epithelial and lymphocytic cells [For review see (112); (17, 37)]. The membranous envelope is studded with numerous glycoproteins, of which EBV is predicted to encode at least 11 although efficient entry of EBV into B cells requires only five glycoproteins (gps): gp350/220, gH, gL, gB and gp42 [For review see (60, 123, 125)] (Table 1.1). The attachment of the virus is mediated by gp350/220 binding to CD21 or complement receptor 2 (CR2) (39, 96, 132). Expression of gp350/220 is not required for membrane fusion, but as a binding factor, greatly enhances infection efficiency, similar to HSV gC (64, 75). Interestingly, antibodies to gp350/220 actually enhance infection of epithelial cells (133). Since CD21 can act as a signal transducer, it is plausible that a gp350/CD21 interaction can induce endocytosis, causing fusion to occur in an endocytic vesicle of B cells, whereas it occurs at the plasma surface of epithelial cells (29-31) (Figure 1.2).

Table 1.1. Epstein-Barr Virus Glycoproteins.

EBV	Other Designations/ Open Reading Frame	HSV (a)	Known or proposed function
gB	gp110/BALF4	gB	virus maturation/fusion
gH	gp85/BXLF2	gH	complexes with gp42 and gL/ binds epithelial receptor/fusion
gL	gp25/BKRF2	gL	complexes with gp42 and gH
gM	BBRF3	gM	virion maturation/expression requires gN
gN	BLRF1	gN	virion maturation/expression requires gM
gp350/220	BLLF1	gC (b)	initial virion binding to CD21
gp150	BDLF3	none	regulates epithelial fusion
gp78	BILF2	none	unknown
gp42	BZLF2	gD (b)	complexes with gL and gH, binds HLA class II/trigger for fusion
BMRF2		none	binds integrins/infection of polarized cells

(a) The HSV glycoproteins which share sequence homology and/or functional homology.

(b) Although no sequence homology with EBV glycoproteins, these HSV glycoproteins may serve as functional homologues.

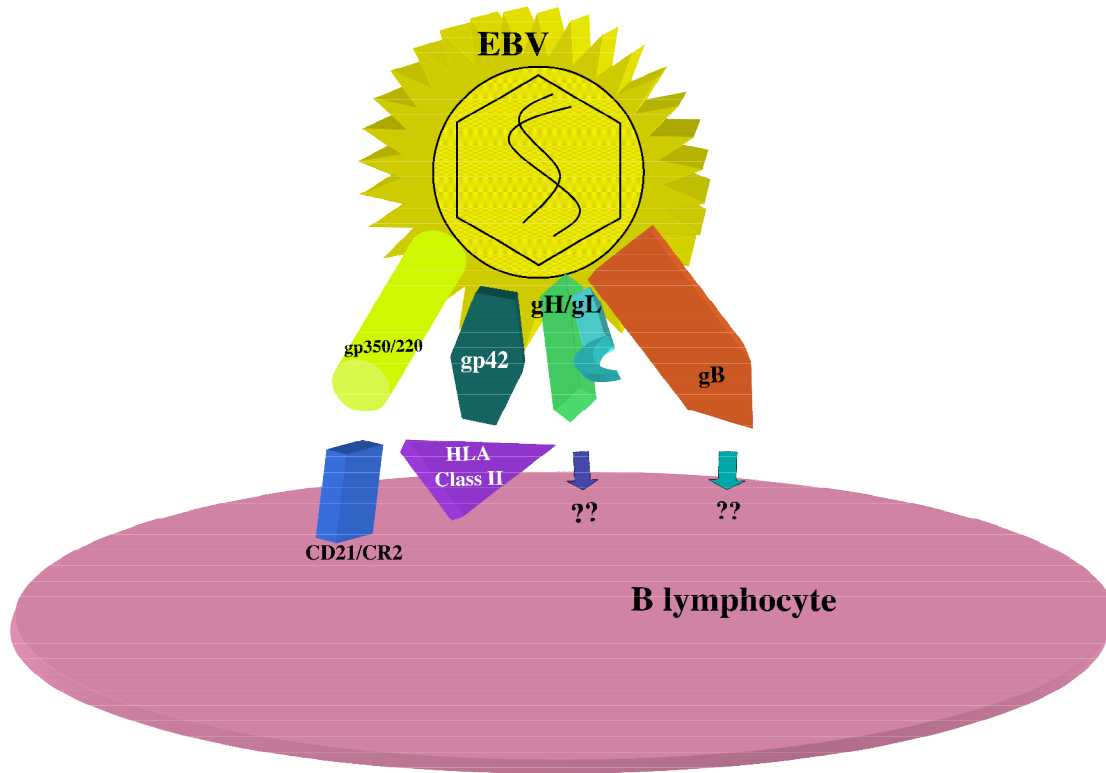


Figure 1.2. Model of EBV infection of B cells.

Cartoon depicting EBV approaching the B lymphocyte (not to scale). The virus has a membranous envelope studded with glycoproteins surrounding the tegument and capsid, which contains the linear double stranded DNA genome. Initial attachment of the virus occurs when gp350/220 binds CD21, followed by gp42 binding the co-receptor, HLA Class II. Membrane fusion requires gp42, gH/gL, and gB. It is unknown if both gH and gB or just gB are inserted into the target membrane, but likely gH is inserted into the outer lipid layer for hemifusion to occur, followed by insertion of gB for complete fusion.

The minimal glycoproteins required for membrane fusion of B cells using experimentally transfected cells are gB, gH, gL, and gp42, while gp42 is dispensable for epithelial cell membrane fusion (47, 88). The glycoproteins gB, gH, and gL all have sequence homology with other herpesviruses. It was previously demonstrated that gB is required for lytic replication as well as the production of transforming virus (59, 79). EBV gB has been shown to be functionally distinct from other human herpesvirus subfamily gBs and this could be due to the different regulatory domains of the cytoplasmic tail that are involved in membrane fusion and virion transport (47, 78). Neuhiel *et al.* demonstrated that EBV gB dramatically enhances infection of human cells and constitutes an important virulence factor that determines infection of non-B cells (97). Mutant gB that had high surface expression due to mutations within the carboxyl-terminal tail was able to mediate membrane fusion of epithelial cells by itself (88). Mutational analysis of the hydrophobic residues in the putative fusion loops demonstrated that they are essential for gB function and its ability to cause fusion with epithelial and B cells (4). The corresponding residues in HSV-1 gB are more hydrophilic and less compatible with membrane insertion, and functional complementation of different herpesvirus gB proteins has not been demonstrated, implying that the mechanisms by which EBV gB mediates membrane fusion could be unique (53, 78, 105). Structural studies of gB revealed rosette structures reminiscent of the postfusion aggregates formed by other viral fusion proteins, but when the putative fusion loops were mutated to contain more hydrophilic residues, trimeric proteins were produced and the ectodomain lost its ability to form rosettes, indicating that EBV gB had similar characteristics to other Class I and Class II viral fusion proteins that are not shared with HSV-1 gB (5).

Nearly all herpesviruses contain a gH/gL complex, which serves an indispensable role in membrane fusion and infection (49, 91, 100, 123, 134, 138, 146). Transmembrane EBV gH

requires the presence of gL, which exists as membrane-bound and soluble forms, in order for EBV gH to fold properly and be transported to the cell membrane, and both EBV gL and the related varicella-zoster virus gL proteins function effectively in mediating the folding and expression of EBV gH protein (51, 80, 82, 149). It has also been established that EBV gH/gL exists as a non-covalently associated heterodimer complex in a 1:1 subunit ratio (70). Mutational studies of gH demonstrated different regions involved in epithelial and B-cell membrane fusion, and that a single point mutation of gH allowed for low levels of B-cell fusion when expressed only with gB, indicating that in B cells, the triggering signal might be transmitted to gH (100, 146, 147). Although early studies implied that gp42 was binding the gH/gL complex via gL, it has since been demonstrated that binding is with gH (82, 101, 138, 147). The N-terminal region of gp42 was demonstrated to be important for interactions with gH/gL, initially using a truncated soluble gp42-Fc chimeric protein lacking the first 58 gp42 residues. This mutant maintained HLA class II binding, and although it did not detectably coprecipitate gH/gL, it did partially inhibit epithelial cell infection, which was attributed to a reduced ability to interact with gH/gL (138). Further studies of purified, soluble proteins revealed that gp42 stably binds gH/gL with 1:1:1 stoichiometry, with residues 33 through 85 being critical for this complex formation. This heterotrimeric complex interestingly acted like soluble gp42 to trigger B-cell membrane fusion, but inhibited epithelial cell membrane fusion. A 30-residue gp42-derived peptide spanning residues 36 to 65 was sufficient to inhibit membrane fusion with epithelial cells with micromolar affinity, partially mimicking the ability of gp42 to bind gH/gL (70). This was in accordance with previous data indicating that due to the lack of surface expression of HLA class II on epithelial cells, gp42 cannot function in entry, and that gp42 acts in an inhibitory manner, likely due to competition for an epithelial cell receptor (13, 82). Although the binding affinities of gp42 with

gH/gL had been examined, the precise binding domain of gp42 that interacts with gH/gL had not been identified.

The type II transmembrane protein gp42 of the BZLF2 open reading frame is unique structurally, but may have functional homology with other glycoproteins such as Herpes Simplex Virus glycoprotein D (HSV gD). The presence of gp42 is required for entry into B-lymphocytes, but not epithelial cells and has two alternately processed forms: a 42 kDa membrane-bound protein and a 38 kDa soluble protein, with varying sizes depending on glycosylation (6, 82, 137). The B cell receptor of gp42 has been identified as the class II human leukocyte antigen (HLA class II) and the -DR, -DP and -DQ alleles are all functional (46, 81, 126). Interestingly, HLA-DQ β^*02 is the only functional DQ allele (48). One requirement for this interaction is the presence of a glutamic acid at the HLA class II beta-chain residue 46, which is present in all HLA-DR and HLA-DP, but only some HLA-DQ alleles (46, 48, 61, 81, 89, 95, 125, 126, 137). A soluble gp42-Fc chimeric protein can stimulate the entry of a gp42-null virus into B cells, and, likewise, the addition of baculovirus-produced, soluble gp42 to cells transfected with gH, gL, and gB allows membrane fusion to occur with B cells (70, 138). However, membrane fusion with epithelial cells is actually inhibited by the presence of gp42 for both virus infection and a cell-cell fusion assay (70, 138). Increasing levels of inhibition occur as exogenous soluble gp42 is added in a cell-cell fusion assay, beginning in the low-nanomolar-concentration range (70). This is likely due to the formation of three-part gH/gL/gp42 complexes that are unable to mediate membrane fusion with epithelial cells, possibly due to steric hindrance of gH/gL receptor binding or direct insertion of gH/gL into the target membrane (14, 61). These studies are consistent with the proposal that levels of gp42 in the virus dictate EBV tropism in vivo (138).

It has been theorized that expression levels of gp42 on the surface of the virion decrease or increase as the virus alternates between infection of epithelial cells and lymphocytes in the human host, the so-called “cell-switching and kissing” model (13). Carefully designed experiments demonstrated *in vitro* that when the virus is produced in epithelial cells, the virion contains abundant gp42, which allows very efficient infection of B cells. However, as gp42 is not required for entry into epithelial cells, the high surface expression might sterically interfere with receptor binding which would lead to the reduced efficiency of epithelial cell infection that was observed. Conversely, when the virus is produced in B cells, the amount of gp42 in the virion is reduced, due to co-localization with the EBV B-cell receptor, which allows efficient infection of epithelial cells, but decreased infection of other B cells as was demonstrated (13, 108, 109). This provides a plausible route of oral EBV infection in humans via epithelial cells and then B cells where the virus can establish latency. Alternatively, Shannon-Lowe *et al.* demonstrated that EBV virions bound to primary B cells *in vitro* were not internalized and that their persistence on the surface allowed the virions to transfer more efficiently to CD21-negative epithelial cells. Infection increased by 10^3 to 10^4 -fold over cell-free virus (120).

When the studies described in this thesis dissertation were initially undertaken, the crystal structure of a baculovirus-produced soluble form of gp42 bound to the HLA-DR1 allele had just been solved (89, 95). The predicted c-type lectin domain (CTLN) lies between residues 94 and 223 of the protein and though it shows some structural homology to other CTLN-containing proteins such as Ly49a, it was revealed that binding of gp42/HLA-DR1 was not homologous to Ly49a binding to its receptor, the major histocompatibility complex (MHC) class I molecule H-2D^d, nor any other CTLN-containing protein and its receptor. A region of the gp42 amino-terminal ectodomain formed dimers in the crystal between residues 87 and 94. Adding to its

inimitable character as a novel herpesvirus glycoprotein is a region of several aliphatic and aromatic residues that create a hydrophobic pocket with a yet unknown binding partner. Structural data indicated that this recess on the surface of the protein consisted of many hydrophobic residues from disparate sequence regions of gp42. It was so hydrophobic and large that it was concluded to be impossible for this particular conformation to remain unoccupied. Recent structural studies of the unbound gp42 crystal reveal that gp42 formed dimers in such a way as to occlude the hydrophobic pocket of both molecules (Kirschner *et al.*, submitted). Comparison of the pre- and post-bound gp42 protein also revealed that the amino-terminal ectodomain closest to the CTLD moves away from the CTLD, possibly allowing dimers to then form, and the hydrophobic pocket opens up, which could allow its ligand to then bind. Dimerization of gp42, either pre- or post-binding to HLA class II, may be important for fusion since it could conceivably bring more glycoproteins and/or receptors together to increase lipid mingling. Membrane fusion is a delicate dance, a careful orchestration of proteins and lipids. At the very tips lies the intricate mingling of amino acid residues, the flirting of atomic bonds, gently hugging and tugging, kissing and shying away. The initiation of fusion by gp42 mediated by its coordinated interactions with gB, gH, and gL likely results from conformational changes in gp42 after its binding to HLA class II. These conformational changes may allow other EBV encoded glycoproteins or additional cellular receptors to bind to the fusion complex, or may rearrange receptors on the virion or cell surface.

The specific tropism gp42 lends EBV along with its unique binding structure and hydrophobic pocket make it an interesting target for functional studies of membrane fusion to not only characterize EBV fusion mechanisms, but also increase our overall understanding of herpesvirus infection. Herpesviruses fusion complexes require more viral proteins than most

other viruses, and therefore will prove to be more difficult in attempts to develop drugs that target membrane fusion. Better understanding of the sequential and conformational requirements of the glycoproteins involved will aid in targeting and designing effective therapies. We have undertaken mutational structure/function studies of gp42 to confirm the predicted interaction of gp42 with HLA class II and also to investigate the function of other gp42 domains such as the amino-terminal ectodomain and the hydrophobic pocket in EBV-induced membrane fusion.

**CHAPTER TWO—MUTATIONAL ANALYSES OF EPSTEIN-BARR VIRUS
GLYCOPROTEIN 42 REVEAL FUNCTIONAL DOMAINS NOT INVOLVED IN
RECEPTOR BINDING BUT REQUIRED FOR MEMBRANE FUSION**

INTRODUCTION

The mechanisms of EBV-induced membrane fusion have not yet been elucidated in complete detail, but mutational studies coupled with x-ray crystallography have already provided much insight into the intricacies of this finely tuned process. Previous work had demonstrated the minimal EBV glycoprotein requirement for B-cell fusion in a virus-free system to be gH, gL, gB and gp42 (47). Preliminary data of the crystal structure of EBV gp42 bound to the HLA class II-DR1 allele along with mutational studies of HLA class II helped guide the generation of several gp42 mutants (89, 95). We wished to confirm the sites of gp42 that directly interacted with HLA class II, but we also wanted to determine if there were other functional domains required for receptor binding and/or membrane fusion.

We randomly generated linker-insertion mutants and also created several site-specific mutants of gp42 and assayed them for proper conformation in both membrane-bound and secreted form. Those that expressed were then tested for their ability to mediate cell-cell fusion using a luciferase reporter system. Many of the mutants did not work in the fusion assay, which was quite surprising. All of the mutants were further tested in the secreted form for their ability to bind HLA class II-expressing B cells, as well as their ability to co-precipitate with gH and gL. From the data gathered, four categories of mutants emerged: (a) unaffected in their ability to bind HLA class II and mediate fusion, (b) mutations located within the core of the protein, distant from any domains, leading to proteins unable to bind HLA class II or mediate fusion, (c) mutations located within the HLA class II binding site leading to loss of both binding and fusion, and (d) mutations located within the hydrophobic pocket resulting in proteins that are able to bind HLA class II but unable to mediate fusion. This last category was quite intriguing because it demonstrated a functional domain involved in membrane fusion but separate from receptor

binding. Although the ligand of this hydrophobic pocket remains unidentified, the domain is a potential target for small molecule inhibitors of membrane fusion and infection. Identification of the binding partner will also help provide a clearer image of how gp42 is able to trigger membrane fusion with B cells in concert with the other glycoproteins.

MATERIALS & METHODS

Cells and plasmids. Chinese hamster ovary cells (CHO-K1) kindly provided by Nanette Susmarski were grown in Ham's F-12 media with 10% fetal bovine serum and 1% penicillin/streptomycin, referred to as complete media (all from BioWhittaker). EBV-positive HLA class II- and CD21-expressing Daudi B lymphocytes were obtained from American Type Culture Collection (Manassas, VA) and were grown in RPMI complete media (BioWhittaker). To more easily monitor membrane fusion, a Daudi cell line stably transfected and expressing T7 RNA polymerase was constructed. Briefly, Daudi cells were electroporated with 40 μ g of pOS2 plasmid DNA, containing a G418 selectable marker and bacteriophage T7 RNA polymerase under transcriptional control of the simian virus 40 promoter. This plasmid was kindly provided by Stanley Lemon (140). Following transfection, the cells were plated at 10,000 and 50,000 cells per well in 96-well plates and selected with G418 (0.9, 1.1, or 1.3 mg/ml). Clones emerged approximately 3 to 4 weeks post plating. Approximately 50 clones were expanded from the 96-well plates and were tested in the fusion assay as described below. Of the tested clones, cell lines 22, 29, 31 and 36 provided the highest levels of luciferase expression in the fusion assay. Of these lines, lines 29 and 36 were used for all subsequent experiments and were maintained in RPMI complete media with 1.1 and 1.3 mg of G418/ml, respectively. Cells were grown in 75-cm² cell culture flasks (Corning), and adherent cells were detached using either trypsin-Versene (BioWhittaker) or Versene (phosphate-buffered saline [PBS]-1 mM EDTA). The various plasmids used in the present studies are shown in Table 2.1.

Generation of mutants. Mutations were generated using either a GPS-LS linker scanning system (New England Biolabs [NEB]) or a QuikChange kit (Stratagene) on an EBV gp42-containing pCAGGS/MCS vector (72) and isolated by cesium chloride density gradients. The

NEB kit uses a transposon-based random mutagenesis to introduce a selection marker. After selection, clones are diagnostically digested and then sequenced to determine the exact location of the mutation. Collapse of the marker leaves a 5-amino-acid insertion introducing a rare PmeI site and a repeat of five host base pairs. The QuikChange kit uses PCR to introduce a specific mutation via primers designed with a silent mutation for diagnostic purposes. The suggested PCR protocol was followed to generate mutant clones, which were then diagnostically digested and sequenced. Some mutants were generated without the QuikChange kit by using two-step PCR to introduce a specific mutation via primers designed with a silent mutation for diagnostic purposes, similar to those used with the kit. After confirmation of the introduced mutation, plasmids were prepared and confirmed similarly.

Transfection. (i) Fusion assay. CHO cells were seeded in plastic 24-well plates (Corning), grown 24 h to approximately 90% confluency, and transiently transfected with 0.125 μg each of EBV gH, gL, and gB, 0.5 μg of gp42 or gp42 mutant, and 0.2 μg of a luciferase-containing reporter plasmid with a T7 promoter (99). Transfections utilized 700 μl of Opti-Mem (Gibco) and 1 μl of Lipofectamine 2000 (Invitrogen) per well.

(ii) Western blotting and cell-based enzyme-linked immunosorbent assay (CELISA). CHO cells were seeded into six-well plastic plates (Corning) and transfected with 4 μg of plasmid DNA with 2.5 mls of Opti-Mem and 5 μl of Lipofectamine 2000. The transfection efficiency was always simultaneously assessed by transfection of pEGFP-N1 and expression of enhanced green fluorescent protein (EGFP).

Expression of mutants. (i) Western blotting. CHO cells were transfected as previously stated. Media was changed 12 h later and cells collected 24 h later. Cells were scraped, washed 2 to 3 times in PBS, and lysed using a 1% Triton X buffer with 1 mM sodium vanadate, 10 mM sodium

fluoride, leupeptin (0.5 mg/ml), pepstatin (0.7 mg/ml) and 0.2 mM phenylmethylsulfonyl fluoride. Lysates were run on Bio-Rad 12.5% criterion gels in sodium dodecyl sulfate running buffer at 120 V for 90 min. Proteins were transferred to Immobilon-P membranes in transfer buffer at 90 V for 90 min with cooling or at 15 V overnight. Blots were blocked in Tris-buffered saline with Tween with 3% milk for an hour at RT or overnight at 4°C and then incubated for an hour at RT with a rabbit polyclonal anti-gp42 antibody (PB1114) diluted at 1:1,000 in blocking solution. Blots were washed, and a secondary protein A-horseradish peroxidase (HRP) conjugated antibody (Amersham) was applied for half an hour at RT. Blots were then mixed in equal volumes of ECL solutions and exposed to hyperfilm (Amersham Biosciences).

(ii) CELISA. CHO cells were transfected as previously stated. After 12 h media was changed, and then 12 h later cells were detached with Versene and transferred to Corning 96-well plates, 3 wells per sample. After 16 h of incubation at 37°C, cells were washed with PBS-ABC (PBS with 0.89 g of CaCl₂ and 0.89 g of MgCl₂·H₂O per 8 liters), incubated for 30 min at RT with a rabbit polyclonal anti-gp42 antibody (PB1112) diluted 1:1,000 in PBS-ABC with 3% bovine serum albumen (PBS-BSA), then fixed for 10 min in PBS with 2% formaldehyde and 0.2% glutaraldehyde. Cells were washed three times with PBS-BSA, incubated with a biotinylated goat anti-rabbit immunoglobulin G (IgG) (Sigma) at 1:500 for 30 min, washed five times, and then incubated with a streptavidin-HRP antibody (1:20,000) (Amersham) for 30 min, all at RT. Cells were then mixed with a peroxide substrate (BioFX Laboratories) and read with a Victor plate reader at 370 nm for 0.1 s.

Cell-cell membrane fusion assay. This assay was slightly modified from a previously published protocol (47). Briefly, CHO cells were transfected as stated previously. After 12 h, these cells were washed and overlaid with 5.0×10^5 target HLA class II-expressing Daudi B cells that had

been stably transfected to express T7 RNA polymerase. After 24 h of incubation, the cells were washed twice with PBS and lysed and 100 μ l of firefly luciferin substrate was added to 20 μ l of lysate (Promega luciferase assay system). Relative luciferase activity was measured in Visibottom 96-well plates by a Victor plate reader at 370 nm for 0.1 s.

Quantification of sgp42 levels by enzyme-linked immunosorbent assay (ELISA). A baculovirus-generated soluble gp42 (sgp42) was used as a positive control in addition to transfected soluble gp42. Twenty-five microliters of transfected CHO cell supernatants diluted in PBSN (PBS with 0.02% sodium azide) were added to NUNC round-bottom plates (3 wells per samples), covered with plastic wrap, and allowed to incubate overnight at RT. Samples were blocked with PBS-1% BSA (blocking buffer) for 1 h at 37°C, followed by PB1112 diluted 1:1,000 in blocking buffer for 2 h at 37°C, goat anti-rabbit IgG diluted 1:500 in blocking buffer for 2 h at 37°C, and streptavidin-HRP diluted 1:20,000 in blocking buffer for 2 h at 37°C. Peroxide substrate was added, and plates were read on a Victor plate reader at 405 nm for 0.1 s.

Binding of sgp42 to HLA class II-expressing cells by flow-cytometry. This assay was slightly modified from the previously published protocol (89). After measuring relative levels of soluble gp42 in CHO cell supernatants by ELISA, supernatants were diluted in Ham's F-12 complete media and incubated with 5.0×10^5 Daudi cells in approximately 250 μ l of RPMI complete media while rotating at 4°C for 20 min. Cells were then washed with fluorescence-activated cell sorting (FACS) buffer (PBS with 0.01% sodium azide, 1% HEPES buffer [BioWhittaker], and 1% fetal bovine serum), followed by incubation with PB1114 (diluted in FACS buffer to 1:250) and a biotinylated anti-DQ Ia₃ antibody (1:100) on ice for 15 min. After washing with FACS buffer, secondary antibodies used were fluorescein isothiocyanate (FITC)-conjugated goat anti-rabbit whole IgG and allophycocyanin-conjugated streptavidin (both at 1:250) (Pharmingen),

also on ice for 15 min. Cells were washed and resuspended in 350 μ l of FACS buffer. Immunofluorescence was measured using a Becton-Dickinson FACS-Sort cytometer and analyzed using Cell Quest Pro. As a positive control, a baculovirus-generated sgp42 of residues 33 to 233 was utilized.

Table 2.1. Plasmids utilized for present studies.

PLASMID OR MUTANT	EXPRESSED PROTEIN ^a	RESTRICTION SITE	REFERENCE
pCAGGS.MCS	Ampicillin selec. marker	Multiple	(72)
pF42	EBV gp42	EcoRI/BglII	(47)
pF25	EBV gL	EcoRI/BglII	(47)
pF85	EBV gH	ClaI/BglII	(47)
pF110	EBV gB	EcoRI/ClaI	(47)
pEGFP-N1	EGFP	Multiple	Clontech
pOS2	T7 RNA Polymerase, G418 selec. marker		(140)
pT7EMCLuc	T7 Luciferase		(99)
LI12	EBV gp42 LFKQL-F	PmeI	(121)
LI27	CLNNF-L	PmeI	(121)
LI82	CLNNW-T	PmeI	(121)
LI93	MFKHQ-N	PmeI	(121)
LI104	CLNSN-T	PmeI	(121)
LI112	CLNTY-K	PmeI	(121)
LI118	CLNIY-F	PmeI	(121)
LI122	MFKQK-K	PmeI	(121)
LI134	CLNSA-E	PmeI	(121)
LI148	MFKHD-I	PmeI	(121)
LI149	CLNNI-L	PmeI	(121)
LI179	CLNID-G	PmeI	(121)
LI193	CLNNC-T	PmeI	(121)
LI195	CLNTY-V	PmeI	(121)
LI206	CLNTH-H	PmeI	(121)
LI210	LFKHS-F	PmeI	(121)
LI216	CLNSF-C	PmeI	(121)
W44A	TRP to ALA	Acc65I	(121)
Q89A	GLN to ALA	Acc65I	(121)
T104A	THR to ALA	XhoI	(121)
Y107A	TYR to ALA	BsaJI	(121)
W125G	TRP to GLY	BsrDI	(121)
R154A	ARG to ALA	MunI	(121)
E160A	GLU to ALA	Esp3I	(121)
Y185F	TYR to PHE	BglII	(121)
F210A	PHE to ALA	AflII	(121)
R220A	ARG to ALA	HindIII	(121)

^aThe mutant EBV gp42-expressed protein either reveals the 5-amino-acid insert followed by the residue (after the hyphen) indicating the location (LI12 contains LFKQL inserted before residue 12F) or the change in point mutation (W44A is tryptophan to alanine).

RESULTS

Construction of gp42 mutants. In order to better understand the mechanism of EBV-induced membrane fusion, we wanted to define functional domains of gp42. Initially we utilized a transposon-based linker insertion mutagenesis to generate random 5-amino-acid inserts spaced throughout gp42. The NEB GPS-LS linker scanning system creates mutants with an insertion of five amino acids containing a 5-bp repeat from the host sequence along with the addition of a unique PmeI site. During this time, the crystal structure of a baculovirus expressed soluble form of gp42 (sgp42) from residues 33 through 223 bound to HLA class II was solved, which revealed a short stretch of residues 104 through 107, an α -helix of residues 149 through 154 with an adjacent loop of residues 155 through 160, and arginine 220 all as areas of interaction with the HLA-DR1 β -chain (Figure 2.1A). The HLA class II E β 46 forms a salt bridge with gp42 R220 and hydrogen bonds with T104 and Y107, R β 72 forms hydrogen bonds with T104 and Y107, and N β 62, S β 63 and K β 65 all form hydrogen bonds with the α -helix (89, 95) (Figure 2.1B). Although the ectodomain up to residue 85 was disordered, other structural features were also discovered. Ten cysteine residues of the native protein form five disulfide bonds (99 with 138, 102 and 115, 128 and 214, 132 and 216, and 192 with 208) and there are four potential N-linked glycosylation sites at residues 64, 93, 98, and 173. A potential dimerization site was delineated between residues 87 and 94, and a hydrophobic pocket was observed consisting of several aliphatic and aromatic residues between residues 161 and 201 (Figure 2.1C). The proposed binding site with the gH/gL dimer located in the amino terminus was in the disordered region. Although the linker-insertion mutants spanned all of these domains, we constructed additional site-directed mutations of individual residues to introduce specific mutations within certain domains. For these mutations, the Stratagene QuikChange kit was utilized. For each site-specific

mutation, a unique restriction site was silently incorporated into the reading frame to allow easy identification of each mutant. More detailed procedures and the various plasmid clones used in these studies are included in Material and Methods and in Table 2.1. Plasmid DNA was isolated by cesium chloride density gradients and sequenced to locate and confirm the nature of each mutation shown in Figure 2.1D. Linker insertion mutants are named based on the residue number that follows the 5-amino-acid insert and are shown along with the locations of the point mutations.

Figure 2.1. Important Structural Features of EBV gp42 and Residue Sequence Mapping

Location of Mutations. (A) Three-dimensional ribbon model of soluble EBV gp42 (rose) bound to HLA class II HLA-DR1 (beige). The amino terminus of residues 33 to 85 was disordered in the crystal structure. Backbones of residues interacting with HLA class II are yellow, oxygen atoms red, and nitrogen atoms are blue. The orange and green arrows indicate the regions enlarged in panels B and C, respectively. (B) Close-up depicting key gp42 contact residues at the HLA class II interface. The color scheme is the same as in panel A. (C) Close-up of gp42 hydrophobic pocket highlighting aliphatic and aromatic residues. (D) The residue sequence of gp42 reveals the locations of point mutations above residues and linker insertion mutations containing 5-amino-acid inserts above arrows. Linker-insertion mutants are named based on the residue that their mutation precedes, e.g. LI 12, and point mutants reveal original and mutation residue, e.g. W44A. The baculovirus-produced soluble gp42 (89) used as a positive control in many experiments spans residues 33 through 223 and was kindly provided by Maureen Mullen. Residues of the potential gH/gL binding site are in green. HLA class II contact sites are indicated as follows: aromatic ring residues in red, α -2-helix in purple, and arginine 220 in blue. Hydrophobic residues in the pocket are in yellow. Mutants are color-coded by their function in the fusion assay: those in green have levels similar to the wild-type levels, those in orange have reduced levels of fusion, and those in red do not mediate fusion.

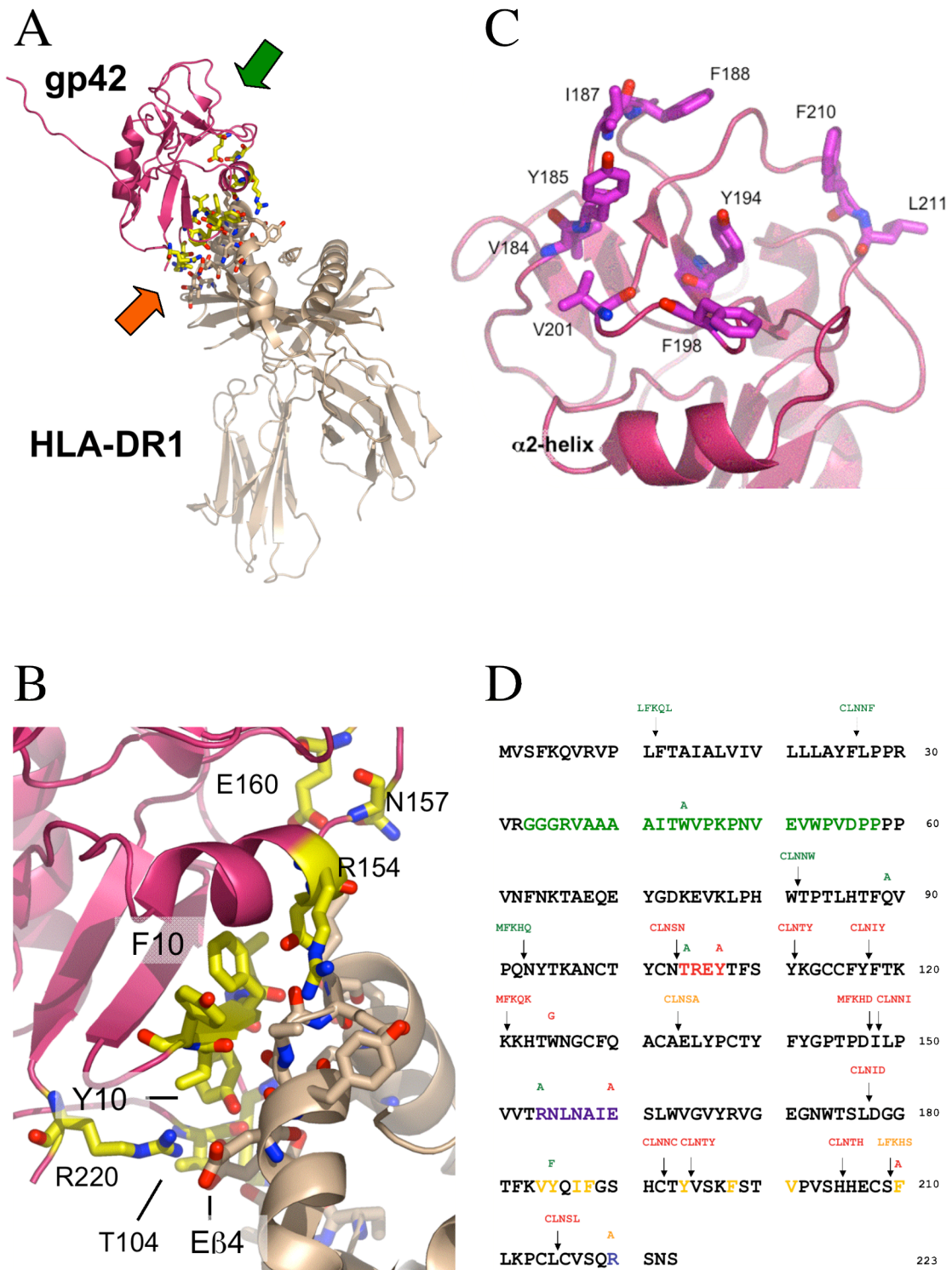


Figure 2.1. Important Structural Features of EBV gp42 and Residue Sequence Mapping Location of Mutations.

Analysis of cell surface expression, whole cell expression, and secretion of the gp42 mutants. Prior to using the gp42 mutants in a cell-based fusion assay, we verified the expression of each of the mutants following transfection in CHO cells. Cell surface expression for each of the mutants was detected by CELISA at 40 h posttransfection. Only a subset of the mutants are shown in Figure 2.2A, but all were tested. All mutants were expressed on the surface at detectable levels (threefold above background at the left of Figure 2.2A), and many were expressed at levels similar to wild-type gp42. The W125G mutant was expressed the least with an approximate 50% reduction compared to wild type gp42. Total cellular expression of the gp42 mutants was measured by Western immunoblotting, and although the expression level for each of the mutants was somewhat variable, each was expressed at levels greater than that observed for wild-type gp42. Fourteen of the seventeen linker insertion mutants are shown in Figure 2.2B. The linker insertion mutant LI193 consistently migrated higher than wild-type or other mutant gp42 samples on a gel (Figure 2.2B, lane LI193). This mutant contains two asparagines residues in the insert, likely introducing a new glycosylation site at the first asparagine, resulting in the altered mobility. Finally, we investigated the levels of a secreted form of gp42 found in the media of the CHO-transfected cells 24 h posttransfection. As shown in Figure 2.2C, the relative levels of gp42 in the media supernatant for each of the gp42 linker insertions mutants were equal to or greater than that observed for wild type gp42. Analyzed but not shown, the gp42 site-specific mutants also had expression levels similar to those of linker insertion mutants shown in Figure 2.2C, except for W125G, which showed reduced levels similar to those obtained with the CELISA.

Figure 2.2. Verification of mutant gp42 surface expression by CELISA and whole-cell expression by Western blotting. (A) CHO cells were transiently transfected to express wild-type or mutant gp42 and transferred to 96 wells, 3 wells per sample. Shown is a representative CELISA experiment with a random sampling of linker insertion mutants followed by point mutants in sequential order from amino terminus to carboxyl terminus. Positive expression is at least a threefold higher average reading of triplicate samples than the vector control shown at left. OD, optical density. (B and C) Mutant gp42 expression was verified as both a transmembrane form in whole lysates (B) and a secreted form in supernatants (C) of transiently transfected CHO cells by Western blotting. Molecular mass (kDa) is noted to the left of blots.

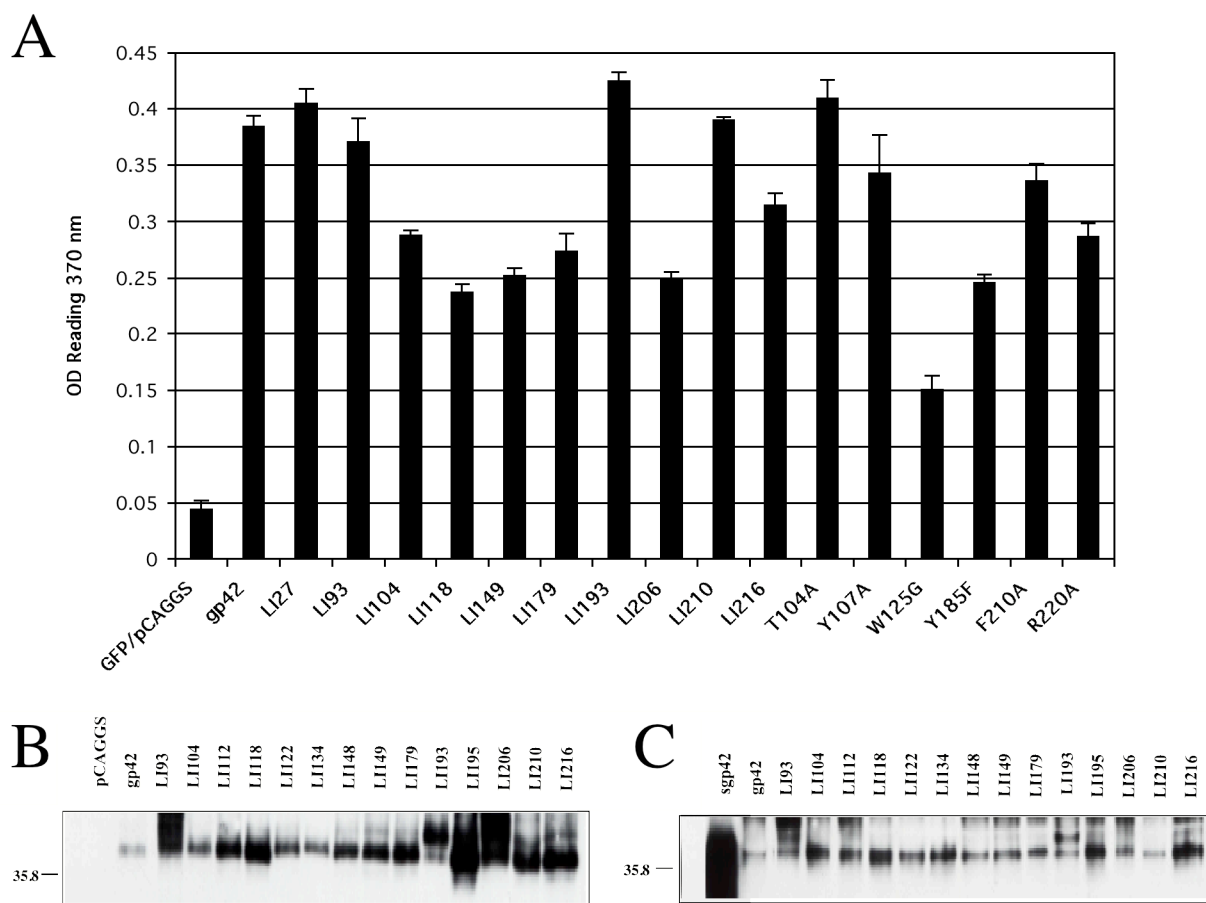


Figure 2.2. Verification of mutant gp42 surface expression by CELISA and whole-cell expression by Western blotting.

Function of gp42 mutants in membrane fusion. Since most gp42 mutants were expressed with levels similar to that of the wild type, we screened them for their ability to mediate membrane fusion in a virus-free assay (Figure 2.3) as previously described (47). Briefly, effector CHO cells were transfected with expression constructs for gH, gL, gB, and either wild-type or one of the mutant forms of gp42. In addition, a plasmid with the luciferase gene under control of the T7 RNA polymerase was included. The effector cells were then overlaid with Daudi cells constitutively expressing T7 RNA polymerase. The T7 RNA polymerase-expressing cells were constructed as detailed in Material and Methods. Upon fusion, luciferase expression is upregulated, which provides a quantitative measure of fusion between the two cell types. The fusion assay was repeated at least five times for each mutant, with clear patterns of the fusion competence of each mutant emerging. Results from a representative experiment with all of the gp42 mutants are shown in Figure 2.3. Although surface expression levels vary as demonstrated in Figure 2.2A, it is not a completely accurate gauge of fusion capability. Fusion levels consistently appear similar even if one mutant surface expression level is measurably higher than another, indicating a quantitative threshold of fusion and that detectable levels of surface expression are sufficient to assess the ability to mediate membrane fusion (compare LI93 and Y185F in Figures 2.2A and 2.3). The mutants can be categorized by their fusion activity and, as might be expected from the crystallization studies, the various groups of mutations localized to specific domains of gp42, some in domains known to be functionally important and, interestingly, in others with no function currently ascribed. The first group of mutants, all located within the amino-terminal domain of gp42 or near the membrane-spanning domain of gp42, is competent in mediating fusion (LI12, LI27, LI82, LI93, W44A, and Q89 [Figure 2.3]). Of the nine gp42 mutants with mutations localized in areas predicted to be important for binding to

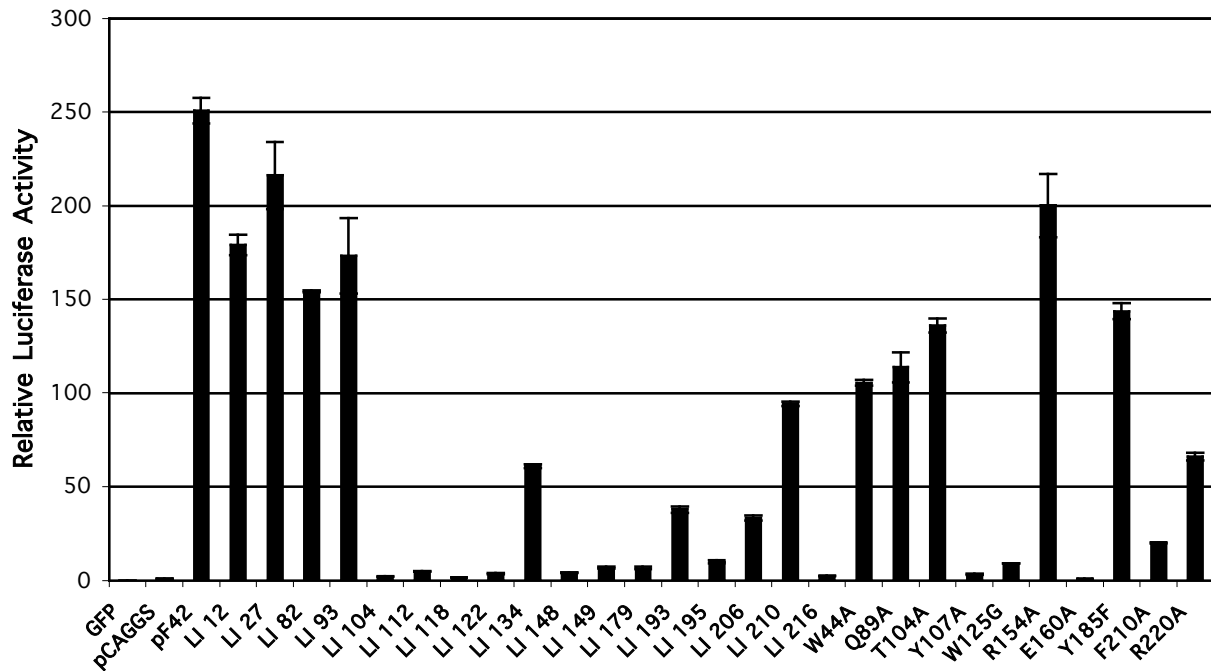


Figure 2.3. Mutant gp42s Vary in Ability to Mediate Cell-Cell Fusion.

CHO cells transiently transfected to express EBV gH, gL, gB, wild-type or mutant gp42, and luciferase driven by a T7 promoter were overlaid with Daudi cells stably transfected to express T7 RNA polymerase. Mutants are in order of location from the amino terminus to carboxyl terminus, linker insertion mutants are followed by point mutants, and readings are averages of two samples.

HLA class II, six had clear defects in fusion (LI104, LI112, LI148, LI149, Y107A, and E160A [Figure 2.3]). Two of the gp42 mutants localized in these regions had no effect on membrane fusion (T104A and R154A [Figure 2.3]), with the mutants having levels of fusion similar to wild-type gp42, whereas the R220A mutant was reduced in membrane fusion when compared to wild-type gp42. With the exception of the Y185F and LI210 gp42 mutants, the gp42 mutants localized to the hydrophobic pocket dramatically reduced membrane fusion when compared to wild-type gp42 (LI193, LI195, LI206, and F210A [Figure 2.3]). All the remaining mutants, with the exception of LI134, were greatly reduced in fusion (LI118, LI122, LI179, LI216 and W125G [Figure 2.3]). LI134 had a defect leading to a roughly fivefold reduction in membrane fusion. These mutations, which do not localize to the gp42 hydrophobic pocket or the HLA class II binding site, can be classified as “core/distant” mutations, since they are localized distant from these two gp42 functional domains. They likely interrupt important structural determinants of gp42, as they either are buried in the central part of the protein or are located in key structural determinants, and they most likely contribute to the overall structural integrity of gp42. They will be more fully discussed later. A summary of the results of the fusion assay is listed in Table 2.2.

Table 2.2. Summary of assays reveals four classes of gp42 mutations.

Classification ^a	Mutant	Function ^b	Fusion ^c	Binding ^d
Unaffected	LI12	TM Domain	+	+
Unaffected	LI27	N-Terminus	+	+
Unaffected	LI82	N-Terminus	+	+
Unaffected	LI93	N-Terminus	+	+
Unaffected	W44A	N-Terminus	+	+
Unaffected	Q89A	N-Terminus	+	+
Unaffected	T104A	HLA class II	+	+
Unaffected	R154A	HLA class II	+	+
Unaffected	Y185F	Pocket	+	+
Core/Distant	LI118	Structural	-	-
Core/Distant	LI122	Structural	-	-
Core/Distant	LI134	Structural	+/-	+/-
Core/Distant	LI179	Structural	-	-
Core/Distant	LI195	Pocket	-	-
Core/Distant	LI216	Structural	-	-
Core/Distant	W125G	Structural	-	-
HLA class II	LI104	HLA class II	-	-
HLA class II	LI112	HLA class II	-	-
HLA class II	LI148	HLA class II	-	-
HLA class II	LI149	HLA class II	-	-
HLA class II	Y107A	HLA class II	-	-
HLA class II	E160A	HLA class II	-	-
HLA class II	R220A	HLA class II	+/-	-
Pocket	LI193	Pocket	-	+
Pocket	LI206	Pocket	-	+
Pocket	LI210	Pocket	+/-	+
Pocket	F210A	Pocket	-	+

^aClassification based on location of mutation and results of cell-cell fusion and HLA class II binding assays.

^bProposed or known functional domain where mutation is located. TM, transmembrane.

^cMutants were tested for ability to mediate membrane fusion in cell-cell fusion assays as described in text and for Figure 2.3. Relative fusion levels were scored as follows: +, greater than 50%; +/-, roughly between 10 and 50%; and -, no fusion.

^dMutants were tested for ability of soluble form to bind HLA class II-expressing human B cells as described in the text and for Figure 2.4.

Binding of gp42 mutants to HLA class II positive B cells. In order to further characterize gp42 mutants, we assayed their ability to bind HLA class II. We reasoned that it was unlikely that all mutants unable to mediate membrane fusion would also be defective in HLA class II binding and that the results might reveal another requirement for membrane fusion. Similar to previous studies in which the binding of a baculovirus expressed gp42 was assayed (89), the Daudi human B-cell line, which expresses abundant levels of all alleles of HLA class II, was used (71). In this assay, supernatants of transfected CHO cells were collected, and the amount of secreted gp42 quantified by ELISA (data not shown) and diluted so that similar amounts of the soluble gp42 were contained in each sample. The concentration-adjusted gp42 was then added to Daudi cells at 4°C to allow binding of gp42 to HLA class II on the cell surface. Binding of gp42 to HLA class II was detected by using rabbit serum directed against gp42 followed by FITC-conjugated secondary antibody. HLA class II expression was monitored by using a biotinylated anti-HLA class II antibody followed by allophycocyanin-conjugated streptavidin antibody. The cells were then analyzed by FACS. Controls are shown in the first column of Figure 2.4. No FITC-positive cells were detected when media alone (Ham's) or cell supernatants from vector control-transfected cells (pCAGGS) were tested, despite the abundance of HLA class II-positive cells. When either the baculovirus-expressed gp42 or supernatants from wild-type gp42 were tested, binding was readily detected (Figure 2.4, sgp42 [baculovirus] and gp42 [CHO cells]). Previous studies have shown that gp42 binding to target cells is dependent on HLA class II expression (81, 126).

Binding of a subset of gp42 mutants to HLA class II is shown in Figure 2.4, and the remaining data with all of the gp42 mutants are summarized in Table 2.2. From this analysis and our previous analysis of the gp42 mutants in fusion, the mutants can be subdivided according to

Figure 2.4. FACS analysis reveals differences among mutants in binding to HLA class II and mediating fusion. Daudi B lymphocytes (5×10^5) expressing HLA class II were incubated with 25 μ l of supernatant from transfected CHO cells expressing wild-type or mutant gp42. Cells were stained for gp42 and HLA class II HLA-DQ and analyzed by flow-cytometry using a Becton-Dickinson FACS-Sort. Columns represent five groups. Column 1 shows controls; the top two are negative media and vector controls, the bottom are baculovirus-produced sgp42 and transfected CHO cell supernatant gp42 (wild-type). Column 2 reveals the mutants that are unaffected in binding to HLA class II and are able to mediate fusion. Column 3 shows those that cannot mediate binding to HLA class II or fusion, but the locations are not in HLA class II contact sites. Column 4 contains mutants unable to bind HLA class II and mediate fusion, but the mutations are localized to HLA class II contact sites. Column 5 contains mutants that are able to bind to HLA class II but are unable to mediate fusion and localize to the hydrophobic pocket.

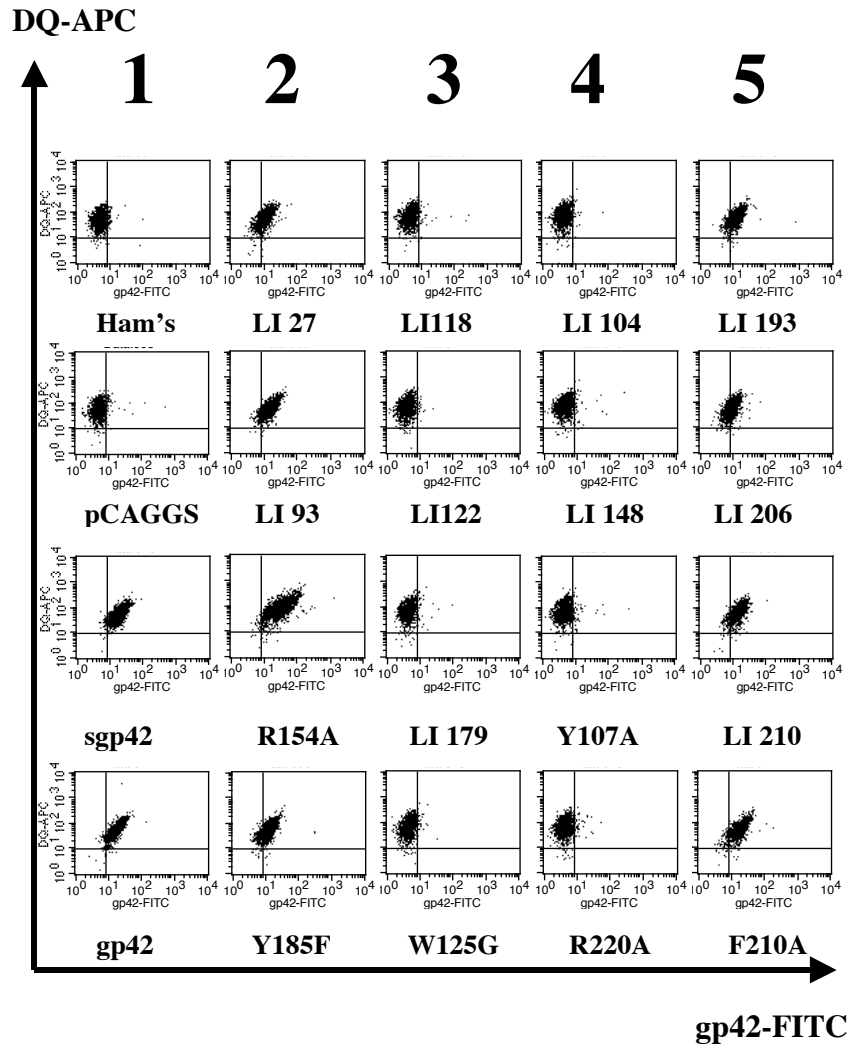


Figure 2.4. FACS analysis reveals differences among mutants in binding to HLA class II and mediating fusion.

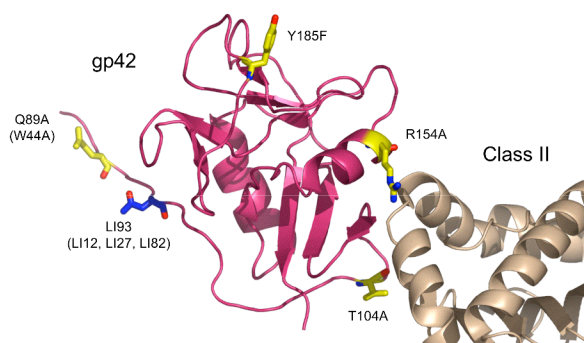
characteristics of binding to HLA class II and fusion competence, resulting in four categories of gp42 mutants. In the second column of Figure 2.4, examples of the first category of mutants are shown. These mutants are unaffected in both binding to HLA class II and fusion. The mutants are LI27, LI93, R154A, Y185F (all shown in Figure 2.4), LI12, LI82, W44A, Q89A, and T104 (data not shown). The second group consists of the so-called core/distant mutants (column 3). These mutations do not localize to HLA class II contact sites or the hydrophobic pocket and are generally negative in binding to HLA class II (LI118, LI122, LI179, and W125G [all shown in Figure 2.4], LI134, LI195 and LI216 [summarized in Table 2.2]). None of these mutants is able to efficiently induce membrane fusion, likely as a consequence of an inability to bind HLA class II. The inclusion of linker-insertion mutant LI195 in this category is somewhat of a surprise. Although the mutation localizes to the gp42 hydrophobic pocket, it appears to be close enough to the α -helix region that mediates HLA class II binding to disrupt the correct conformation, rendering the mutant unable to bind HLA class II. In the fourth column, representative mutants are shown which have mutations that localize to HLA class II binding sites, are unable to bind HLA class II, and as a consequence are unable to mediate fusion (LI104, LI148, Y107A, and R220A [Figure 2.4]). Other mutants tested that were also unable to bind HLA class II are summarized in Table 2.2 (LI112, LI149, and E160A). The T104A and R154A mutants, whose mutations localize to HLA class II binding sites, are able to bind HLA class II and mediate fusion, indicating that these sites tolerate mutation without affecting HLA class II binding. The final group consists of gp42 mutants that localize to the hydrophobic pocket and is represented in the fifth column. These mutants generally are not affected in binding to HLA class II (with the exception of LI195, as described above), yet these mutants cannot mediate fusion (LI193, LI206,

LI210, and F210A [Figure 2.4]). Y185F is the only mutant in the hydrophobic pocket able to mediate fusion similar to the wild type (summarized in Table 2.2).

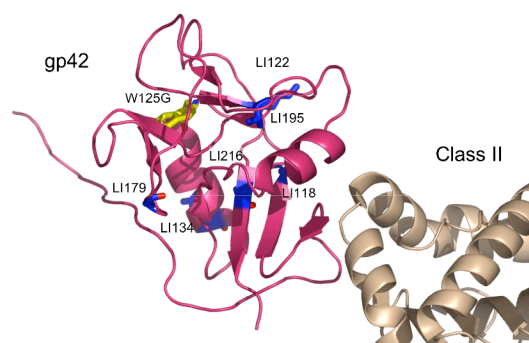
DISCUSSION

We wished to confirm crystallization studies of EBV gp42 bound to HLA class II and also ascertain if domains not binding HLA class II were involved in membrane fusion. The analyses of gp42 mutants provide additional clues as to how gp42 may be involved in the initiation of membrane fusion, an essential process for the entry of EBV into B lymphocytes. From these studies, four general categories of gp42 mutants were identified and are summarized in Table 2.2. Figure 2.5 shows three-dimensional ribbon models with the locations of the mutations based on these categories that are explained further below. The four categories define mutants that (A) are unaffected for binding and fusion, (B) likely induce folding defects in the gp42 structure, disrupting HLA class II binding and fusion, (C) are located in the HLA class II binding site, do not bind to HLA class II, and also do not mediate fusion, or (D) are located in the hydrophobic pocket and are able to bind HLA class II but unable to mediate fusion. Interestingly, for each of these categories we were able to identify a single point mutant.

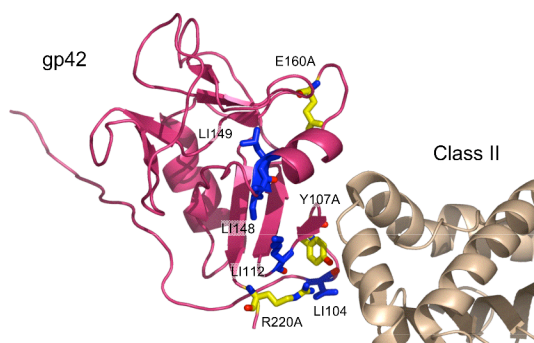
Locations of Inconsequential gp42 Mutations



Locations of Core/Distant gp42 Mutations



Locations of Class II Binding Site Mutations



Locations of Hydrophobic Pocket Site Mutations

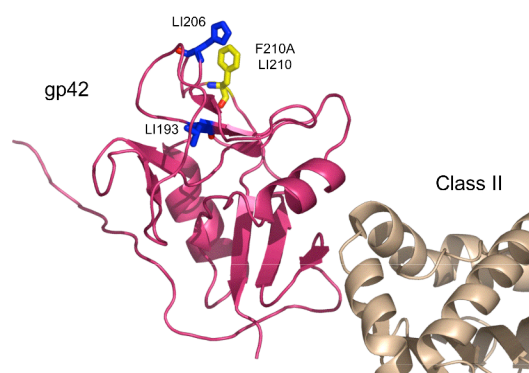


Figure 2.5. Ribbon models identifying locations of all gp42 mutants based on classes identified from Table 2.2.

The classes are inconsequential, core/distant, HLA class II binding, or hydrophobic pocket. In each panel, the sites of the linker-insertions (LI) mutants are indicated in blue and the site-specific mutants are indicated in yellow. Abbreviations and color scheme follow those in previous figures.

Mutations in the transmembrane domain and amino-terminal domain located near the membrane-spanning domain are unaffected in HLA class II binding and fusion (Figure 2.5, upper-left). LI12, LI27, LI82, LI93, W44A and Q89A, all located within the amino-terminal domain of gp42, were unaffected in their ability to bind HLA class II and mediate fusion. These results are compatible with results from our structural studies of gp42 bound to HLA class II that indicate this region is not involved in the contact of gp42 with HLA class II. Interestingly, this region may be important for the dimerization of gp42, as observed in our previous structural studies, and the interaction of gp42 with the gH and gL complex. Previous studies have shown by deletion that a region in the first 58 amino acids of gp42 is critical for the interaction of gp42 with gH and gL (138). In addition, this gp42 deletion mutant was unable to complement a gp42-deficient recombinant virus, indicating that complex formation between gp42 and gH/gL is likely essential for EBV infectivity. None of the present mutants within this region of gp42, the HLA class II interface, or the hydrophobic pocket had any defect in the association of gp42 with gH/gL (data not shown) indicating that additional mutants should be isolated to determine the functional significance of the interaction of gp42 with gH/gL and its importance in fusion. Although gp42 was observed as dimers in the crystal structure, formation of gp42 dimers has not been detected by other analyses; thus specific mutants within the dimerization region of gp42 may directly test the functional significance of gp42 dimer formation.

Mutations that localize to neither the HLA class II binding site nor the hydrophobic pocket are unable to mediate fusion and binding (Figure 2.5, upper-right). Surprisingly, several mutants with linker insertions in regions that neither make contact with HLA class II nor are located in the hydrophobic pocket do not bind HLA class II HLA-DQ and are unable to mediate fusion. These include LI118, LI122, LI134, LI179, and LI216, although LI134 seems to allow

low levels of binding and fusion. Since each of the mutations is distant to the HLA class II binding site but blocks HLA class II binding, with the possible exception of LI134, it is likely that these mutants alter the overall structure of gp42. Compatible with this idea, many of these mutants fall within major structural features of gp42. LI118 and LI216 fall within two antiparallel β -sheets, for which the insertion of the 5-amino-acid linker would be expected to have dramatic structural consequences. LI134 is located at the base of one of two α -helices within the gp42 structure. Although not within the core, this mutation may also be expected to alter the gp42 conformation. Compatible with this, LI134 binds weakly to HLA class II and does not mediate fusion at wild-type levels.

The linker insertion site for the mutants LI122 and LI179 are contained within exterior loops that connect structural determinants of the gp42 core. Since both insertion sites are fairly distant from the HLA class II binding site and are not near cysteines forming gp42 disulfide bonds, these results may indicate that the overall gp42 structure is easily perturbed, as indicated by the inability to bind HLA class II, but still sufficiently folded to result in expression and secretion of gp42, as was observed with all of the mutants. The point mutant W125G would also appear to globally alter the gp42 structure, as demonstrated by lack of binding to HLA class II and fusion competence. The tryptophan residue mutated is within the core of gp42 and may act as a platform for the gp42 hydrophobic pocket to rest on. The dramatic substitution to a glycine residue, if the tryptophan does serve as a major structural determinant, may alter the stability of the protein. Consistent with this idea, of all of the mutations described in the present study, the W125G mutant exhibited both a decrease in cell surface expression and in the supernatant of transfected cells.

It was surprising that most of the mutations introduced did not drastically affect the expression levels of gp42. This is in stark contrast to HSV-1 gB, which contains five main domains and insertion of five amino acid residues in all of these domains can lead to loss of cell surface expression (83). Based on CELISA and Western blot analysis, gp42 appears to tolerate mutations quite well in comparison. However, subsequent characterization of newly generated gp42-specific mouse monoclonal antibodies revealed that all three antibodies recognized the gp42 Core/Distant mutants less than the other three classes of mutants, both in immunoprecipitations and CELISA (data not shown). This indicates that although these mutants are expressed well on the cell surface, the mutations in the core of the CTLD indeed perturb the overall structure of the protein, interfering with receptor binding and required conformational changes for membrane fusion.

Not all mutants localized to HLA class II binding domains disrupt gp42 function (Figure 2.5, lower-left). Y107A, E160A, and R220A mutants all lost their ability to bind HLA class II and are unable to mediate fusion, highlighting the requirement of gp42 binding to HLA class II in fusion. Surprisingly, low levels of fusion are consistently detected with the R220A, which does not detectably bind to HLA class II expressed on Daudi cells. One possible explanation is that perhaps the salt bridge is not as critical as the hydrogen bonds and some low-level binding may occur that is not readily apparent in the binding assay, allowing for some measurable fusion to occur. All of the linker insertion mutants that are within or close to HLA class II contact sites are unable to bind HLA class II and are also unable to mediate fusion (LI104, LI112, LI148, and LI149). A 5-amino-acid insert clearly eliminates all binding activity in this region. Although T104A and R154A localize to HLA class II binding sites, they are able to bind to HLA class II as well as mediate fusion. Previous structural studies of the gp42 HLA class II complex indicated

that the carbonyl oxygens from the main chains of T104 and Y107 of gp42 form hydrogen bonds with R β 72 of HLA class II (95). Mutational analysis of R β 72 of HLA class II indicated that this residue is essential for gp42 binding to HLA class II and EBV entry (89). The T104A mutation, which would be predicted not to disrupt the hydrogen bond between T104 and R β 72, has no effect on gp42 binding to HLA class II or EBV-induced membrane fusion, as might be expected. However, mutation of Y107 blocks both, probably due to multiple effects by potentially changing the local conformation of the region that binds HLA class II as well as blocking a hydrogen bond with E β 46. In regard to the mutation of R154 of gp42, previous mutational studies of HLA class II S β 63, which hydrogen bonds with gp42 R154, indicated that this interaction of R154 with S β 63 is not important for gp42 binding to HLA class II or EBV entry since mutation of S β 63 to either an alanine or lysine did not block gp42 binding to HLA class II or EBV entry (89). This result is further supported by the present results indicating that R154 of gp42 is not important for gp42 binding to HLA class II or EBV-mediated fusion.

Though gp42 is structurally similar to some other C-type lectin superfamily members, the gp42/HLA class II interaction is unique compared to other natural killer (NK) receptor complexes, namely, Ly49A/MHC class I and NKG2D/MHC class I homolog (MICA) (95). The interaction is also different from the HSV gD/HveA binding complex. McShane *et al.* clearly showed that a single residue mutation of HLA-DQ could ablate sgp42 binding and EBV infection, whereas single mutations of HveA did not affect HSV entry, suggesting that most of those contact residues contribute to receptor function collectively rather than individually (28, 89).

Many mutations that localize to the hydrophobic pocket are unaffected in HLA class II binding but do not mediate fusion (Figure 2.5, lower-right). LI193, LI206, LI210, Y185F and

F210A are all able to bind to class II-expressing cells. However, of these, only Y185F is able to efficiently mediate fusion similar to wild type. In the hydrophobic pocket, it is interesting to see that a single point mutant can distinguish HLA class II binding from the ability to mediate membrane fusion. It is perhaps not surprising that the relatively conservative substitution of tyrosine to phenylalanine at amino acid 185 does not alter fusion activity. In contrast, the more drastic change of phenylalanine to alanine at amino acid 210 does disrupt fusion significantly. It is likely, as with the case of HLA class II binding, that some of these hydrophobic residues are more critical than others for generating a strong interaction with a potential unknown binding partner. Interestingly, all of the linker insertion mutants within the gp42 hydrophobic pocket have greatly reduced fusion when compared to wild type, LI210 clearly being positive for fusion but at reduced levels, whereas LI193 and LI206 having fusion consistently above background but not nearly as high as LI210. Of the linker insertions, only LI195 appears to be entirely negative for fusion. Importantly, the site of this insertion is close to the α -helix HLA class II binding site, resulting in a mutant gp42 that is unable to bind HLA class II. This may be the primary defect in this mutant and not due to the gp42 hydrophobic pocket. It is likely that proximity of the mutation to the HLA class II binding site coupled with the insertion of five amino acids disrupts the HLA class II binding function of gp42 in the LI195 mutant. Therefore, this mutant has been classified as a core/distant mutant, as it does not show the hydrophobic pocket mutant phenotype, that is, the ability to bind HLA class II but not mediate fusion.

The mutants described in this report have helped to define functional domains required for fusion. We have demonstrated that, in addition to a functional gp42/HLA class II binding site, a structurally intact hydrophobic pocket is required to initiate membrane fusion. The discovery of this hydrophobic pocket is interesting for two reasons: the functional requirement

(i) adds to our current model of EBV-induced membrane fusion and (ii) provides a potential target for antiviral strategies. Like the HSV gD/HveA interface, only a handful of the EBV gp42/HLA class II contact residues that comprise the interface are actually required for binding (27). Structural studies of gD by Carfi *et al.* suggested that the N-terminal gD hairpin was conformationally flexible and that a conformational change accompanying binding might be part of the viral entry mechanism (20). Although structurally distinct from gD, gp42 could have a similar functional mechanism and such a conformational change might also be required for membrane fusion. Binding of HLA class II might induce a conformational change that reveals the hydrophobic pocket, which is then able to bind its viral or cellular ligand. If the pocket is occupied before binding to HLA class II, the structure could reposition the viral ligand to come in contact with the host membrane. The functional requirement of the hydrophobic pocket makes it an excellent target for antiviral inhibitors. Modis *et al.* discovered a ligand-binding hydrophobic pocket in the dengue virus envelope glycoprotein E that is briefly exposed as fusion-competent trimers form, implicating a multi-conformational mechanism of membrane fusion (92). This hydrophobic pocket was discovered to bind a single molecule of the detergent *n*-octyl- β -D-glucoside, indicating a potential site for small-molecule inhibitors. The hydrophobic pocket of the human immunodeficiency virus gp120/41 trimer has already proven fruitful in identifying both synthetic peptides and screening small-molecules to inhibit binding and fusion (32, 36). Such results are encouraging for future studies of potential inhibitors of gp42-mediated membrane fusion. The mutants generated from these experiments will be used to supplement our knowledge of binding requirements with the gH/gL complex and with gB if there is a direct interaction. We will next use these mutants to identify the ligand of this hydrophobic pocket,

which could be viral or cellular, which would further characterize requirements and mechanisms involved with initiating membrane fusion and provide a target to block viral entry.

**CHAPTER THREE—BINDING-SITE INTERACTIONS BETWEEN EPSTEIN-BARR
VIRUS FUSION PROTEINS GP42 AND GH/GL REVEAL A PEPTIDE THAT INHIBITS
BOTH EPITHELIAL AND B-CELL MEMBRANE FUSION**

INTRODUCTION

The interaction of EBV gp42 with gH/gL allows for membrane fusion and infection of B cells, but inhibits fusion and infection of epithelial cells (13, 47, 82, 88, 138). It has been demonstrated that the heterodimeric complex of gH/gL binds gp42 in a 1:1:1 ratio, and that gH binds gp42 somewhere between residues 58 and 86 of the gp42 amino-terminus (70, 95, 101, 138, 147). Linker-insertion and point mutants of the gp42 amino-terminus did not affect binding HLA class II receptor binding and had at most a modest effect on membrane fusion with B cells (121). In order to precisely define the gH/gL binding site of the gp42, several five residue deletion mutants were created along with double deletion mutants and one mutant deleted of a large portion of the amino-terminus.

The characterization of the gH/gL binding site on gp42 has revealed some surprising results. The mutants were screened for the ability to mediate fusion with B cells in addition to being tested for their ability to bind both transfected gH/gL by co-immunoprecipitation and soluble gH/gL by CELISA. Based on the results, several peptides were designed, two of which showed inhibition of both epithelial and B cell fusion. Determining the binding kinetics demonstrated that a 46-mer peptide bound gH/gL at the same concentrations as soluble gp42. A shorter 30-mer peptide was also able to inhibit, but at much higher concentrations. Shorter peptides were unable to inhibit epithelial cell fusion alone, nor could they complement B-cell fusion when used in combination. Greater inhibition of epithelial cell fusion was seen when using the 30-mer peptide with another peptide (67-81), but not as high as the 46-mer. That data indicated that there are two separate domains involved in gH/gL binding. There are also regions adjacent to these two domains that are not involved in gH/gL binding but required for fusion. The amino-terminal end of the first domain is near a putative cleavage site and hints at the

requirement of soluble gp42 for fusion, while the carboxyl-terminal end of the second domain indicates that either a linker-domain or possibly dimerization is required.

MATERIALS AND METHODS

Cells and proteins. High Five insect cells (BTI-TN-5B1-4; Invitrogen) were grown in shaker flasks in Excell-405 medium (JRH Biosciences). Sf9 insect cells (Invitrogen) were grown in shaker flasks in Sf900 medium (Gibco).

All media for mammalian cell growth were made complete by supplementing with 10% FetalPlex animal serum complex (Gemini Bio-Products) and 1% penicillin-streptomycin (BioWhittaker), and all mammalian cells were grown in 75-cm² cell culture flasks (Corning). Mammalian epithelial cells were human embryonic kidney 293 cells that express simian virus 40 large T antigen (293T; ATCC, Manassas, VA) and modified to stably express T7 RNA polymerase under selection of 100 µg/ml zeocin in complete Dulbecco's modified Eagle medium (BioWhittaker), which is known as line 14, as described previously (100). Mammalian B cells were Daudi B lymphocytes that are EBV positive and express HLA class II and CD21 (ATCC) and that are modified to stably express T7 RNA polymerase under selection of G418 (700 to 900 µg/ml) in complete RPMI 1640 medium (BioWhittaker) (121). Chinese hamster ovary cells (CHO-K1) were kindly provided by Nanette Susmarski and were grown in complete Ham's F-12 medium (BioWhittaker). Versene (1 mM EDTA in phosphate-buffered saline [PBS]) or trypsin-versene (BioWhittaker) was used to detach adherent cells.

Monoclonal antibodies E1D1 (anti-gH/gL) and F-2-1 (anti-gp42) were gifts generously provided by L. Hutt-Fletcher (Louisiana State University Health Sciences Center, Shreveport, LA) (7, 128). Monoclonal antibody 3H3 (anti-gp42) was obtained as previously described (70). Polyclonal anti-gp42 antibody serum PB1114 was used as previously described (89). Milligram quantities of antibodies were produced by the Northwestern Monoclonal Antibody Facility and the National Cell Culture Center. For cell enzyme-linked immunosorbent assay (CELISA)

experiments with soluble gH/gL, monoclonal antibodies 3H3 and E1D1 were purified by a HiTrap protein G agarose column (Amersham Biosciences), eluted with 0.2 M glycine-HCl, pH 2.5, immediately neutralized to pH ~7 by adding 1/10 volume of 1 M Tris, pH 9.0. Purity was >95% as demonstrated by sodium dodecyl sulfate (SDS)-polyacrylamide gel electrophoresis. Purified antibodies were exchanged into PBS, and concentration was determined by absorbance at 280 nm using a theoretical extinction coefficient (0.1%) of 1.4 for immunoglobulin G (IgG).

Soluble EBV gp42 and soluble EBV gH/gL were produced and purified as described elsewhere (70). Briefly, gp42 and gH/gL proteins were obtained using the baculovirus expression system in High Five and Sf9 insect cells, respectively. Soluble gp42 was purified by cobalt metal affinity chromatography, and soluble gH/gL was purified by affinity purification using monoclonal anti-gH/gL antibody E1D1. Gel filtration using a Superdex-200 HR 10/30 analytical column (Amersham Biosciences) provided the final purification in running buffers consisting of PBS or 25 mM Tris (pH 7.4)-150 mM NaCl (TBS).

Peptides. Synthetic peptides were obtained commercially (EZBiolab) at 95% purity, as determined by high-performance liquid chromatography and mass spectrometry, and used without further purification. Lyophilized peptides were reconstituted in TBS or PBS. Peptide concentration was measured by absorbance at 280 nm using the theoretical 0.1% value. For peptide labeled with fluorescein isothiocyanate (FITC), the absorbance maximum at 495 nm for FITC was additionally used to confirm peptide concentration. Peptide 36-81 is N-terminally labeled with FITC and corresponds to gp42 residues 36 to 81 (RVAAAAITWVPKPNVEVWPVDP PPPVNFNKTAEQEYGDKEVKLPHW). Peptide 36-65 corresponds to gp42 residues 36 to 65 (RVAAAAITWVPKPNVEVWPVDP PPPVNFNK) (70). Peptide 36-56 corresponds to gp42 residues 36 to 56 (RVAAAAITWVPKPNVEVWPVD).

Peptide 42-56 corresponds to gp42 residues 42 to 56 (ITWVPKPNVEVWPVD). Peptide 67-81 corresponds to gp42 residues 67 to 81 (AEQEYGDKEVKLPHW).

Mutants. Mutants were generated using a double-arm PCR approach. Mutant primers were generated to incorporate either five-residue deletions or single-residue changes as well as silent restriction enzyme cutting sites. The first PCR used primers matched to flank the EBV gp42 gene in the pCAGGS.mcs vector (5' primer p-1, TCCTGGGCAACGTGCTGGTTGTTG; 3' primer p-2, GCCAGAAGTCAGATGCTCAAGGGG) paired with their complementary directional mutant primer on a wild-type EBV gp42 plasmid template. The PCR Tails program was used as follows: (i) 94°C for 2 min, (ii) 94°C for 15 s, (iii) 58°C for 1 min, (iv) 72°C for 90 s (40 cycles of steps ii to iv), (v) 72°C for 15 min, and (vi) 4°C for an unlimited period. PCR products were confirmed by gel electrophoresis and then used as templates with the flanking primers in the second PCR to generate full-length mutant gp42, which was confirmed by gel electrophoresis, cut with EcoR1 and BglII, and ligated overnight at 16°C with vector that had been digested under the same conditions. Ligated products were transformed and selected on ampicillin plates. Colonies were picked and grown overnight to generate mini-preparations, which were double digested to confirm the introduction of the mutation. Mini-preparations were sequenced, and positive clones were then grown in large quantities and isolated in cesium chloride density gradients by ultracentrifugation and sequenced again. Double mutants were generated similarly except mutant gp42 plasmids were used for the first PCR template. The first deletion mutant was used as a template with a different pair of mutant primers to generate the second deletion; e.g., d37-41/67-71 (where d37-41 is a deletion mutant lacking gp42 residues 37 to 41) was created using d37-41 plasmid template with d67-71 mutant primers for the first PCR. Two mutants studied had incorporated inconsequential extra point mutations: mutant K47A gained P48S and

d67-71 gained T13I. These mutations were detected after sequencing of CsCl preparations, so new mutants were generated and confirmed to lack any incidental mutations introduced by PCR. Table 3.1 identifies mutants used in this study. Mutant W44A was generated as previously described (121).

Transfection. CHO-K1 cells were transfected in Opti-MEM I medium (Gibco) by a uniform protocol using Lipofectamine 2000 (Invitrogen) as previously described (121). Cells were plated in a six-well format, and after 24 h each well received 5 μ l of Lipofectamine 2000, and various combinations of pCAGGS expression vector containing the gene of interest were used in the following amounts: 0.5 μ g for gH, 0.5 μ g for gL, 0.8 μ g for gB, 0.8 μ g for luciferase, and 1.7 μ g for the pCAGGS vector control (47, 99). In the case of gp42-transfected CHO cells, pCAGGS vector control plasmid was replaced by 1.7 μ g of gp42 vector. For fusion assays (see Figure 3.1), amounts of DNA were changed to 0.5 μ g for gB, 2.0 μ g of wild-type or mutant gp42, and 1.0 μ g each of pCAGGS and enhanced green fluorescent protein (GFP) to allow for negative control and visual confirmation of transfection. For immunoprecipitations, gB and luciferase plasmids were excluded, and 1.0 μ g of gH and gL was transfected with 2.0 μ g of wild-type or mutant gp42. For negative control and visualization, 2.0 μ g each of pCAGGS and enhanced GFP was included with no other glycoprotein.

Fusion assay. CHO-K1 cells were transiently transfected as described above. At 12 h posttransfection, the cells were detached by versene, counted either by hand with a hemocytometer or using a Beckman Coulter Z1 particle counter, and 2.0×10^5 to 2.5×10^5 cells/well in 0.5 ml were transferred to a 24-well format, incubated for about 10 min after the addition of peptide and/or soluble proteins (in TBS or PBS without azide), and subsequently overlaid with 0.5 ml of target cells, either Daudi B cells or 293T epithelial cells. For

simultaneous surface expression readings by CELISA, 4.0×10^4 to 5.0×10^4 CHO cells were also plated in 96-well plates (described below). To induce fusion, equal or greater numbers of Daudi or 293T cells were overlaid on CHO cells, and total volume was 1 ml or more per well. Both of the target cell types, Daudi and 293T, used in the fusion assay stably expressed T7 RNA polymerase and were under selection by G418 and zeocin, respectively (100, 140). After a 24-h overlay, cells were washed with PBS and lysed with 100 μ l of passive lysis buffer (Promega) per well. Luciferase activity was quantified by transferring triplicate 20- μ l aliquots of lysed cells to 96-well opaque plates with clear bottoms (Wallac), and luminescence was measured on a Perkin-Elmer Victor plate reader immediately after adding 100 μ l of luciferase assay reagent (Promega).

CELISA. For testing gp42 mutant binding to soluble gH/gL, 1.7 μ g of gp42 (wild type or mutant) DNA was added with 5 μ l of Lipofectamine 2000 per well in the six-well format. After 12 h posttransfection, CHO cells were replated in the 96-well format. After a 24-h incubation, the medium was removed, cells were washed with PBS-ABC (PBS with 0.89 g of CaCl_2 and 0.89 g of $\text{MgCl}_2 \cdot \text{H}_2\text{O}$ per 8 liters), and soluble gH/gL was added in PBS-ABC with 3% bovine serum albumin (BSA) (Sigma). After a 30-min incubation, cells were washed, and primary antibody at a 50 nM final concentration was added in PBS-ABC with 3% BSA. Cells were fixed for 10 min in PBS with 2% formaldehyde and 0.2% glutaraldehyde and then blocked with 3% BSA in PBS-ABC. Biotinylated anti-mouse-IgG at 1:500 was added as the secondary antibody, followed by streptavidin-horseradish peroxidase at 1:20,000. TMB (3,3',5,5'-tetramethylbenzidine; Sigma) substrate was added, and quantitative colorimetric measurement was performed at 370 nm using a Victor plate reader, typically achieving a high signal over background measurement by 30 to 60 min. Background measurements were obtained from negative control wells that omitted the transfected glycoprotein expression plasmid and/or

omitted primary antibody. Surface expression of transfected gp42 was measured using 50 nM 3H3 antibody, and binding of soluble gH/gL to transfected gp42 was measured using 50 nM E1D1 antibody. Percent soluble gH/gL binding to gp42 was determined by dividing the background-subtracted binding of soluble gH/gL by the background-subtracted surface expression for each gp42 mutant. The wild-type gp42 sample binding to soluble gH/gL was then set to 100%, and gp42 mutants were normalized to that value. For measurement of cell surface expression simultaneous with fusion assays, CHO cells transfected for fusion were also plated in the 96-well format 12 h posttransfection, and CELISA was performed 24 h later. The primary antibody was F-2-1 hybridoma supernatant used at a dilution of 1:150.

Immunoprecipitation. CHO cells were transfected with plasmids encoding EBV gH, gL, and either wild-type or mutant gp42. Opti-MEM medium was removed 12 h posttransfection and replaced with complete Ham's F-12 medium. After 24 h of incubation, cells were detached with versene, counted, washed twice in PBS, and lysed as previously described (121). Equal volumes of lysates were either added to 5X sample buffer or incubated with no antibody, anti-gH/gL E1D1 monoclonal antibody, or anti-gp42 F-2-1 monoclonal antibody and rotated at 4°C for at least 1 h. Agarose beads cross-linked to protein G (Amersham Biosciences) were incubated with lysates at 4°C for at least 1 h and used to pull down IgG complexes by centrifugation. Samples were washed at least three times with complete lysis buffer, and 100 µl of 2X SDS sample buffer was added. Samples of whole-cell lysate and immunoprecipitate were run on 12.5% or 10% Criterion Tris-HCl gels (Bio-Rad) at 120 V for 110 min, followed by transfer at 90 V for 90 min to Immobilon-P transfer membranes (Millipore). Western blotting immunodetection of gp42 was carried out using anti-gp42 antibody serum PB1114 as previously described (121). All the gp42 mutants with the exception of the d45-89 mutant were readily detected by Western blotting. The

absence of the detection of the d45-89 mutant may be a result of the extensive deletion compared to the other mutants.

Fluorescence polarization. A Beacon 2000 instrument (Invitrogen) was used to measure the fluorescence polarization signal that occurs when FITC-labeled gp42-derived peptide binds to soluble gH/gL. Samples were made in parallel in 100- μ l volumes using 10-fold serial dilutions of protein and peptides, with subdivisions in between. To reduce nonspecific interactions and reduce protein losses at low concentrations, samples contained 0.1% Tween-20 detergent. To reduce pipetting errors, parallel samples were mixed in individual tubes (Kimble Glass) and prepared identically using the same volumes for each dilution. Samples were allowed to incubate at room temperature for at least 20 min before measurement. For competition assays, the two competitors were mixed together (FITC-labeled peptide and competitor protein or peptide), and then soluble gH/gL was added last. Data were collected at 25°C.

Cell-free virus infection assay. GFP-positive EBV was produced by Akata cells (a gift from L. Hutt-Fletcher), as previously described (62, 94, 131). Briefly, Akata cells were grown in RPMI 1640 medium (BioWhittaker) with 10% fetal bovine serum (HyClone), 1% penicillin-streptomycin, and 500 μ g/ml neomycin (Gemini Bio-Products). At a high cell concentration, 4×10^7 cells were induced with 50 μ g/ml anti-human Ig (MP Biomedicals) for 5 days. After the cells were removed, 100 μ g/ml bacitracin (Sigma Aldrich) was added, and virus was pelleted by centrifugation at 16,000 X g at 4°C for 90 min. Virus was resuspended in 1 ml of RPMI medium containing bacitracin and passed through a 0.8- μ m-pore-size filter.

Virus aliquots were preincubated for 24 h at 37°C under conditions for testing viral inhibition, during which time human embryonic kidney 293 epithelial cells were plated in the 96-well format nearly at confluence. The infection assay was performed using 50 μ l of cell-free

virus per well that was centrifuged at 2,500 rpm for 1 h at 33°C. Subsequently, virus was removed by aspiration, cells were washed with 200 µl of RPMI complete medium, and cells were left with 200 µl of fresh RPMI complete medium to incubate for 72 h. Infected cells could be observed producing GFP after 24 h. Fluorescence-activated cell sorting (FACS) with a BD LSR II 488-nm laser was used to quantify GFP-expressing cells at 72 h postinfection. The percentage of infected cells was measured by collecting 30,000 total events and gating on the live cell population.

Table 3.1. Activity summary of gp42 deletion mutants.^a

Category and mutant ^b	Surface Expression	Fusion	gH/gL binding	
			Immunoprecipitation	CELISA
Category 1				
R30A	+	+	Y	ND
R32A	+	+	Y	ND
R36A	+	+	Y	ND
W44A	+	+	Y	ND
K47A	+	+	Y	ND
K47A/P48S	+	+	Y	ND
E51A	+	+	Y	ND
d32-36	+	+	Y	+
d57-61 ^c	+	+	Y	-
d62-66	+	+	Y	+
Category 2				
NT1				
d37-41	+	-	Y	+
d42-46	+	-	Y	+
NT2				
d82-86	+	-	Y	+
d87-91	+	-	Y	+
d92-96	+	-	Y	+
Category 3				
NT1				
d47-51	+	-	Y	+/-
d52-56	+	-	Y	-
NT2				
d67-71	+	+/-	Y	-
d72-76	+	-	Y	-
d77-81	+	-	Y	+/-
NT1 & NT2				
d45-89	+	-	ND	-
d37-41/d67-71	+	-	Y	-
d42-46/d72-76	+	-	N	-
d47-51/d77-81	+	-	N	ND
d52-56/d77-81	+	-	ND	ND
d77-81/d47-51	+	-	ND	-

^aActivity is defined as 100% wild-type to 50% (+), between 50% and 25% (+/-), or less than 25% (-). ND; not done; Y, observed by immunoprecipitation with Western blotting; N, greatly reduced or not observed by immunoprecipitation with Western blotting.

^bCategory 1, functional; category 2, fusion impaired, not due to gH/gL binding; category 3, fusion impaired due to altered gH/gL binding.

^c Mutant d57-61 exhibits near wild-type fusion but reduced interactions with soluble gH/gL.

RESULTS

Mutants of the gp42 N-terminal region. Mutants of gp42 were engineered to span the N-terminal region from residues 30 to 96 (Figure 3.1A). Initially, six point mutants were made to substitute alanine for charged residues or tryptophan (Figure 3.1A, bold amino acids). Since none of these mutants dramatically altered fusion, a more systematic approach was employed to remove five contiguous residues throughout the N-terminal region from amino acids 32 to 96 (Figure 3.1A). Cell surface expression of gp42 mutants was similar to wild-type gp42 in transfected CHO cells as shown by CELISA (Figure 3.1B, black diamonds). The mutants were tested for their ability to mediate membrane fusion using CHO cells transfected with gH, gL, gB, and mutant or wild-type gp42 and overlaid with B cells. Mutants with five-residue deletions between residues 37 to 56 or 72 to 96 showed significantly reduced membrane fusion activity, less than 25% of wild type (Figure 3.1B, bar graph). In contrast, deletion of residues 57 to 61 or 62 to 66 showed only moderate reduction in membrane fusion activity to ~50% of wild-type gp42. Mutant d67-71 averaged between 25% and 50% of wild-type fusion. These data suggest that there are two functional regions within the gp42 N terminus that we designate N-terminal region 1 (NT1) for residues 37 to 56 and N-terminal region 2 (NT2) for residues 67 to 96.

Figure 3.1. Schematic of gp42 mutants, fusion assay, and CELISA data. (A) Map of EBV gp42 amino-terminal ectodomain residues 30 to 100 depicting mutant constructs of either five-residue and longer deletions or single-residue substitutions. Individual residues that were mutated to alanine are shown in bold. Italics highlight predicted glycosylation sites. Putative cleavage and crystal (Xtal) dimerization sites are indicated by dotted lines from above. Soluble gp42 starts at residue 33 and is indicated by an angled arrow. Important functional domains designated NT1 and NT2 are represented by double arrows, and peptides derived from gp42 are shown below. The core binding residues based on concordance between activity in fusion and binding soluble gH/gL in CELISA are below black boxes. Gray lines depict the peptides used in this study. (B) Relative luciferase activity measured in a cell-cell fusion assay using CHO cells transfected with gH, gL, gB, and wild-type or mutant gp42 and overlaid with B cells (bar graph). Surface expression of gp42 is measured by CELISA using monoclonal F-2-1 antibody, secondary biotinylated-anti-mouse-IgG antibody, tertiary streptavidin-horseradish peroxidase, and TMB substrate (black diamonds). Line indicates 100% of wild-type gp42. Color development was measured by absorbance at 370nm. Data shown are averages of at least three independent experiments with wild-type gp42 luciferase activity and expression set at 100%, and standard deviations are represented by the error bars.

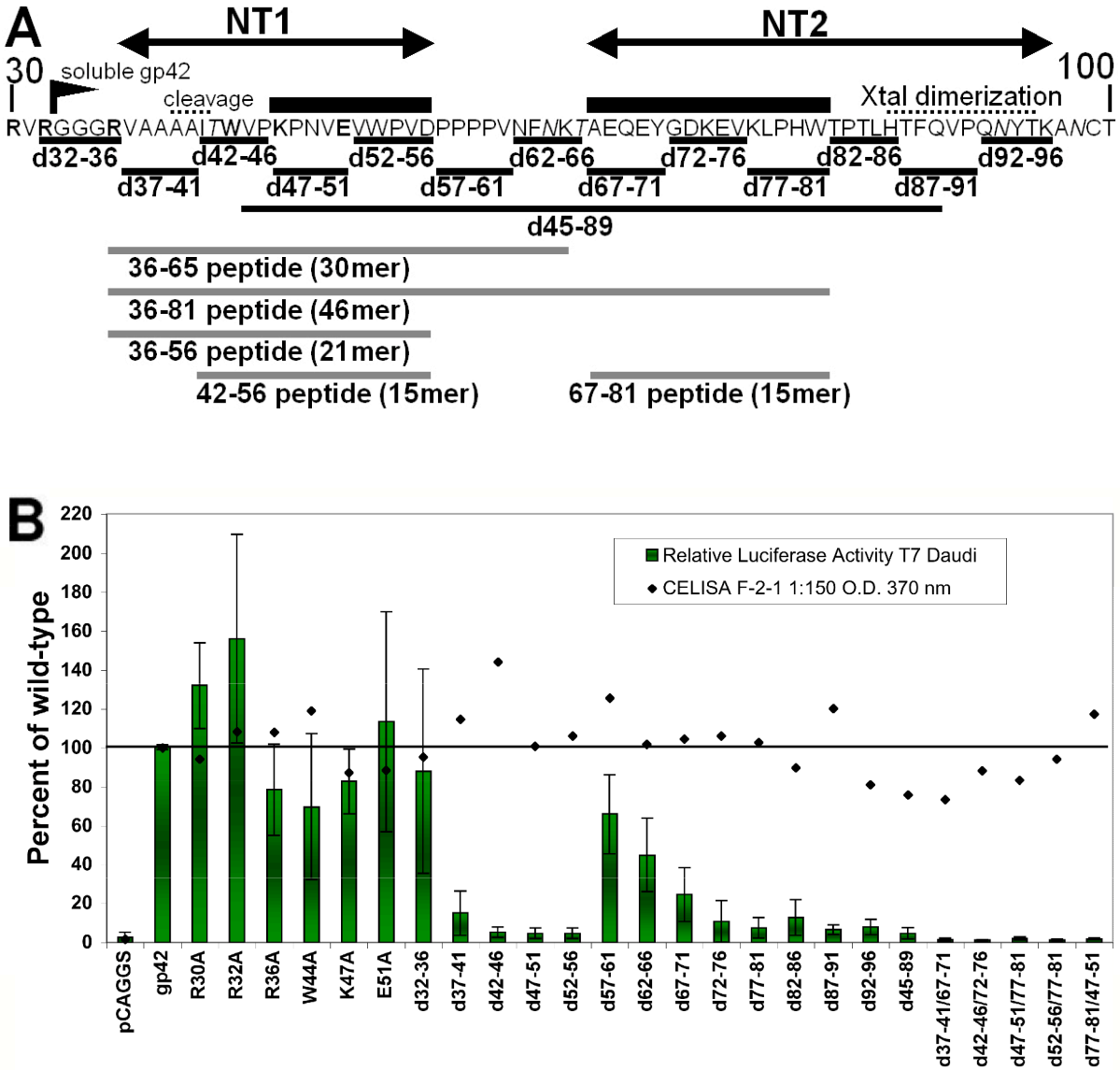


Figure 3.1. Schematic of gp42 mutants, fusion assay, and CELISA data

Representative Western blotting of lysates immunoprecipitated with anti-gp42 mouse monoclonal antibody demonstrated that the expression and size of mutant gp42 protein are nearly the same as wild-type gp42, except for d62-66 and d92-96, where two and one, respectively, potential glycosylation sites were removed (Figure 3.2B and data not shown). Loss of the glycosylation sites did not affect the ability of the d62-66 mutant to trigger fusion, although the d92-96 mutant was unable to mediate fusion (Figure 3.1B). This may indicate that glycosylation, at least at the second site, may be important for gp42 function. This would be in contrast to HSV-1 gD in which glycosylation is not essential for function (122). The observation with the d92-96 mutant may also indicate another role of this region in gp42 function such as dimerization, which was observed in the crystal structure (95). Immunoprecipitation with anti-gH/gL E1D1 antibody followed by Western blotting for gp42 was performed to monitor gH/gL binding with gp42 (Figure 3.2A to C). Surprisingly, none of the deletion mutants with the exception of d45-89 was deficient in gH/gL binding as assessed by immunoprecipitation (representative data in Figure 3.2A to C and summarized in Table 3.1). The d45-89 mutant is not readily detected by Western blotting even though surface expression was confirmed by CELISA (Figure 3.1B).

Figure 3.2. Binding of gp42 mutants with transfected gH/gL in coimmunoprecipitations and soluble gH/gL in CELISA. (A to C) SDS-polyacrylamide gel electrophoresis and Western blotting of wild-type and mutant gp42 expressed in CHO cells, using rabbit polyclonal PB1114 anti-gp42 antibody at 1:1,000 for detection, reveal gp42 levels in immunoprecipitations using either F-2-1 anti-gp42 antibody or E1D1 anti-gH/gL antibody as labeled. Samples are from the same transfection and were simultaneously run in non-adjacent lanes. (D) CELISA-based quantitative measurements of soluble gH/gL binding to transfected gp42. CELISA experiments were performed in collaboration with Austin Kirschner. Detection of bound gH/gL is carried out with E1D1 anti-gH/gL antibody, as in the CELISA described in the legend of Figure 3.1B. Data shown are a representative example of three or more independent experiments, and error bars represent standard deviations across triplicate measurements within an experiment. Data for all mutants are summarized in Table 3.1.

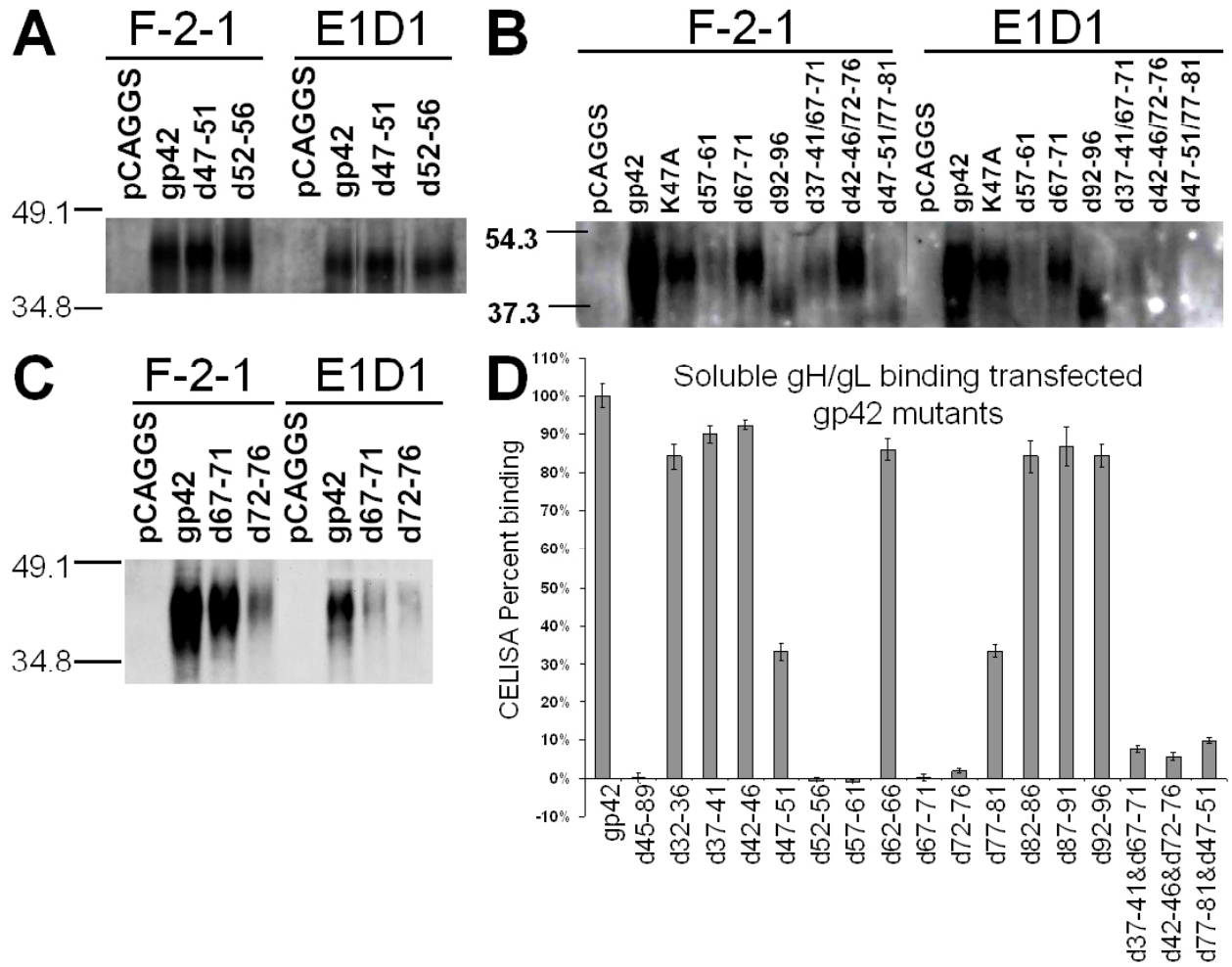


Figure 3.2. Binding of gp42 mutants with transfected gH/gL in coimmunoprecipitations and soluble gH/gL in CELISA

As an alternative approach to further understand gp42 domains required for interaction with gH/gL, more quantitative analysis was performed using CELISA experiments with 50 nM soluble gH/gL to determine gp42 mutants that retain near wild-type binding, bind at a reduced level, and completely lose binding function (Figure 3.2D). These experiments were performed in collaboration with Austin Kirschner. Interestingly, these results did not entirely agree with the immunoprecipitation data (Figure 3.2 and summarized in Table 3.1). Whereas all of the single five-residue deletions in either NT1 or NT2 were able to bind to gH/gL in immunoprecipitation, one deletion mutant in NT1 and two deletions in NT2 were completely deficient in binding soluble gH/gL, while one in each category showed approximately half of wild-type binding. These results appeared to more quantitatively characterize gH/gL binding, demonstrating that some mutants at the beginning of NT1 and the end of NT2 were deficient for fusion but were still able to bind soluble gH/gL (Figure 3.2D and Table 3.1). Most surprising was the d57-61 mutant that bound gH/gL in immunoprecipitation but did not appear to bind gH/gL in CELISA. Double deletion gp42 mutants were constructed to completely disrupt gH/gL binding since the immunoprecipitation results with the single deletion mutants suggested that both NT1 and NT2 are important for gp42 binding to gH/gL. Many of the double deletion mutants were similar to d45-89 in that although they appeared to express well on the surface of transfected cells, they were unable to mediate membrane fusion (even lower than single deletion mutants), and some were difficult to detect in Western blots (Figure 3.1A and 3.2B). However, d42-46/72-76 was easily detected by Western blotting, and binding to gH/gL was greatly reduced (Figure 3.2B). Although d37-41/67-71 was not detected well by Western blotting, gp42 levels in F-2-1 and E1D1 immunoprecipitation were often nearly similar, implying that there was more gH/gL

binding than in other double mutants (Figure 3.2B and data not shown). However, soluble gH/gL binding to these double mutants showed little to no binding (Figure 3.2D).

Peptide from gp42 residues 36 to 81 binds to soluble gH/gL with strong affinity. The gp42 mutants investigated here demonstrate that much of the N-terminal region of gp42 is critical for membrane fusion and interactions with gH/gL. We have previously demonstrated that a peptide corresponding to residues 36 to 65 binds to gH/gL with micromolar affinity, but this peptide appears to cover only one of the two N-terminal regions important for gH/gL binding (70). In particular the gH/gL CELISA data indicate that residues between 67 and 81, but not 82 and 96, are important for gH/gL binding (Figure 3.2D). A FITC-labeled peptide containing residues 36 to 81 was therefore synthesized by Austin Kirschner to determine in fluorescence polarization experiments the strength of binding to soluble gH/gL. This peptide was found to bind with low nanomolar affinity, with 50% binding calculated to be 5.1 nM by a nonlinear least squares fit (Figure 3.3A). Compared to the gp42 peptide consisting of residues 36 to 65, which binds with a low micromolar K_d , the longer 46-mer peptide gains about 500-fold affinity by extending the 30-mer by 16 C-terminal amino acids to residue 81 (70). These binding data are consistent with the gp42 five-residue deletion mutants, demonstrating that mutants lacking residues between 72 and 81 were noticeably impaired in their ability to bind soluble gH/gL (Figure 3.2D). Key interaction residues exist in the N-terminal region from residues 36 to 65 (based on activity of the peptide 36-65) and in the extended region from residues 66 and 81. These interaction regions were further investigated by studying shorter peptides.

Figure 3.3. Equilibrium binding of gp42 peptides to soluble gH/gL measured by fluorescence polarization. (A) Binding between soluble gH/gL and FITC-labeled gp42-peptide 36-81 shows increased fluorescence polarization signal as the concentration of soluble gH/gL is increased. The concentration of peptide was kept constant at 10 nM, and 50% of binding occurs at 5.1 ± 1.1 nM gH/gL. (B to D) Fluorescence polarization measurements using constant 10 nM concentrations of soluble gH/gL and 10 nM FITC-labeled gp42-peptide 36-81 with added competitor (100% corresponds to no competitor): soluble gp42 protein, EC_{50} at 8.5 ± 1.0 nM (B); peptide 36-65, EC_{50} at 1.5 μ M (C); peptides 36-56, 42-56, and 67-81, the extrapolated theoretical EC_{50} for 42-56 is 150 μ M (D). Competitor was premixed with labeled peptide 36-81, and soluble gH/gL was added to initiate binding. The experiments in this figure were performed by Austin Kirschner.

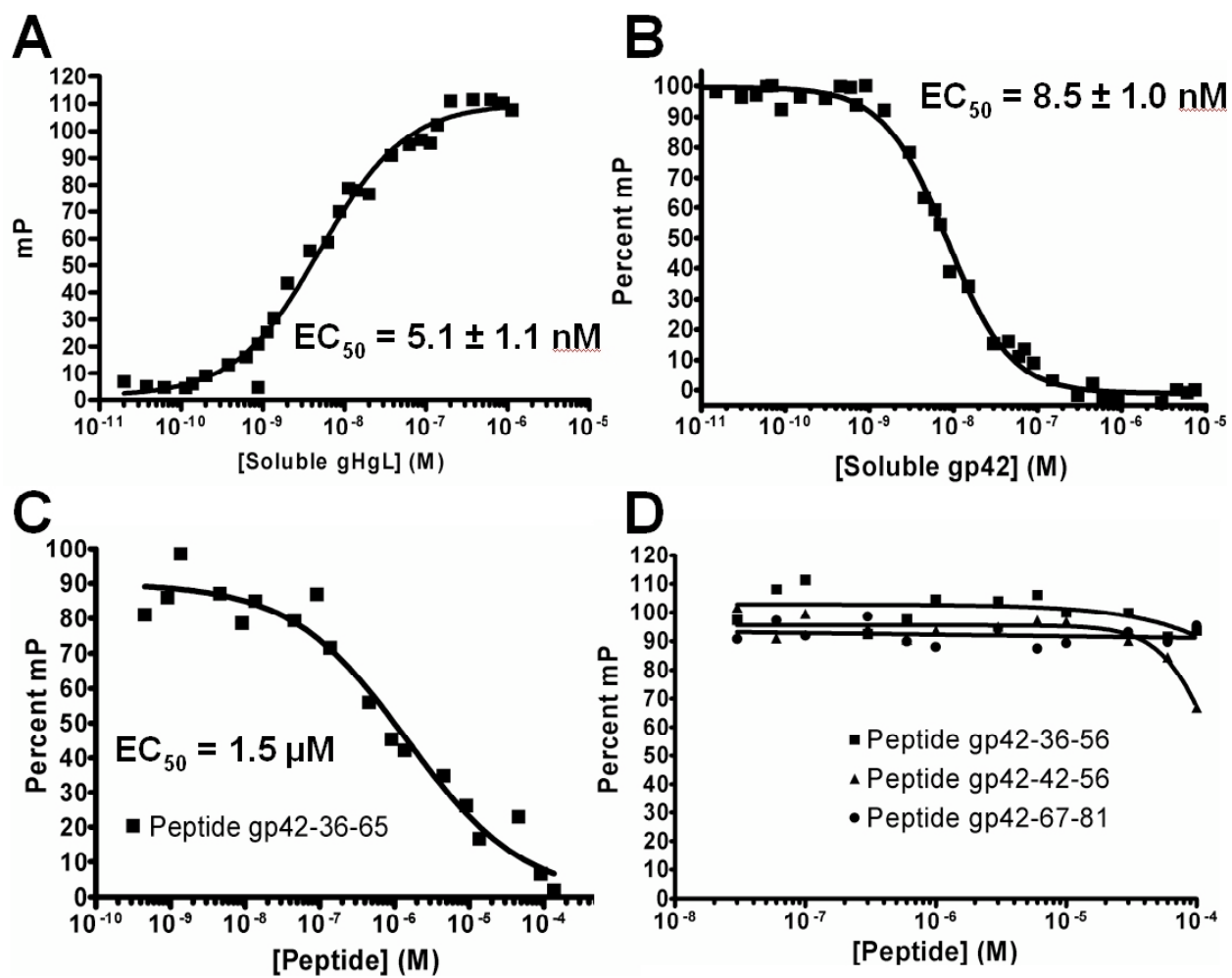


Figure 3.3. Equilibrium binding of gp42 peptides to soluble gH/gL measured by fluorescence polarization

Fluorescence polarization experiments with soluble gp42, an N-terminally truncated form of gp42 beginning at residue 86, and short gp42-derived peptides 36-65, 36-56, 42-56, and 67-81. In order to further map the gp42 regions involved in binding to gH/gL, competition fluorescence polarization experiments were performed by Austin Kirschner using 10 nM soluble gH/gL and 10 nM FITC-labeled gp42-peptide 36-81 with the addition of a competitor gp42 protein (Figure 3.3B). Following the competitive reduction of the peptide polarization signal, titrations of soluble gp42 demonstrated a binding affinity for gH/gL that is very similar to that of the FITC-labeled 46-mer peptide. A nonlinear least squares fit calculated 50% inhibition of binding to be at 8.5 nM soluble gp42. Addition of peptides 36-65, 36-56, 42-56, and 67-81 revealed their relative abilities to compete with peptide 36-81 for binding to gH/gL (Figure 3.3C and 3.3D). Only peptides 36-65 and 42-56 were able to diminish the polarization signal, albeit at significantly higher concentrations, with 50% binding inhibition at 1.2 μ M for peptide 36-65 and at an extrapolated value of approximately 150 μ M for peptide 42-56. Peptides 36-56 and 67-81 did not show significant binding to soluble gH/gL up to the highest concentration tested (100 μ M). Compared to the low nanomolar range for soluble gp42, these short peptides have much lower affinity for gH/gL (Table 3.2).

Table 3.2. Activity summary of gp42-derived peptides.

Soluble EBV gp42 residues	50% binding to gH/gL (nM) ^a	50% inhibition of B-cell fusion (nM) ^b	50% inhibition of epithelial cell fusion (nM) ^c
33-223	8.5	–	5
36-81	5.1	~2 ^d	5
36-65	1,500	>10,000	5,000
36-56	>100,000	>50,000	>50,000
42-56	~150,000 ^e	>50,000	>50,000
67-81	>100,000	>50,000	>50,000

^aMeasured by fluorescence polarization competition experiments with 10 nM purified soluble gH/gL and 10 nM FITC-labeled gp42-peptide 36-81.

^bMeasured by luciferase activity in fusion assay using CHO cells transfected with gH, gL, and gB and addition of known concentrations of soluble gp42, overlaid with Daudi B cells.

^cMeasured by luciferase activity in fusion assay using CHO cells transfected with gH, gL, and gB and overlaid with 293T epithelial cells.

^dMeasured using lowest gp42 concentration tested.

^eTheoretical extrapolated value based on trend of measured data.

The binding kinetics for FITC-labeled gp42-derived peptide 36-81 and soluble gH/gL were also studied. Fluorescence polarization measurements were taken by Austin Kirschner at 30-s time points after mixing 10 nM peptide and 10 nM soluble gH/gL (Figure 3.4A). Maximum binding signal was achieved by 10 min, and the nonlinear least squares exponential fit for one-site binding shows a binding rate of $0.908 \pm 0.039 \text{ min}^{-1}$. For dissociation experiments, excess soluble gp42 was added to preincubated 10 nM peptide and 10 nM soluble gH/gL. Time points measured over 2 h were fit to an exponential dissociation curve with a calculated half-life of the gH/gL/peptide complex at $9.86 \pm 0.6 \text{ min}$ (Figure 3.4B). A control sample with 1 μM soluble gp42- $\Delta\text{N}86$ added to 10 nM peptide and 10 nM soluble gH/gL did not show any peptide dissociation (Figure 3.4B).

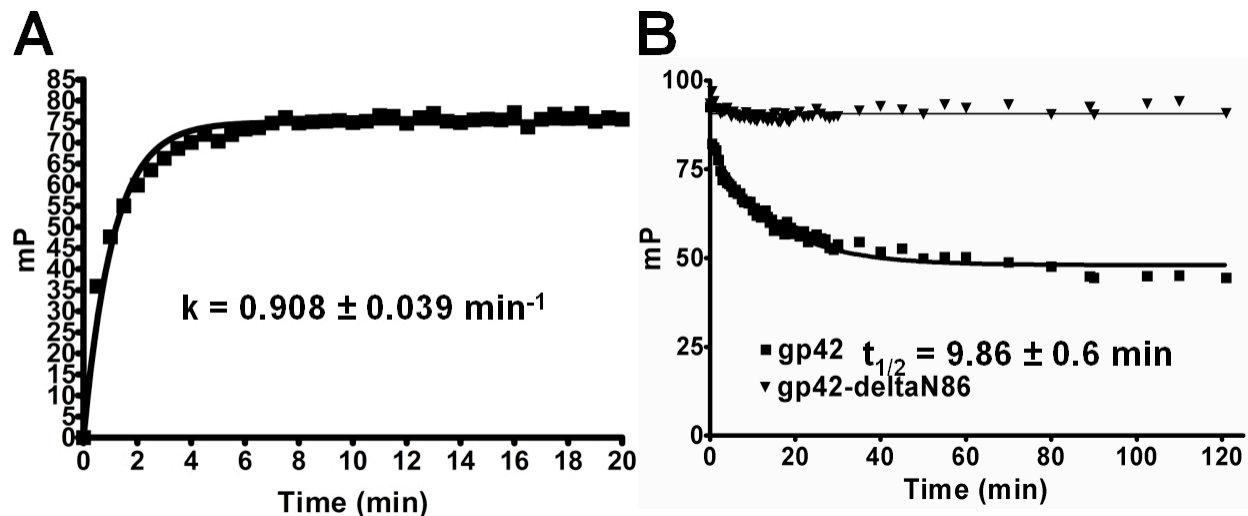


Figure 3.4. Kinetics of FITC-labeled gp42 peptide 36-81 binding soluble gH/gL as determined by fluorescence polarization.

The fluorescence polarization signal from FITC-labeled gp42 peptide 36-81 was monitored at time points immediately after mixing samples. (A) Peptide 36-81 binding to soluble gH/gL, each present at 10 nM concentration. Binding is nearly complete by 10 min with a rate constant of $0.908 \pm 0.039 \text{ min}^{-1}$. (B) Dissociation of premixed 10 nM gH/gL and 10 nM FITC-labeled gp42-peptide 36-81 is observed by adding soluble gp42 at 1 μM . The half-life ($t_{1/2}$) of the gH/gL/peptide complex is $9.86 \pm 0.6 \text{ min}$. The experiments in this figure were performed by Austin Kirschner.

Peptide from gp42 residues 36 to 81 is an efficient inhibitor of EBV-mediated membrane fusion. Previous work with peptide 36-65 revealed that it acted as an inhibitor of EBV-mediated epithelial cell membrane fusion in a dose-dependent manner in the low micromolar range (70). This finding is consistent with the ability of peptide 36-65 to inhibit binding of peptide 36-81 in the polarization assay. Since the longer peptide 36-81 bound gH/gL with much higher affinity than peptide 36-65, peptide 36-81 was also tested for inhibition of cell fusion. As shown in Figure 3.5A, Austin Kirschner demonstrated that peptide 36-81 is a significantly stronger inhibitor of epithelial cell fusion, with an apparent 50% effective concentration (EC_{50}) of approximately 5 nM. Both soluble gp42 and peptide 36-81 had a very similar inhibitory effect over comparable concentration ranges on epithelial cell membrane fusion (see Figure 5A in reference (70). Further testing of the peptide in fusion assays with B cells by Austin Kirschner revealed that the long peptide is also capable of inhibiting membrane fusion in the presence of gp42. With CHO cells transfected with gH, gL, gB, and gp42, the degree of inhibition is ~25% of the control, which is a significant amount (P value of < 0.05) as determined by a Student's *t* test (Figure 3.5B). This decrease in fusion is modest and likely attributable to difficulties in competing the membrane-bound gH/gL/gp42 complexes, which form over a 12-h transfection incubation. A significant amount of preformed gH/gL/gp42 complexes likely remain intact after the peptide is incubated with the CHO cells for only 10 min before it is overlaid with target B cells, especially as the half-life for dissociation is approximately 10 min, based on our peptide polarization results. Even greater inhibition of B cell fusion was observed by Austin Kirschner when the peptide was allowed to incubate for longer times (data not shown). To examine direct competition between gp42 and the peptide for binding cell-associated gH/gL, the B cell fusion assay was performed by Austin Kirschner using known concentrations of soluble

Figure 3.5. Peptide from gp42 residues 36 to 81 inhibits epithelial and B-cell membrane fusion. Fusion assay graphs showing concentration-dependent effects of peptide 36-81 on the cell-cell fusion assay. (A) Epithelial cell fusion. (B and C) B-cell fusion. CHO cells were transfected with gH, gL, and gB (A and C) and additionally transfected with gp42 (B). (The data at the far right of graph A are for cells also transfected with gp42). For panel C, soluble gp42 was added to trigger B-cell fusion and demonstrate efficient competition between the peptide and soluble protein. Data shown are the mean of triplicate measurements from at least three independent experiments, and error bars indicate standard deviations. The experiments in this figure were performed in collaboration with Austin Kirschner.

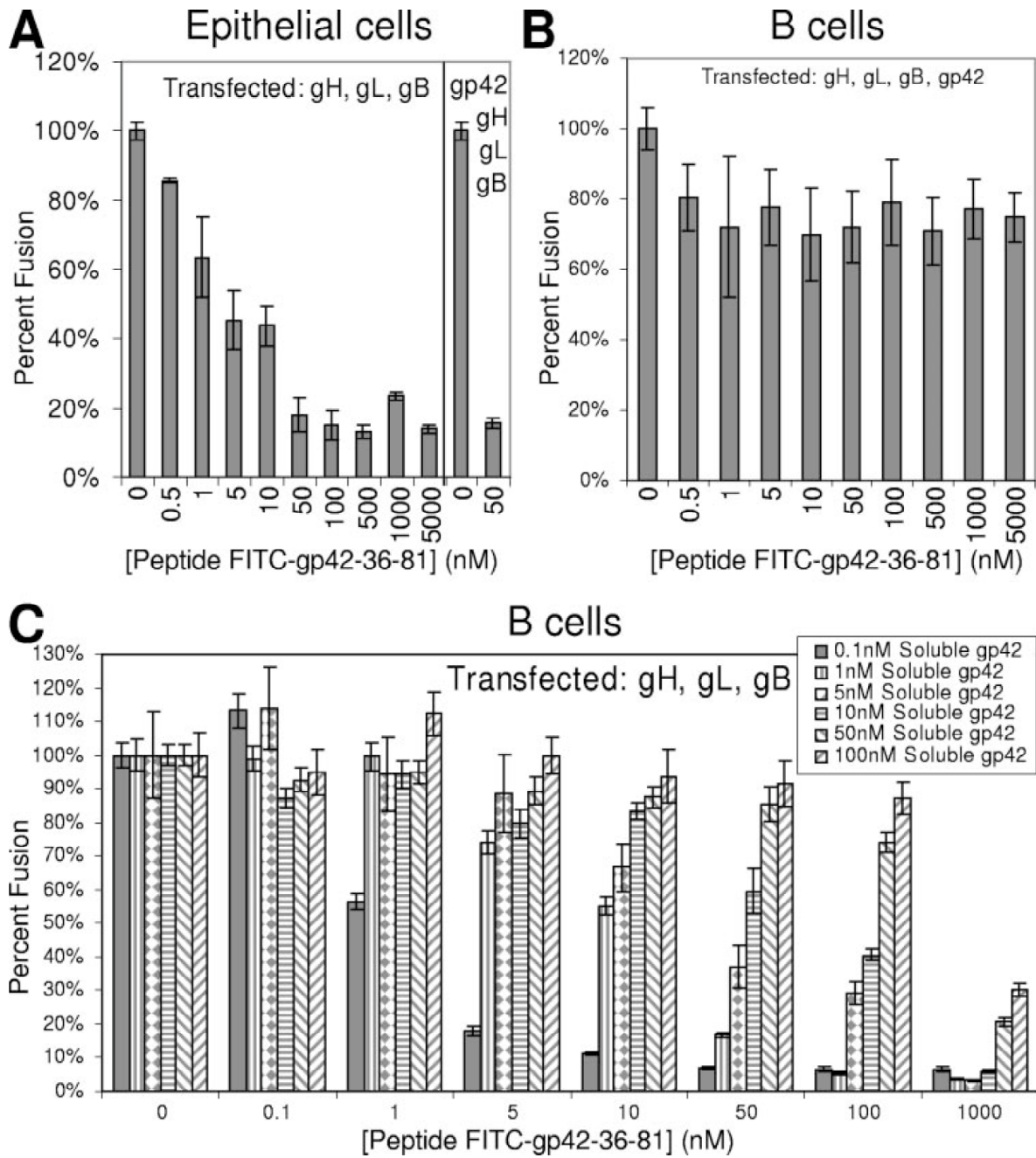


Figure 3.5. Peptide from gp42 residues 36 to 81 inhibits epithelial and B-cell membrane fusion.

gp42 added to CHO cells transfected with gH, gL, and gB. A clear dose-dependent inhibitory effect on B cell fusion is observed when peptide and soluble gp42 compete for binding gH/gL on the same timescale (Figure 3.5C). The data show a logical trend that as more soluble gp42 is added, more peptide is needed to inhibit fusion. Soluble gp42 and the 46-mer peptide are competitive in the same concentration ranges, suggesting that their binding affinities for gH/gL are similar.

Complementation assays with peptides and gp42 deletion mutants. The membrane fusion assay was used to test if B cell fusion with nonfunctional gp42 deletion mutants could be rescued by adding gp42-derived peptides *in trans* by Austin Kirschner. First, the soluble truncated gp42- Δ N86 protein was added along with the longest gp42-derived peptide (residues 36 to 81), but no membrane fusion occurred (data not shown). This lack of fusion was observed with or without transfected gp350 that might provide more favorable contacts between the fusion proteins and the target B cell (data not shown).

Next, the short gp42-derived peptides spanning residues 36 to 56, 42 to 56, and 67 to 81 were tested by Austin Kirschner for the ability to inhibit epithelial cell fusion. Based on their inability to block peptide 36-81 binding in the polarization assay, we did not expect the peptides to block fusion, and indeed no inhibitory activity was detected up to a 50 μ M final peptide concentration (Figure 3.6A). The peptides were also added in combination to see if their inhibitory effects would become apparent at micromolar concentrations, but none of these three peptides exhibited any activity when added simultaneously. However, using the peptide derived from residues 36 to 65, which has an inhibitory effect on epithelial cell fusion in the low micromolar range in combination with the peptide from residues 67 to 81, we did observe consistently enhanced inhibition, although the effect was still moderate and required peptide

Figure 3.6. Shorter gp42-derived peptides tested in epithelial and B-cell fusion assays. (A)

Fusion assay graphs showing no inhibitory effect on epithelial cell fusion with individual gp42-derived peptides tested up to 50 μ M final concentration. (B) Enhanced inhibition of epithelial cell fusion using simultaneous addition of gp42 peptide 36-65 and 67-81 compared to peptide 36-65 alone. (C) There was no restoration of B-cell fusion using transfected gp42 deletion mutants deficient in membrane fusion activity with added peptides, although wild-type soluble gp42 restored fusion. Brackets above the solid bars indicate the peptides added. Data shown are representative from at least two independent experiments, and error bars indicate standard deviations. The experiments in this figure were performed in collaboration with Austin Kirschner.

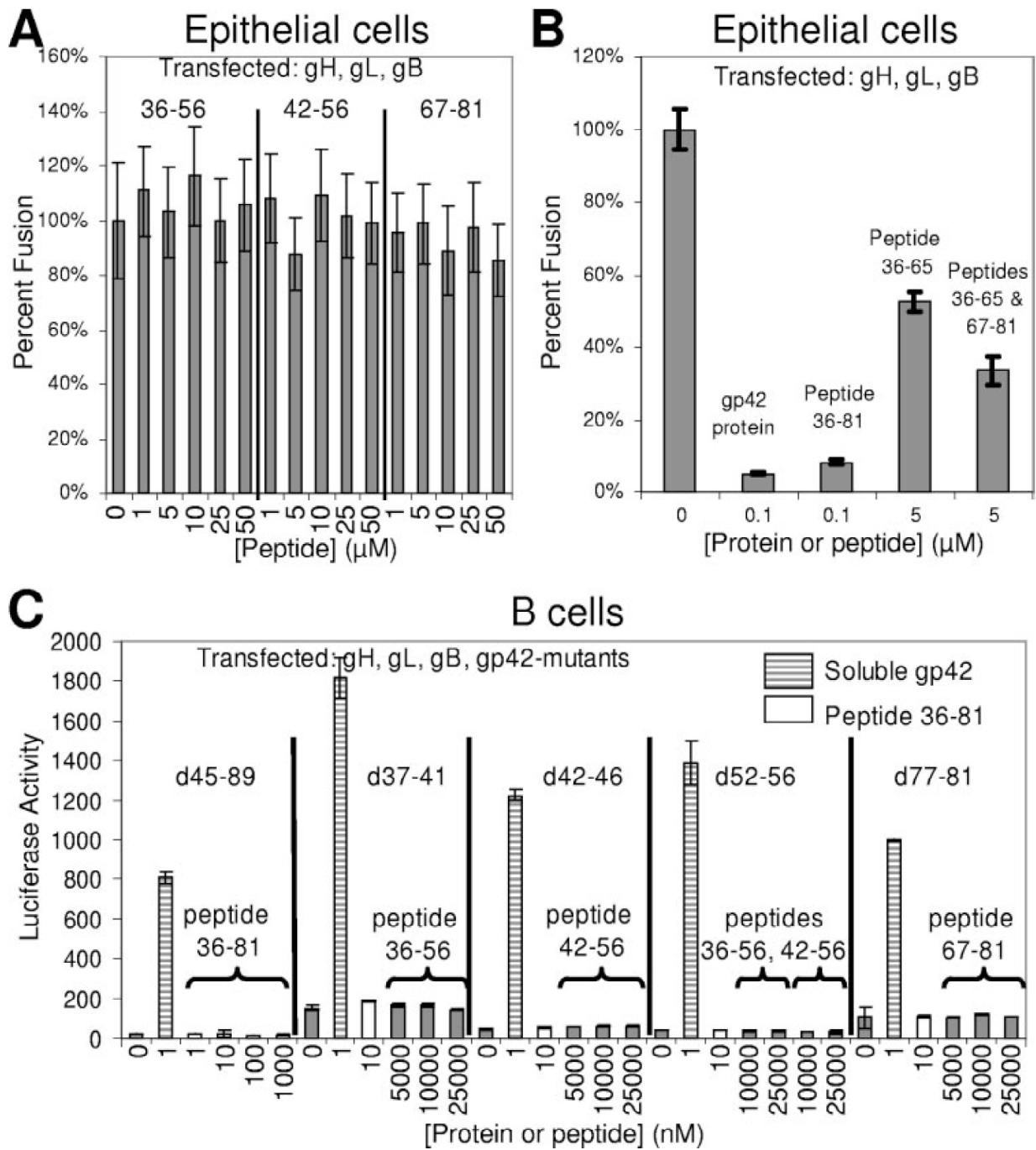


Figure 3.6. Shorter gp42-derived peptides tested in epithelial and B-cell fusion assays.

concentrations in the low micromolar range (Figure 3.6B). Simultaneous addition of peptides spanning residues 36 to 65 and 67 to 81 in the low micromolar range did not inhibit as strongly as the single peptide spanning residues 36 to 81 used in the nanomolar range, indicating that their covalent linkage is important for full binding and inhibition activity.

Subsequently, the reverse experiments were performed by Austin Kirschner to see if the short peptides could complement gp42 deletion mutants deficient in membrane fusion activity. Data were collected from the cell-cell fusion assay using CHO cells transfected with gH, gL, gB, and mutant gp42 (five-residue and longer deletions), and micromolar concentrations of short peptides were added immediately before overlay with B cells (Figure 3.6C). Fusion assay data revealed that these short N-terminal gp42 peptides added in *trans* could not restore the function of gp42 deletion mutants that lost the ability to trigger fusion with B cells. The longest peptide from gp42 residues 36 to 81, which has nanomolar binding to gH/gL, was unable to rescue membrane fusion with any of the gp42 mutants, including the gp42 mutant lacking residues 45 to 89. These data indicate that the contiguity of the gp42 C-terminal lectin domain with N-terminal gp42/gH/gL complexes is important for full fusogenic activity.

EBV infection assay with gp42-derived peptide 36-81. In order to test the effect of peptide 36-81 on entry of the whole virus, Austin Kirschner infected epithelial cells with GFP-expressing EBV, which was produced by Akata cells. Virus was preincubated with a 20 nM concentration of anti-gH/gL antibody E1D1, soluble gp42, or peptide 36-81 for 24 h at 37°C prior to a 1-h spin infection of cells in a 96-well format. The effect of peptide 36-81 on the infection of epithelial cells by EBV was measured by FACS analysis. Each of the three experimental conditions showed a reduction of infection to approximately 25% of the uninhibited EBV control (Figure 3.7). These data demonstrate that a low nanomolar concentration of peptide 36-81 is able to

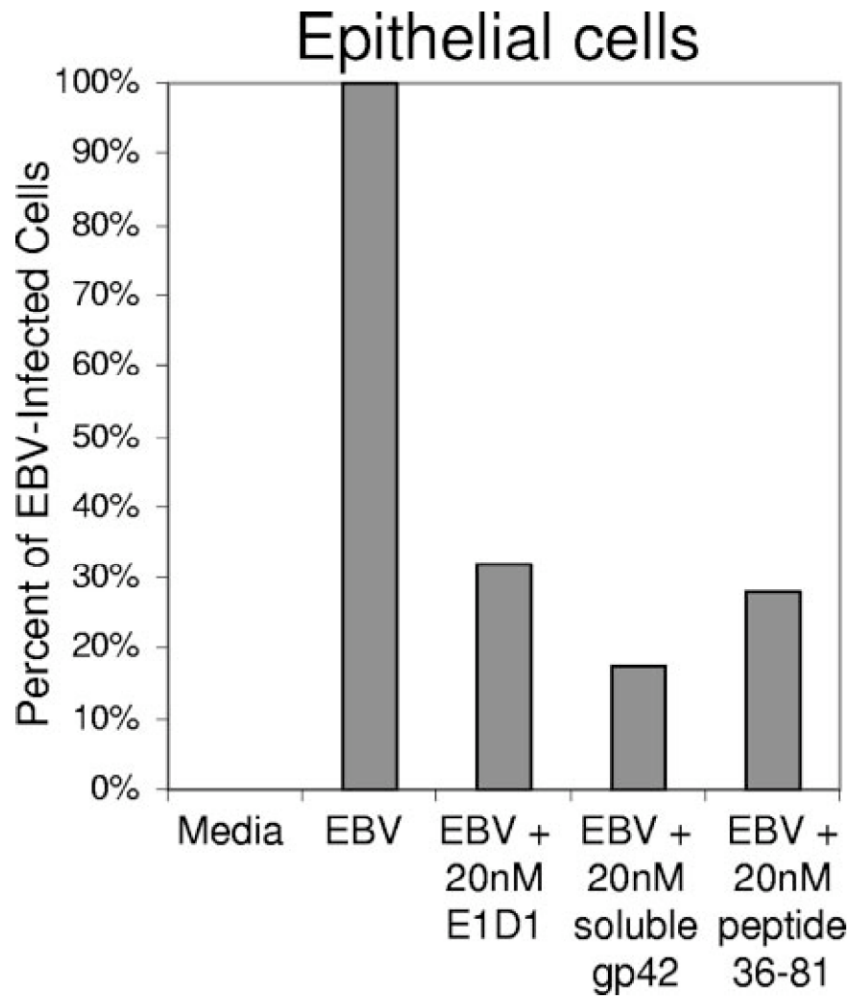


Figure 3.7. Peptide 36-81 inhibits EBV entry into epithelial cells.

A graph of a representative EBV infection assay shows the inhibitory effect of gp42-derived peptide 36-81. Virus was incubated with anti-gH/gL antibody E1D1, soluble gp42, or peptide 36-81 at 20 nM. FACS analysis was used to measure the GFP-expressing cells, and data were transformed to set the medium-only control to 0% infected and the EBV-only control to 100% infected so that each experimental condition demonstrates a fraction of the uninhibited 100% infection. The data shown are representative of at least three independent experiments.

inhibit the intact virus from entering epithelial cells, consistent with observations made in the cell-cell fusion assays.

DISCUSSION

N-terminal deletion mutants of gp42 lose the ability to function in membrane fusion. The deletion of five-residue segments within the N terminus of gp42 did not substantially affect protein expression levels compared to wild type. Membrane fusion experiments with B cells demonstrated that some mutants retain nearly wild-type fusion function, some allow moderate levels of fusion, and some are inactive in fusion. These deletion mutants reveal that residues 37 to 56 and 72 to 96 are absolutely required functional regions of the N terminus of gp42 to trigger fusion and suggest that some of the residues within residues 67 to 71 are also required (Figure 3.1B). The gp42 mutants defective in membrane fusion can be rescued by the addition of soluble gp42 in the fusion assay but not with any gp42-derived peptides that span the regions deleted (Figure 3.6C). Thus, there is a requirement for direct linkage between a gp42 lectin domain (residues 111 to 217) and the N-terminal gH/gL binding site to be within the same molecule.

CELISA with gp42 five-residue deletion mutants quantitatively measures binding to soluble gH/gL. The loss of membrane fusion activity for some gp42 mutants may be due to a lack of binding to gH/gL or to deletion of gp42 residues otherwise important for fusion activation. To investigate this hypothesis, a gH/gL-based CELISA was employed in addition to immunoprecipitation, and the data revealed that some defective gp42 mutants are similar to wild-type gp42 in binding gH/gL, some show moderately diminished binding, and some completely lose any interaction with gH/gL. Correlating the ability of mutants to function in membrane fusion with the ability to bind soluble gH/gL distinguishes three categories of mutants (Table 3.1): category 1, inconsequential mutants remaining fully functional; category 2, loss of fusion but maintenance of wild-type gH/gL binding; and category 3, reduced or complete loss of fusion due to altered binding to gH/gL. Category 1 mutants are innocuous deletions and/or single

substitutions that have no major effect on gp42 or gH/gL function. The d57-61 mutant appears to lack gH/gL binding in the CELISA but could mediate fusion. However, there are a few discrepancies between the immunoprecipitation data and CELISA measurements for the binding of gp42 mutants to gH/gL. These differences may be due to interactions gp42 may have with transfected gH/gL during protein expression and folding, possibly within the proteins' membrane spanning domains.

Mutant d57-61 is able to promote near wild-type membrane fusion but completely loses binding to soluble gH/gL as detected in CELISA. This is a peculiar mutant that was difficult to detect in Western blotting even though surface expression levels were consistently higher than wild-type gp42 (Figures 3.1B and 3.2B). There may be a significant contribution by the unusual tetra-proline structure (residues 57 to 60) in binding gH/gL, but a nearly wild-type degree of fusion is maintained in its absence. For HSV gD, which is a functional homolog for gp42, it is thought that a flexible proline-rich region becomes exposed upon receptor binding, thus activating gH/gL and gB for membrane fusion (19, 23, 40, 74). We reasoned that the N-terminal region of gp42 might play an analogous role and that for gp42 the presence of the tetra-proline motif might enable a gH/gL-dependent regulation of the gp42-N-terminal peptide. In this scenario, the d57-61 mutant might be capable of activating gB-dependent fusion in the absence of gH/gL. However, fusion assays performed by Austin Kirschner revealed that the d57-61 mutant is not capable of membrane fusion without gH/gL, i.e., transfected gB and the d57-61 mutant do not cause membrane fusion (data not shown). Furthermore, epithelial cell membrane fusion was inhibited in the presence of the d57-61 gp42 mutant, although d57-61 gp42 was somewhat less effective than wild-type gp42 (data not shown). These data suggest that the d57-61 mutant still binds gH/gL but with a lower affinity and significantly increased dissociation

rate. As a preliminary test for altered binding kinetics, preformed E1D1-gH/gL complexes (500 nM E1D1 and 50 nM gH/gL) were tested by Austin Kirschner in CELISA for binding d57-61, but no binding was detected even though the antibody complex is bivalent and thereby might be expected to interact more strongly with the mutant (data not shown). However, when the gp42 d57-61 mutant is transfected instead of wild-type gp42 in membrane fusion assays with B cells, peptide 36-81 does inhibit fusion somewhat more efficiently (data not shown). These data collected by Austin Kirschner also suggest that the d57-61 mutant forms complexes with gH/gL with a lower binding affinity than wild-type gp42 and that this complex can be dissociated by adding peptide 36-81.

Interestingly, category 2 mutants that are at the beginning of NT1 and the end of NT2 are able to bind soluble gH/gL in the gH/gL CELISA but are still unable to mediate membrane fusion (Figures 3.1B and 3.2; Table 3.1). At the N terminus of NT1, mutants d37-41 and d42-46 both appear to bind gH/gL well but are impaired in membrane fusion. The NT1 mutant d37-41 removes the cleavage site of residues 40 to 42 and does not secrete soluble gp42 (data not shown), potentially indicating that soluble gp42 plays an important role in membrane fusion (109). However, it is not clear why d42-46, which can bind soluble gH/gL, does not mediate fusion. Perhaps these missing residues are essential for triggering gH/gL function, even though binding to gH/gL occurs at wild-type levels. The NT2 mutants d82-86, d87-91, and d92-96 were also able to bind gH/gL but not mediate fusion. These mutants fall in or near the dimerization domain that was seen in the crystal structure of gp42-HLA-DR1 that includes residues 86 to 95 (95). The dimerization site might therefore be important for membrane fusion; alternatively, conceivably a linker region between the gH/gL binding site and the lectin domain is required. A five-residue insertion mutant previously studied (LI93) at this site does not affect membrane

fusion, consistent with the idea that a minimal, but perhaps sequence-independent, linker region is important rather than dimerization (121). The d82-86 mutant had very low levels of fusion, and these residues link the end of the gH/gL binding domain to the putative dimerization site. Further studies are required to determine whether specific sequences, dimerization, or simply linker residues are required for gp42 function in these regions of NT1 and NT2. For example, it is possible that five-residue deletions between residues 82 to 96 primarily result in a loss of fusion function due to altered geometry of the lectin domain relative to gH/gL in the complex. These residues may act as a linker between the gH/gL binding site and the lectin domain, providing needed flexibility for the fusion process to proceed. Nevertheless, category 3 mutants reveal the "core" gp42 residues that interact with gH/gL. These residues are important for binding soluble gH/gL and essential for membrane fusion function (Figure 3.1A).

The gp42-derived peptides directly bind to gH/gL. Fluorescence polarization experiments performed by Austin Kirschner reveal that the FITC-labeled gp42-derived peptide from residues 36 to 81 binds to gH/gL with high affinity. This direct measurement allows quantitative data to be gathered on the binding. Both binding at equilibrium and kinetics of binding were studied. The measured values for the on-rate and off-rate of FITC-labeled peptide 36-81 binding to soluble gH/gL are consistent with values obtained in equilibrium binding experiments. The affinity of peptide 36-81 for gH/gL was found to be nearly equivalent to the binding affinity of soluble gp42 protein. Thus, the residues sufficient for wild-type level binding to gH/gL appear to be present in the 46-mer peptide. Additional competition experiments with shorter peptides showed significantly weaker binding affinities. Peptide from residues 36 to 65 competes in the low-micromolar-concentration range, while the peptide from residues 42 to 56 just begins

binding soluble gH/gL in the mid-micromolar range, confirming that the minimum residues required for high-affinity gH/gL binding cover a large residue range (Table 3.2).

Peptides derived from gp42 inhibit epithelial cell fusion. Membrane fusion studies by Austin Kirschner investigating the effect of soluble gp42 and peptides derived from the N-terminal region of gp42 revealed that they can effectively inhibit epithelial cell fusion. The soluble gp42 protein and the long peptide 36-81 inhibit in the low nanomolar range, the peptide 36-65 inhibits in the low micromolar range, and the shorter peptides do not show inhibition up to 50 μ M. Nevertheless, a synergistic effect was found when adding peptides 36-65 and 67-81 in the low micromolar range, somewhat enhancing the inhibitory effect compared to peptide 36-65 alone. The small synergistic effect of peptides 36-65 and 67-81 suggests that these segments bind with an extended peptide binding site on gH/gL, which exhibits only mild cooperativity in binding. The fact that the longer peptide 36-81 gains nearly 1,000-fold binding affinity and concentration for 50% inhibition compared to the shorter peptides demonstrates the importance of having these two binding regions within a single peptide chain. Given that gp42 and gp42-derived peptides function by binding to gH/gL, it can be inferred that the inhibitory mechanism is either blockage of a critical binding site on gH/gL, such as an interaction of gH/gL with a gH/gL receptor, or inhibition or induction of a conformational change in gH/gL rendering it unable to mediate fusion.

Peptide from gp42 residues 36 to 81 inhibits B cell fusion when competing with soluble gp42. The long peptide from gp42 residues 36 to 81 binds soluble gH/gL with approximately the same affinity as the soluble protein gp42. This suggests that their activities in membrane fusion may be in the same functional range, namely, the low nanomolar concentration. Indeed, when tested in direct competition with soluble gp42, peptide 36-81 is able to inhibit B-cell fusion when

its concentration is above that of soluble gp42. However, membrane fusion with B cells proceeds only when the N-terminal region of gp42 is connected to the lectin domain, which engages the HLA class II receptor. B cell fusion did not occur in experiments with peptide 36-81 and soluble gp42- Δ N86 added together (data not shown). Therefore, membrane fusion requires the combination of the N-terminal region of gp42 occupying the gH/gL binding site and the same protein's proximal C-type lectin domain engaging the HLA class II receptor. In addition, none of the short gp42-derived peptides (peptides 36-56, 42-56, and 67-81) has any inhibitory effect on B cell or epithelial cell fusion, testing even at 50 μ M peptide. Moreover, none of the gp42-derived peptides can rescue B cell fusion with transfected five-residue gp42 deletion mutants. Nevertheless, the gp42 residues in this region are critical for binding to gH/gL and triggering membrane fusion. It remains unclear why the presence of these residues is insufficient to stimulate membrane fusion, even when the high-affinity peptide 36-81 and the gp42- Δ N86 protein are present.

Peptide 36-81 inhibits epithelial cell infection by whole virus. Since peptide 36-81 inhibited EBV-mediated epithelial cell fusion in the low nanomolar range, its ability to inhibit intact virus infection of epithelial and B cells was examined by Austin Kirschner. For epithelial cell infections, virus was produced by Akata cells, which are thought to make virus with lower levels of gp42 that is therefore more efficient at infecting epithelial cells. At a concentration of 20 nM, which is approximately four times the EC_{50} for inhibiting epithelial cell fusion, the peptide acts similarly to anti-gH/gL antibody E1D1 and soluble gp42, reducing the infection to nearly one-quarter of the uninhibited control (Figure 3.7). The peptide inhibits intact virus as effectively as it inhibits epithelial cell membrane fusion in the virus-free cell-cell fusion assay. Since the peptide is known to bind directly to gH/gL in competition for gp42, the infection assay data

strongly suggest that the peptide is capable of binding gH/gL on the intact virus surface to inhibit its ability to enter epithelial cells.

In contrast, when peptide 36-81 was examined in a B-cell infection assay, using virus produced by B95-8 cells, it did not demonstrate inhibition (data not shown). This was likely due to the presence of higher concentrations of viral gp42 forming tight membrane-bound gH/gL/gp42 complexes, in which gp42 could not be displaced by the peptide. This finding is consistent with the results observed for peptide inhibition of B cell membrane fusion in which even high concentrations of peptide could achieve only a modest decrease in cell-cell fusion when transfected gp42 was present (Figure 3.5B). Design of other peptides or peptidomimetics might reveal a better inhibitor of viral entry into B cells.

Characterization of the gp42 residues important for gH/gL-mediated membrane fusion.

The gp42 residues found to primarily contribute to binding gH/gL (47 to 61 and 67 to 81) contain seven prolines, 10 charged residues, and three aromatic residues. Other residues important for triggering fusion function, are hydrophobic (residues 37 to 46) and mostly neutral (residues 82 to 96). However, there are putative glycosylation sites that suggest that these regions are not likely to mediate direct protein-protein interactions. In addition, gp42 has a cleavage site from residues 40 to 42 and a possible dimerization or linker region from residues 86 to 95. We must await a crystal structure of the N-terminal region of gp42 and the structure of the gH/gL complex to complete our understanding of this herpesvirus membrane fusion mechanism.

Based on the data gathered using the gp42-derived peptide 36-81 in vitro and in cell-based assays, a model of its inhibition of EBV-mediated membrane fusion is proposed (Figure 3.8). Contacts mimicking gp42 are retained, and membrane fusion is inhibited when peptide 36-81 is bound to gH/gL.

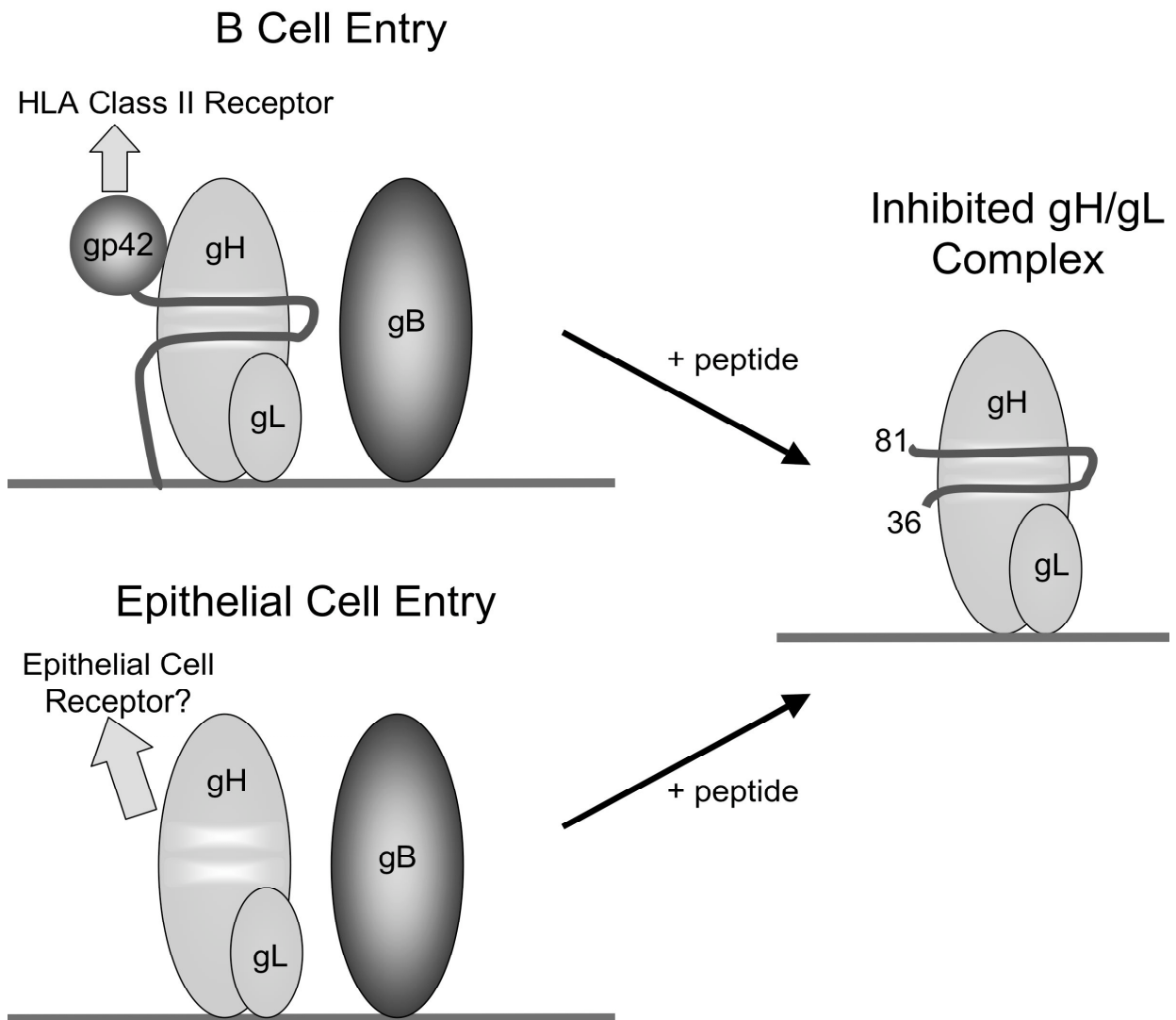


Figure 3.8. Model of peptide inhibition of EBV membrane fusion apparatus.

The N-terminal region of gp42 binds gH/gL with high affinity, and the peptide from gp42 residues 36 to 81 mimics that interaction. Epithelial cell fusion is inhibited by nanomolar concentrations of gp42, and the peptide 36-81 is sufficient to inhibit at those concentrations as well. B-cell membrane fusion only proceeds when a gp42 lectin domain is supplied in *cis* with the N-terminal region. Thus, peptide 36-81 is a strong inhibitor of both epithelial and B-cell membrane fusion.

The peptide derived from residues 36 to 81 acts as a low nanomolar inhibitor of B-cell membrane fusion, and it is as potent as gp42 at inhibiting epithelial cell membrane fusion and viral entry. This peptide proves useful for future drug development to treat EBV-mediated diseases of both B cell and epithelial cell origin. The gp42-derived peptides, and others like them, provide new tools for studying herpesvirus entry and designing effective therapeutics.

CHAPTER FOUR—CONCLUSIONS AND FUTURE DIRECTIONS

Epstein-Barr virus glycoprotein 42 has at least three functional domains required for B-cell membrane fusion. EBV is able to infect both epithelial cells and B cells, with membrane fusion occurring at the plasma surface of epithelial cells involving gH, gL, and gB, while B-cell membrane fusion occurs after endocytosis and is mediated by gp42, gH/gL, and gB [(138); For review see (60)]. Virion levels of EBV gp42 determine which cell type the virus is able to infect. High levels of gp42 sterically hinder infection of epithelial cells, but allow for efficient infection of B cells, whereas virus that is lacking gp42 can bind but not infect B cells (81, 137). Shortly after biosynthesis in B cells, gp42 molecules associate intracellularly with -DR, -DP, or -DQ alleles of its co-receptor, the class II human leukocyte antigen (HLA class II) (46, 48, 109, 126). This leads to the emergence of virus with low levels of gp42, and these virions are able to efficiently infect epithelial cells, but not other B cells (13). The alternating tropism of the virus provides a model of how the virus is able to spread within and between human hosts to establish latency.

Although the role of gp42 had been established in membrane fusion and infection, very little was known specifically about the protein and how it interacted with other glycoproteins or its receptor. Crystal studies of soluble gp42 (residues 33 – 223) bound to HLA-DR1 revealed three sites on the gp42 C-type lectin domain (CTLD) that contact HLA-DR1: an α -2-helix, an aromatic ring, and a single arginine residue (95). Although the majority of the gp42 amino-terminal ectodomain was unresolved in the structure, dimerization was observed along residues 87 – 94 in the crystal lattice. Although it could merely be an artifact of crystallization, the formation of gp42 dimers after receptor binding could play a role in membrane fusion. A hydrophobic pocket was also discovered on the surface of the CTLD, which was separated from the HLA class II binding site by the α -2-helix. Mutational studies of individual residues of the

HLA-DR1 β 1 chain confirmed that glutamic acid 46, lysine 65, and arginine 72 were all required for efficient binding of soluble gp42 and infection by EBV (89). To determine the functional significance of the various gp42 structures revealed by the structural and mutational studies of HLA class II, we created several linker-insertion and point mutations in gp42 (Chapter 2). Our data confirmed that the gp42 aromatic ring, α -2-helix, and arginine 220 are all required to interact with the three key residues of HLA class II for receptor binding and fusion with B cells. Mutations along the amino-terminal domain had modest if any effects on binding and fusion, while mutations buried within the CTLD appeared to perturb the overall structure of gp42 and disrupt both binding and fusion. Most interesting, mutations in the hydrophobic pocket did not disrupt receptor binding, but mutants were unable to mediate fusion, demonstrating a functional requirement separate from receptor binding to trigger B-cell membrane fusion.

Because the mutants from chapter 2 only had modest effects at most on membrane fusion, additional mutants were created to further characterize the gp42 amino-terminal ectodomain (Chapter 3). It had been demonstrated that soluble gp42.Fc missing the first 58, 90, and 122 residues (Δ 58, Δ 90, and Δ 122) could bind HLA class II but not co-immunoprecipitate gH/gL (138). The mutants were unable to rescue gp42-null EBV infection of B cells, or block infection of epithelial cells, although Δ 58 appeared to weakly bind gH/gL based on a faint EBNA1 signal from infection. Binding studies of soluble gp42 with soluble gH/gL also proved that the three proteins bind in a high affinity complex in a 1:1:1 ratio, and that this binding occurs somewhere between residues 33 and 86 (70). We sought to precisely define the gp42 amino-terminal binding site of gH/gL by creating five residue deletions and testing them for gH/gL binding and fusion. Our data proved that there are actually two separate domains of gp42, both of which are required to bind soluble and transmembrane gH/gL, as well as to mediate B-

cell membrane fusion. The data also hinted that both cleavage and dimerization of gp42 might also play a role in fusion. Several peptides were designed to bind these domains separately, but it was peptide 36-81 that spanned both, which could effectively inhibit gH/gL binding, epithelial and B-cell membrane fusion, and infection of epithelial cells. Taken together these studies have identified and helped to characterize three separate gp42 domains that are all required for membrane fusion: the HLA class II binding site on the CTLD, the gH/gL binding sites on the amino-terminal ectodomain, and the hydrophobic pocket on the CTLD, whose ligand remains to be identified.

EBV gp42 and HSV-gD are functionally similar, but uniquely trigger membrane fusion.

EBV and other herpesviruses use a multicomponent system for membrane fusion, which is different from other known viral fusion systems that utilize a single fusion protein [For review see (65)]. However, it remains unclear as to how all these proteins interact to accomplish entry. Studies have solved the crystal structures of the EBV gp42-HLA class II complex and the herpes simplex virus type 1 (HSV-1) functional homolog gD bound to the herpesvirus entry mediator receptor (HVEM) (19, 95). The similarities between these herpesvirus proteins can provide us insight into the mechanisms of EBV-triggered membrane fusion. The unliganded HSV-1 gD crystals revealed a flexible N-terminus, the conformation of which is clearly altered when bound to receptor (74). This similarly occurs in gp42 after HLA class II engagement (Kirschner *et al.*, submitted). Like EBV, HSV can infect epithelial cells as well as cells where the virus establishes latency, i.e., neurons for the α -herpesviruses. However, unlike EBV gp42, HSV gD can bind multiple receptors to trigger membrane fusion: HVEM, a member of the tumor necrosis factor receptor family; nectin-1 or nectin-2, cell adhesion molecules belonging to the immunoglobulin

superfamily; and specifically modified heparan sulfate (3-*O*-S HS) catalyzed by particular isoforms of 3-*O*-sulfotransferase (124). Although HSV gD receptors HVEM and Nectin-1 bind overlapping but distinct epitopes of gD, the conformationally flexible C-terminal region of gD is clearly open when receptor-bound. In the case of HVEM, there is an N-terminal hairpin loop that is formed upon receptor binding. This loop is not seen when gD binds nectin-1. Before binding, the C-terminal ectodomain occupies this same space as the loop (19, 20, 74). The C terminus also lies on top of residues involved in nectin-1 binding (26, 86). The movement of the C terminus of gD was postulated to be required for receptor binding, rather than as a result of the event (74). However, current studies also favor the hypothesis that interaction of gD with its receptors alters its conformation and exposes the C-terminal of gD to fusogenic glycoproteins B, H, and L (152). Kirschner *et al.* clearly demonstrated EBV gp42 receptor-induced conformational changes, and preliminary data from our lab suggest that HLA class II engagement with gp42 alters gH/gL binding from the amino-terminus to the hydrophobic pocket, a step required for fusion to proceed (data not shown).

We have demonstrated that the EBV gp42 hydrophobic pocket is not involved with HLA class II receptor binding, but still required for fusion (Chapter 2). HSV gD was similarly demonstrated to have a defined region of residues 262 and 285 that are required for membrane fusion, but not involved in receptor binding and has been termed the profusion domain (23, 150). Lazear *et al.* proposed that this profusion domain is more tightly associated with the core of HSV gD and that receptor binding is required for stable unwinding of the C terminus to expose that domain (76). In the case of EBV gp42, the hydrophobic pocket might be similarly occluded before receptor engagement, and interaction with B cells exposes the pocket, allowing ligand binding and triggering of fusion. Another potential structural parallel discovered is that gD

formed dimers before receptor engagement, which occludes receptor binding sites, although this, too, could be an artifact of crystallization (74). Dimers of gp42 were seen whether receptor bound or not, but in different sites (95, Kirschner *et al.*, submitted). It is interesting to speculate that dimerization might also play a role in herpesvirus membrane fusion.

The steps following these required conformational changes and receptor binding remain unclear for EBV, but a few creative and well-executed studies with HSV have given some insight into the specific mechanisms of membrane fusion. HSV-1 gD has been shown to form complexes sequentially with both gH and gB (34, 66, 103, 129). Subramanian and Geraghty developed an exquisite assay to detect hemifusion as well as complete fusion, demonstrating the sufficiency of gD with gH/gL for hemifusion. Interestingly, gB was not required for hemifusion, but was necessary for complete fusion, providing an elegant model of sequential glycoprotein involvement in HSV-1 membrane fusion. It was later demonstrated using bimolecular complementation that HSV gD associates with gB, and gD associates with gH/gL, but no association was seen between gB and gH/gL unless gD was present (3). Results indicated that gD binding its receptor concurrently triggers both fusion and the interaction between gB and gH/gL. Most recently, Maurer *et al.* used small vesicles reconstituted from the ends of neurons to catalog images of these synaptosomes fusing with virions. Fusion pores were very difficult to observe due to their transience, but based on identified fusion intermediates, it was proposed that receptor binding of gD induces a conformational change, followed by interaction with gH/gL. This in turn causes a conformational change in gH/gL, leading to binding of gH/gL to the plasma membrane, followed by recruitment of gB, which then also binds the plasma membrane (87). We have yet to demonstrate such sequential recruitment of EBV glycoproteins to induce membrane fusion, but since the presence or absence of EBV gp42 appears to act as a switch for virus entry into B cells

or epithelial cells, respectively, its interaction with gH/gL is a fundamental feature in EBV-mediated membrane fusion (13). However, our work has added to the field by delineating required functional domains of gp42 to trigger B-cell membrane fusion and suggesting an order in which proteins must interact with gp42 for this to proceed.

Proposed model. The EBV gH/gL interaction with gp42 appears more complex than previously hypothesized. Not only are two separate regions along the amino-terminal ectodomain of gp42 involved in both gH/gL binding and membrane fusion, the hydrophobic pocket, which is required for membrane fusion, may also be involved in gH/gL binding for fusion to proceed. We therefore propose that during EBV gp42-induced membrane fusion with B cells, the two amino-terminal domains of gp42 initially bind gH/gL by “hugging” the heterodimeric complex via gH and that gH either binds or occludes the gp42 hydrophobic pocket (Figure 4.1). Molecules of gp42 that are not in complex with gH/gL dimerize to occlude the hydrophobic pockets of both molecules. Receptor binding of HLA class II to gp42 induces a conformational change in the amino-terminus that causes gp42 to release gH/gL, allowing gH/gL to now bind exclusively at the hydrophobic pocket. The conformational change that also occurs in the hydrophobic pocket not only allows gH/gL binding, but also brings gH/gL closer to the target membrane, which then allows gH to insert the fusogenic domain into the membrane. Dimerization of gp42 along the amino-terminal ectodomain closest to the CTLD would enable more gH to be drawn to the target membrane. Hemifusion occurs at the outer leaflet of the membrane involving just gH/gL, while gB is required for complete fusion. Alternately, the shift in gH/gL conformation with gp42 could cause a shift in gB nearby, bringing gB in closer proximity to the cell and allowing gB to insert

Figure 4.1. Proposed model of Epstein-Barr virus glycoprotein 42-induced B-cell membrane fusion. Upper panel) EBV gp42 (multi-colored), gH (yellow), gL (light green), and gB (blue) are depicted along the virus membrane (dark green) as they approach HLA class II molecules (purple) on the surface of the B cell (red). Structural determinants of gp42 include the amino-terminal ectodomain (striped in light blue and black), the C-type lectin domain (CTLD) (large black ball), HLA class II receptor binding site (concave portion of CTLD), the hydrophobic pocket (protruding semi-circle in cayenne red), and the 158 loop of residues 156 – 161 adjacent to the α -2-helix between the receptor binding site and the hydrophobic pocket (small protruding loop in dark blue) and are represented here as gp42 protein alone and in heterotrimeric complex with gH/gL. The gp42 N-terminus binds the gH/gL complex in two separate regions before HLA class II receptor engagement. The gp42 hydrophobic pocket binds gH/gL or is occluded by gH/gL on the virus surface. Not depicted is gp350, which initially tethers the virus to the cell by binding CD21. This adhesion enhances infection, but is not essential for membrane fusion. Lower panel) After receptor binding, the gp42 N-terminus extends away from the CTLD, the 158 loop is drawn in closer to the CTLD and the hydrophobic pocket widens, depicted now as a partial-triangle in cayenne red (Kirschner *et al.*, submitted). Binding of gp42 to HLA class II allows gH/gL to shift its position from the gp42 N-terminus and thus to bind exclusively at the hydrophobic pocket. This shift repositions gH to insert itself directly into the target membrane, and/or brings gB closer for insertion into the target membrane.

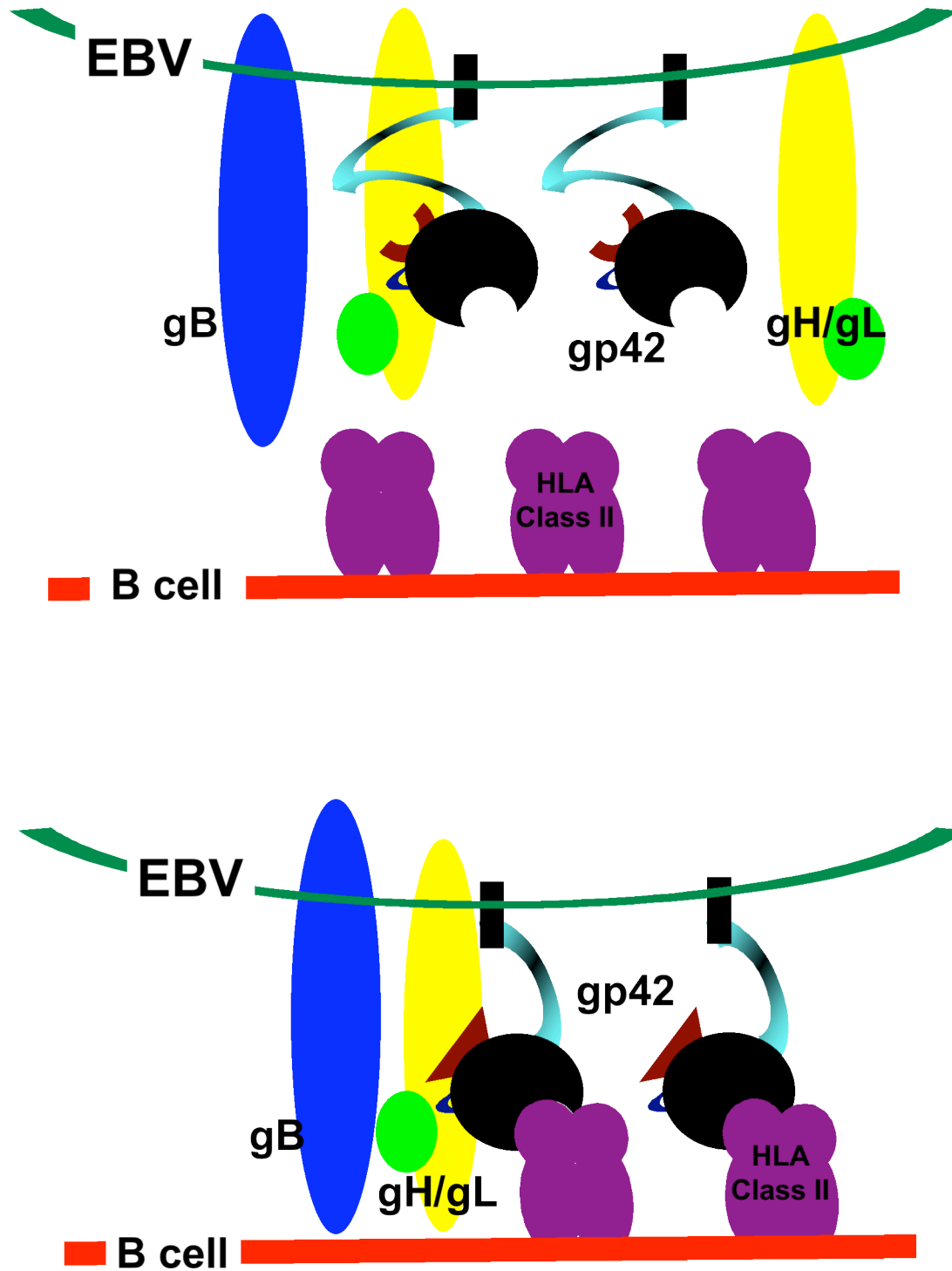


Figure 4.1. Proposed model of Epstein-Barr virus glycoprotein 42-induced B-cell membrane fusion.

itself into the target membrane. Insertion of either gH or gB would further tether the virion to the cell to allow fusion to proceed. Our studies provide a simple model of gp42 triggered-membrane fusion whereby HLA class II receptor-binding induces conformational changes in gp42. These alterations may cause gH/gL to shift binding from the gp42 amino-terminus to the hydrophobic pocket, providing the signal for fusion to proceed.

Future studies. To gain further insight into the mechanisms of gp42-triggered membrane fusion, future studies should focus on viral complementation assays, which are more sensitive than the fusion assay, and which will verify the mutant phenotypes in a viral system. The results should be confirmed by both real-time PCR and clonal outgrowth of B cells. To further characterize gp42 functional domains, more gp42-specific monoclonal antibodies should be generated and tested. Furthermore, it is important to positively identify the hydrophobic pocket ligand. We have no direct evidence that gH/gL binds the pocket, but have developed ways to demonstrate this or identify the intermediate between gH/gL and the hydrophobic pocket. Future directions also include investigation of the role of gp42 cleavage and dimerization in fusion.

One of the most exciting prospects is the targeting of the gp42 hydrophobic pocket for the development of anti-viral therapies. It is possible to perform a small molecule inhibitor screen using DOCK, a software program created by Dr. Brian Schoichet, which generates a 3-D grid based on a protein structure and then screens known molecules from existing databases. The parameters of the program allow adjustments for shape, size, and molecular bonds to identify the best-fit candidates for the gp42 hydrophobic pocket. Our aim was to develop a rapid 96-well format screen of molecules that had been selected by DOCK. Preliminary data from collaboration with the Jardetzky lab indicated that compound AK0026 inhibited membrane

fusion in a dose-dependent manner, and it was further tested for its ability to neutralize HSV-1 & HSV-2 infection, and inhibit membrane fusion of KSHV, HSV-1 and HSV-2 glycoproteins. Although AK0026 inhibited membrane fusion in an EBV-independent manner, these results suggest that this methodology can be used for high-throughput screening of potential inhibitory compounds of EBV fusion and infection, and that such studies can be undertaken even without complete knowledge of the mechanisms of membrane fusion. The amino-terminus has already proven to be an excellent target for inhibitory peptides, and the hydrophobic pocket provides an even better opportunity for development of antiviral therapies such as small molecule inhibitors.

The studies described in this dissertation have laid the groundwork to identify all the key players both spatially and temporally in gp42-triggered membrane fusion and infection of B cells. We have defined the gp42-HLA class II receptor-binding site, the gp42/gH/gL binding site, and demonstrated the functional requirement of the hydrophobic pocket for membrane fusion. The pocket may bind gH/gL after receptor engagement to trigger fusion. Coupled with structural and functional analyses, we are confident that future studies will elucidate precisely how the altered interaction of gp42 with gH/gL triggers EBV fusion with B cells and enhance our understanding of the mechanisms of herpesvirus entry, paving the way for the development of novel and effective therapeutic agents.

REFERENCES

1. 1999. Palivizumab (Synagis) for prevention of RSV infection. *Med Lett Drugs Ther* **41**:3-4.
2. **Allison, S. L., J. Schlich, K. Stiasny, C. W. Mandl, C. Kunz, and F. X. Heinz.** 1995. Oligomeric rearrangement of tick-borne encephalitis virus envelope proteins induced by an acidic pH. *J Virol* **69**:695-700.
3. **Atanasiu, D., J. C. Whitbeck, T. M. Cairns, B. Reilly, G. H. Cohen, and R. J. Eisenberg.** 2007. Bimolecular complementation reveals that glycoproteins gB and gH/gL of herpes simplex virus interact with each other during cell fusion. *Proc Natl Acad Sci U S A* **104**:18718-23.
4. **Backovic, M., T. S. Jardetzky, and R. Longnecker.** 2007. Hydrophobic residues that form putative fusion loops of Epstein-Barr virus glycoprotein B are critical for fusion activity. *J Virol* **81**:9596-600.
5. **Backovic, M., G. P. Leser, R. A. Lamb, R. Longnecker, and T. S. Jardetzky.** 2007. Characterization of EBV gB indicates properties of both class I and class II viral fusion proteins. *Virology* **368**:102-13.
6. **Baer, R., A. T. Bankier, M. D. Biggin, P. L. Deininger, P. J. Farrell, T. J. Gibson, G. Hatfull, G. S. Hudson, S. C. Satchwell, C. Seguin, and et al.** 1984. DNA sequence and expression of the B95-8 Epstein-Barr virus genome. *Nature* **310**:207-11.
7. **Balachandran, N., D. E. Oba, and L. M. Hutt-Fletcher.** 1987. Antigenic cross-reactions among herpes simplex virus types 1 and 2, Epstein-Barr virus, and cytomegalovirus. *J Virol* **61**:1125-35.
8. **Baldwin, C. E., R. W. Sanders, Y. Deng, S. Jurriaans, J. M. Lange, M. Lu, and B. Berkhout.** 2004. Emergence of a drug-dependent human immunodeficiency virus type 1 variant during therapy with the T20 fusion inhibitor. *J Virol* **78**:12428-37.
9. **Barocchi, M. A., V. Massignani, and R. Rappuoli.** 2005. Opinion: Cell entry machines: a common theme in nature? *Nat Rev Microbiol* **3**:349-58.
10. **Beitia Ortiz de Zarate, I., L. Cantero-Aguilar, M. Longo, C. Berlioz-Torrent, and F. Rozenberg.** 2007. Contribution of endocytic motifs in the cytoplasmic tail of herpes simplex virus type 1 glycoprotein B to virus replication and cell-cell fusion. *J Virol* **81**:13889-903.
11. **Bender, F. C., J. C. Whitbeck, H. Lou, G. H. Cohen, and R. J. Eisenberg.** 2005. Herpes simplex virus glycoprotein B binds to cell surfaces independently of heparan sulfate and blocks virus entry. *J Virol* **79**:11588-97.
12. **Bennett, M. K.** 1995. SNAREs and the specificity of transport vesicle targeting. *Curr Opin Cell Biol* **7**:581-6.

13. **Borza, C. M., and L. Hutt-Fletcher.** 2002. Alternate Replication in B cells and epithelial cells switches tropism of Epstein-Barr virus. *Nat Medicine* **8**:594-599.
14. **Borza, C. M., A. J. Morgan, S. M. Turk, and L. M. Hutt-Fletcher.** 2004. Use of gHgL for attachment of Epstein-Barr virus to epithelial cells compromises infection. *J Virol* **78**:5007-14.
15. **Bressanelli, S., K. Stiasny, S. L. Allison, E. A. Stura, S. Duquerroy, J. Lescar, F. X. Heinz, and F. A. Rey.** 2004. Structure of a flavivirus envelope glycoprotein in its low-pH-induced membrane fusion conformation. *Embo J* **23**:728-38.
16. **Bullough, P. A., F. M. Hughson, J. J. Skehel, and D. C. Wiley.** 1994. Structure of influenza haemagglutinin at the pH of membrane fusion. *Nature* **371**:37-43.
17. **Burkitt, D.** 1962. A children's cancer dependent on climatic factors. *Nauchni Tr Vissh Med Inst Sofiia* **194**:232-234.
18. **Burkitt, D.** 1962. A tumour syndrome affecting children in tropical Africa. *Postgrad Med J* **38**:71-9.
19. **Carfi, A., H. Gong, H. Lou, S. H. Willis, G. H. Cohen, R. J. Eisenberg, and D. C. Wiley.** 2002. Crystallization and preliminary diffraction studies of the ectodomain of the envelope glycoprotein D from herpes simplex virus 1 alone and in complex with the ectodomain of the human receptor HveA. *Acta Crystallogr D Biol Crystallogr* **58**:836-8.
20. **Carfi, A., S. H. Willis, J. C. Whitbeck, C. Krummenacher, G. H. Cohen, R. J. Eisenberg, and D. C. Wiley.** 2001. Herpes Simplex Virus Glycoprotein D Bound to the Human Receptor HveA. *Mol. Cell* **8**:169-179.
21. **Chen, E. H., and E. N. Olson.** 2005. Unveiling the mechanisms of cell-cell fusion. *Science* **308**:369-73.
22. **Chen, J., K. H. Lee, D. A. Steinhauer, D. J. Stevens, J. J. Skehel, and D. C. Wiley.** 1998. Structure of the hemagglutinin precursor cleavage site, a determinant of influenza pathogenicity and the origin of the labile conformation. *Cell* **95**:409-17.
23. **Cocchi, F., D. Fusco, L. Menotti, T. Gianni, R. J. Eisenberg, G. H. Cohen, and G. Campadelli-Fiume.** 2004. The soluble ectodomain of herpes simplex virus gD contains a membrane-proximal pro-fusion domain and suffices to mediate virus entry. *Proc Natl Acad Sci U S A* **101**:7445-50.
24. **Cole, N. L., and C. Grose.** 2003. Membrane fusion mediated by herpesvirus glycoproteins: the paradigm of varicella-zoster virus. *Rev Med Virol* **13**:207-22.
25. **Colman, P. M., and M. C. Lawrence.** 2003. The structural biology of type I viral membrane fusion. *Nat Rev Mol Cell Biol* **4**:309-19.

26. **Connolly, S. A., D. J. Landsburg, A. Carfi, J. C. Whitbeck, Y. Zuo, D. C. Wiley, G. H. Cohen, and R. J. Eisenberg.** 2005. Potential nectin-1 binding site on herpes simplex virus glycoprotein d. *J Virol* **79**:1282-95.
27. **Connolly, S. A., D. J. Landsburg, A. Carfi, D. C. Wiley, G. H. Cohen, and R. J. Eisenberg.** 2003. Structure-based mutagenesis of herpes simplex virus glycoprotein D defines three critical regions at the gD-HveA/HVEM binding interface. *Journal of Virology* **77**:8127-8140.
28. **Connolly, S. A., D. J. Landsburg, A. Carfi, D. C. Wiley, R. J. Eisenberg, and G. H. Cohen.** 2002. Structure-based analysis of the herpes simplex virus glycoprotein D binding site present on herpesvirus entry mediator HveA (HVEM). *J Virol* **76**:10894-904.
29. **D'Addario, M., A. Ahmad, A. Morgan, and J. Menezes.** 2000. Binding of the Epstein-Barr virus major envelope glycoprotein gp350 results in the upregulation of the TNF-alpha gene expression in monocytic cells via NF-kappaB involving PKC, PI3-K and tyrosine kinases. *J Mol Biol* **298**:765-78.
30. **D'Addario, M., A. Ahmad, J. W. Xu, and J. Menezes.** 1999. Epstein-Barr virus envelope glycoprotein gp350 induces NF-kappaB activation and IL-1beta synthesis in human monocytes-macrophages involving PKC and PI3-K. *Faseb J* **13**:2203-13.
31. **D'Addario, M., T. A. Libermann, J. Xu, A. Ahmad, and J. Menezes.** 2001. Epstein-Barr Virus and its glycoprotein-350 upregulate IL-6 in human B-lymphocytes via CD21, involving activation of NF-kappaB and different signaling pathways. *J Mol Biol* **308**:501-14.
32. **Debnath, A. K., L. Radigan, and S. Jiang.** 1999. Structure-based identification of small molecule antiviral compounds targeted to the gp41 core structure of the human immunodeficiency virus type 1. *Journal of Medicinal Chemistry* **42**:3203-3209.
33. **Deshpande, C. G., S. Badve, N. Kidwai, and R. Longnecker.** 2002. Lack of expression of the Epstein-Barr Virus (EBV) gene products, EBERs, EBNA1, LMP1, and LMP2A, in breast cancer cells. *Lab Invest* **82**:1193-9.
34. **Diakidi-Kosta, A., G. Michailidou, G. Kontogounis, A. Sivropoulou, and M. Arsenakis.** 2003. A single amino acid substitution in the cytoplasmic tail of the glycoprotein B of herpes simplex virus 1 affects both syncytium formation and binding to intracellular heparan sulfate. *Virus Res* **93**:99-108.
35. **Eckert, D. M., and P. S. Kim.** 2001. Mechanisms of viral membrane fusion and its inhibition. *Annu Rev Biochem* **70**:777-810.
36. **Eckert, D. M., V. N. Malashkevich, L. H. Hong, P. A. Carr, and P. S. Kim.** 1999. Inhibiting HIV-1 entry: discovery of D-peptide inhibitors that target the gp41 coiled-coil pocket. *Cell* **99**:103-115.

37. **Epstein, M. A., B. G. Achong, and Y. M. Barr.** 1964. Virus Particles in Cultured Lymphoblasts from Burkitt's Lymphoma. *Lancet* **15**:702-703.
38. **Farnsworth, A., T. W. Wisner, M. Webb, R. Roller, G. Cohen, R. Eisenberg, and D. C. Johnson.** 2007. Herpes simplex virus glycoproteins gB and gH function in fusion between the virion envelope and the outer nuclear membrane. *Proc Natl Acad Sci U S A* **104**:10187-92.
39. **Fingeroth, J. D., J. J. Weis, T. F. Tedder, J. L. Strominger, P. A. Biro, and D. T. Fearon.** 1984. Epstein-Barr virus receptor of human B lymphocytes is the CR2 receptor CR2. *Proc Natl Acad Sci U S A* **81**:4510-4.
40. **Fusco, D., C. Forghieri, and G. Campadelli-Fiume.** 2005. The pro-fusion domain of herpes simplex virus glycoprotein D (gD) interacts with the gD N terminus and is displaced by soluble forms of viral receptors. *Proc Natl Acad Sci U S A* **102**:9323-8.
41. **Galdiero, S., M. Vitiello, M. D'Isanto, A. Falanga, C. Collins, K. Raieta, C. Pedone, H. Browne, and M. Galdiero.** 2006. Analysis of synthetic peptides from heptad-repeat domains of herpes simplex virus type 1 glycoproteins H and B. *J Gen Virol* **87**:1085-97.
42. **Gianni, T., P. L. Martelli, R. Casadio, and G. Campadelli-Fiume.** 2005. The ectodomain of herpes simplex virus glycoprotein H contains a membrane alpha-helix with attributes of an internal fusion peptide, positionally conserved in the herpesviridae family. *J Virol* **79**:2931-40.
43. **Gianni, T., L. Menotti, and G. Campadelli-Fiume.** 2005. A heptad repeat in herpes simplex virus 1 gH, located downstream of the alpha-helix with attributes of a fusion peptide, is critical for virus entry and fusion. *J Virol* **79**:7042-9.
44. **Gianni, T., A. Piccoli, C. Bertucci, and G. Campadelli-Fiume.** 2006. Heptad repeat 2 in herpes simplex virus 1 gH interacts with heptad repeat 1 and is critical for virus entry and fusion. *J Virol* **80**:2216-24.
45. **Gibbons, D. L., M. C. Vaney, A. Roussel, A. Vigouroux, B. Reilly, J. Lepault, M. Kielian, and F. A. Rey.** 2004. Conformational change and protein-protein interactions of the fusion protein of Semliki Forest virus. *Nature* **427**:320-5.
46. **Haan, K. M., W. W. Kwok, R. Longnecker, and P. Speck.** 2000. Epstein-Barr virus entry utilizing HLA-DP or HLA-DQ as a coreceptor. *J Virol* **74**:2451-4.
47. **Haan, K. M., S. K. Lee, and R. Longnecker.** 2001. Different functional domains in the cytoplasmic tail of glycoprotein B are involved in Epstein-Barr virus-induced membrane fusion. *Virology* **290**:106-14.
48. **Haan, K. M., and R. Longnecker.** 2000. Coreceptor restriction within the HLA-DQ locus for Epstein-Barr virus infection. *Proc Natl Acad Sci U S A* **97**:9252-7.

49. **Haddad, R. S., and L. M. Hutt-Fletcher.** 1989. Depletion of glycoprotein gp85 from virosomes made with Epstein-Barr virus proteins abolishes their ability to fuse with virus receptor-bearing cells. *J Virol* **63**:4998-5005.
50. **Harrison, S. C.** 2008. Viral membrane fusion. *Nat Struct Mol Biol* **15**:690-8.
51. **Heineman, T., M. Gong, J. Sample, and E. Kieff.** 1988. Identification of the Epstein-Barr virus gp85 gene. *J Virol* **62**:1101-7.
52. **Heldwein, E. E., and C. Krummenacher.** 2008. Entry of herpesviruses into mammalian cells. *Cell Mol Life Sci* **65**:1653-68.
53. **Heldwein, E. E., H. Lou, F. C. Bender, G. H. Cohen, R. J. Eisenberg, and S. C. Harrison.** 2006. Crystal structure of glycoprotein B from herpes simplex virus 1. *Science* **313**:217-20.
54. **Helenius, A., J. Kartenbeck, K. Simons, and E. Fries.** 1980. On the entry of Semliki forest virus into BHK-21 cells. *J Cell Biol* **84**:404-20.
55. **Henle, G., W. Henle, and V. Diehl.** 1968. Relation of Burkitt's tumor-associated herpes-type virus to infectious mononucleosis. *Proc Natl Acad Sci U S A* **59**:94-101.
56. **Henle, W.** 1977. [Factors involved in the development of human tumors using the Epstein-Barr virus as an example (author's transl)]. *Klin Wochenschr* **55**:847-55.
57. **Henle, W., and G. Henle.** 1970. Evidence for a relation of Epstein-Barr virus to Burkitt's lymphoma and nasopharyngeal carcinoma. *Bibl Haematol*:706-13.
58. **Henle, W., and G. Henle.** 1969. The relation between the Epstein-Barr virus and infectious mononucleosis, Burkitt's lymphoma and cancer of the postnasal space. *East Afr Med J* **46**:402-6.
59. **Herrold, R. E., A. Marchini, S. Fruehling, and R. Longnecker.** 1996. Glycoprotein 110, the Epstein-Barr virus homolog of herpes simplex virus glycoprotein B, is essential for Epstein-Barr virus replication in vivo. *J Virol* **70**:2049-54.
60. **Hutt-Fletcher, L. M.** 2007. Epstein-Barr virus entry. *J Virol* **81**:7825-32.
61. **Hutt-Fletcher, L. M., and C. M. Lake.** 2001. Two Epstein-Barr virus glycoprotein complexes. *Curr Top Microbiol Immunol* **258**:51-64.
62. **Hutt-Fletcher, L. M., and S. M. Turk.** 2001. Virus isolation. *Methods Mol Biol* **174**:119-23.
63. **Jahn, R., T. Lang, and T. C. Sudhof.** 2003. Membrane fusion. *Cell* **112**:519-33.

64. **Janz, A., M. Oezel, C. Kurzeder, J. Mautner, D. Pich, M. Kost, W. Hammerschmidt, and H. J. Delecluse.** 2000. Infectious Epstein-Barr virus lacking major glycoprotein BLLF1 (gp350/220) demonstrates the existence of additional viral ligands. *J Virol* **74**:10142-52.
65. **Jardetzky, T. S., and R. A. Lamb.** 2004. Virology: a class act. *Nature* **427**:307-8.
66. **Jones, N. A., and R. J. Geraghty.** 2004. Fusion activity of lipid-anchored envelope glycoproteins of herpes simplex virus type 1. *Virology* **324**:213-28.
67. **Kadlec, J., S. Loureiro, N. G. Abrescia, D. I. Stuart, and I. M. Jones.** 2008. The postfusion structure of baculovirus gp64 supports a unified view of viral fusion machines. *Nat Struct Mol Biol* **15**:1024-30.
68. **Kaye, J. F., U. A. Gompels, and A. C. Minson.** 1992. Glycoprotein H of human cytomegalovirus (HCMV) forms a stable complex with the HCMV UL115 gene product. *J Gen Virol* **73 (Pt 10)**:2693-8.
69. **Kinzler, E. R., and T. Compton.** 2005. Characterization of human cytomegalovirus glycoprotein-induced cell-cell fusion. *J Virol* **79**:7827-37.
70. **Kirschner, A. N., J. Omerovic, B. Popov, R. Longnecker, and T. S. Jardetzky.** 2006. Soluble Epstein-Barr virus glycoproteins gH, gL, and gp42 form a 1:1:1 stable complex that acts like soluble gp42 in B-cell fusion but not in epithelial cell fusion. *J Virol* **80**:9444-54.
71. **Klein, G., G. Clements, J. Zeuthen, and A. Westman.** 1976. Somatic cell hybrids between human lymphoma lines. II. Spontaneous and induced patterns of the Epstein-Barr virus (EBV) cycle. *Int J Cancer* **17**:715-724.
72. **Kobasa, D., M. Rodgers, K. Wells, and Y. Kawaoka.** 1997. Neuraminidase hemadsorption activity, conserved in avian influenza A viruses, does not influence viral replication in ducks. *J. Virol.* **71**:6706-6713.
73. **Kost, T. A., J. P. Condreay, and D. L. Jarvis.** 2005. Baculovirus as versatile vectors for protein expression in insect and mammalian cells. *Nat Biotechnol* **23**:567-75.
74. **Krummenacher, C., V. M. Supekar, J. C. Whitbeck, E. Lazear, S. A. Connolly, R. J. Eisenberg, G. H. Cohen, D. C. Wiley, and A. Carfi.** 2005. Structure of unliganded HSV gD reveals a mechanism for receptor-mediated activation of virus entry. *Embo J* **24**:4144-53.
75. **Langeland, N., A. M. Oyan, H. S. Marsden, A. Cross, J. C. Glorioso, L. J. Moore, and L. Haarr.** 1990. Localization of the herpes simplex virus type 1 genome of a region encoding proteins involved in adsorption to the cellular receptor. *J Virol* **64**:1271-1277.

76. **Lazear, E., A. Carfi, J. C. Whitbeck, T. M. Cairns, C. Krummenacher, G. H. Cohen, and R. J. Eisenberg.** 2008. Engineered disulfide bonds in herpes simplex virus type 1 gD separate receptor binding from fusion initiation and viral entry. *J Virol* **82**:700-9.
77. **Lazzarin, A., B. Clotet, D. Cooper, J. Reynes, K. Arasteh, M. Nelson, C. Katlama, H. J. Stellbrink, J. F. Delfraissy, J. Lange, L. Huson, R. DeMasi, C. Wat, J. Delehanty, C. Drobnes, and M. Salgo.** 2003. Efficacy of enfuvirtide in patients infected with drug-resistant HIV-1 in Europe and Australia. *N Engl J Med* **348**:2186-95.
78. **Lee, S. K., T. Compton, and R. Longnecker.** 1997. Failure to complement infectivity of EBV and HSV-1 glycoprotein B (gB) deletion mutants with gBs from different human herpesvirus subfamilies. *Virology* **237**:170-81.
79. **Lee, S. K., and R. Longnecker.** 1997. The Epstein-Barr virus glycoprotein 110 carboxy-terminal tail domain is essential for lytic virus replication. *J Virol* **71**:4092-7.
80. **Li, Q., C. Buranathai, C. Grose, and L. M. Hutt-Fletcher.** 1997. Chaperone functions common to nonhomologous Epstein-Barr virus gL and Varicella-Zoster virus gL proteins. *J Virol* **71**:1667-70.
81. **Li, Q., M. K. Spriggs, S. Kovats, S. M. Turk, M. R. Comeau, B. Nepom, and L. M. Hutt-Fletcher.** 1997. Epstein-Barr virus uses HLA class II as a cofactor for infection of B lymphocytes. *J Virol* **71**:4657-62.
82. **Li, Q., S. M. Turk, and L. M. Hutt-Fletcher.** 1995. The Epstein-Barr virus (EBV) BZLF2 gene product associates with the gH and gL homologs of EBV and carries an epitope critical to infection of B cells but not of epithelial cells. *J Virol* **69**:3987-94.
83. **Lin, E., and P. G. Spear.** 2007. Random linker-insertion mutagenesis to identify functional domains of herpes simplex virus type 1 glycoprotein B. *Proc Natl Acad Sci U S A* **104**:13140-5.
84. **Little, S. J., S. Holte, J. P. Routy, E. S. Daar, M. Markowitz, A. C. Collier, R. A. Koup, J. W. Mellors, E. Connick, B. Conway, M. Kilby, L. Wang, J. M. Whitcomb, N. S. Hellmann, and D. D. Richman.** 2002. Antiretroviral-drug resistance among patients recently infected with HIV. *N Engl J Med* **347**:385-94.
85. **Longnecker, R.** 1998. Molecular Biology of Epstein-Barr Virus. *In* D. J. McCance (ed.), *Human tumor viruses*. American Society for Microbiology, Washington, D.C.
86. **Manoj, S., C. R. Jogger, D. Myscofski, M. Yoon, and P. G. Spear.** 2004. Mutations in herpes simplex virus glycoprotein D that prevent cell entry via nectins and alter cell tropism. *Proc Natl Acad Sci U S A* **101**:12414-21.
87. **Maurer, U. E., B. Sodeik, and K. Grunewald.** 2008. Native 3D intermediates of membrane fusion in herpes simplex virus 1 entry. *Proc Natl Acad Sci U S A* **105**:10559-64.

88. **McShane, M. P., and R. Longnecker.** 2004. Cell-surface expression of a mutated Epstein-Barr virus glycoprotein B allows fusion independent of other viral proteins. *Proc Natl Acad Sci U S A* **101**:17474-9.
89. **McShane, M. P., M. M. Mullen, K. M. Haan, T. S. Jardetzky, and R. Longnecker.** 2003. Mutational analysis of the HLA class II interaction with Epstein-Barr virus glycoprotein 42. *J Virol* **77**:7655-62.
90. **Mettenleiter, T. C., B. G. Klupp, and H. Granzow.** 2006. Herpesvirus assembly: a tale of two membranes. *Curr Opin Microbiol* **9**:423-9.
91. **Miller, N., and L. M. Hutt-Fletcher.** 1988. A monoclonal antibody to glycoprotein gp85 inhibits fusion but not attachment of Epstein-Barr virus. *J Virol* **62**:2366-72.
92. **Modis, Y., S. Ogata, D. Clements, and S. C. Harrison.** 2003. A ligand-binding pocket in the dengue virus envelope glycoprotein. *Proc Natl Acad Sci U S A* **100**:6986-91.
93. **Modis, Y., S. Ogata, D. Clements, and S. C. Harrison.** 2004. Structure of the dengue virus envelope protein after membrane fusion. *Nature* **427**:313-9.
94. **Molesworth, S. J., C. M. Lake, C. M. Borza, S. M. Turk, and L. M. Hutt-Fletcher.** 2000. Epstein-Barr virus gH is essential for penetration of B cells but also plays a role in attachment of virus to epithelial cells. *J Virol* **74**:6324-32.
95. **Mullen, M. M., K. M. Haan, R. Longnecker, and T. S. Jardetzky.** 2002. Structure of the Epstein-Barr virus gp42 protein bound to the MHC class II receptor HLA-DR1. *Mol Cell* **9**:375-85.
96. **Nemerow, G. R., C. Mold, V. K. Schwend, V. Tollefson, and N. R. Cooper.** 1987. Identification of gp350 as the viral glycoprotein mediating attachment of Epstein-Barr virus (EBV) to the EBV/C3d receptor of B cells: sequence homology of gp350 and C3 complement fragment C3d. *J Virol* **61**:1416-20.
97. **Neuhierl, B., R. Feederle, W. Hammerschmidt, and H. J. Delecluse.** 2002. Glycoprotein gp110 of Epstein-Barr virus determines viral tropism and efficiency of infection. *Proc Natl Acad Sci U S A* **99**:15036-15041.
98. **Oda, T., S. Imai, S. Chiba, and K. Takada.** 2000. Epstein-Barr virus lacking glycoprotein gp85 cannot infect B cells and epithelial cells. *Virology* **276**:52-8.
99. **Okuma, K. M., S. Nakamura, S. Nakano, Y. Niho, and Y. Matsuura.** 1999. Host range of human T-cell leukemia virus type I analyzed by a cell fusion-dependent reporter gene activation assay. *Virology* **254**:235-244.
100. **Omerovic, J., L. Lev, and R. Longnecker.** 2005. The Amino Terminus of Epstein-Barr Virus Glycoprotein gH Is Important for Fusion with Epithelial and B Cells. *J Virol* **79**:12408-15.

101. **Omerovic, J., and R. Longnecker.** 2007. Functional homology of gHs and gLs from EBV-related gamma-herpesviruses for EBV-induced membrane fusion. *Virology* **365**:157-65.
102. **Parry, C., S. Bell, T. Minson, and H. Browne.** 2005. Herpes simplex virus type 1 glycoprotein H binds to alphavbeta3 integrins. *J Gen Virol* **86**:7-10.
103. **Perez-Romero, P., A. Perez, A. Capul, R. Montgomery, and A. O. Fuller.** 2005. Herpes simplex virus entry mediator associates in infected cells in a complex with viral proteins gD and at least gH. *J Virol* **79**:4540-4.
104. **Pertel, P. E.** 2002. Human herpesvirus 8 glycoprotein B (gB), gH, and gL can mediate cell fusion. *J Virol* **76**:4390-400.
105. **Pertel, P. E., P. G. Spear, and R. Longnecker.** 1998. Human herpesvirus-8 glycoprotein B interacts with Epstein-Barr virus (EBV) glycoprotein 110 but fails to complement the infectivity of EBV mutants. *Virology* **251**:402-13.
106. **Reeves, J. D., F. H. Lee, J. L. Miamidian, C. B. Jabara, M. M. Juntilla, and R. W. Doms.** 2005. Enfuvirtide resistance mutations: impact on human immunodeficiency virus envelope function, entry inhibitor sensitivity, and virus neutralization. *J Virol* **79**:4991-9.
107. **Reske, A., G. Pollara, C. Krummenacher, B. M. Chain, and D. R. Katz.** 2007. Understanding HSV-1 entry glycoproteins. *Rev Med Virol* **17**:205-15.
108. **Ressing, M. E., D. van Leeuwen, F. A. Verreck, R. Gomez, B. Heemskerk, M. Toebes, M. M. Mullen, T. S. Jardetzky, R. Longnecker, M. W. Schilham, T. H. Ottenhoff, J. Neefjes, T. N. Schumacher, L. M. Hutt-Fletcher, and E. J. Wiertz.** 2003. Interference with T cell receptor-HLA-DR interactions by Epstein-Barr virus gp42 results in reduced T helper cell recognition. *Proc Natl Acad Sci U S A* **100**:11583-8.
109. **Ressing, M. E., D. van Leeuwen, F. A. Verreck, S. Keating, R. Gomez, K. L. Franken, T. H. Ottenhoff, M. Spriggs, T. N. Schumacher, L. M. Hutt-Fletcher, M. Rowe, and E. J. Wiertz.** 2005. Epstein-Barr virus gp42 is posttranslationally modified to produce soluble gp42 that mediates HLA class II immune evasion. *J Virol* **79**:841-52.
110. **Rey, F. A.** 2006. Molecular gymnastics at the herpesvirus surface. *EMBO Rep* **7**:1000-5.
111. **Rey, F. A., F. X. Heinz, C. Mandl, C. Kunz, and S. C. Harrison.** 1995. The envelope glycoprotein from tick-borne encephalitis virus at 2 Å resolution. *Nature* **375**:291-8.
112. **Rickinson, A. B., and E. Kieff.** 1996. Epstein-Barr Virus. *In* B. N. Fields, D. M. Knipe, and P. M. Howley (ed.), *Virology*, 3rd ed. Raven Press, New York.
113. **Roche, S., S. Bressanelli, F. A. Rey, and Y. Gaudin.** 2006. Crystal structure of the low-pH form of the vesicular stomatitis virus glycoprotein G. *Science* **313**:187-91.

114. **Roche, S., F. A. Rey, Y. Gaudin, and S. Bressanelli.** 2007. Structure of the prefusion form of the vesicular stomatitis virus glycoprotein G. *Science* **315**:843-8.
115. **Roizman, B., R. J. Whitley, and C. Lopez.** 1993. *The Human herpesviruses*. Raven Press, New York.
116. **Ruel, N., A. Zago, and P. G. Spear.** 2006. Alanine substitution of conserved residues in the cytoplasmic tail of herpes simplex virus gB can enhance or abolish cell fusion activity and viral entry. *Virology* **346**:229-37.
117. **Santoro, F., H. L. Greenstone, A. Insinga, M. K. Liszewski, J. P. Atkinson, P. Lusso, and E. A. Berger.** 2003. Interaction of glycoprotein H of human herpesvirus 6 with the cellular receptor CD46. *J Biol Chem* **278**:25964-9.
118. **Santoro, F., P. E. Kennedy, G. Locatelli, M. S. Malnati, E. A. Berger, and P. Lusso.** 1999. CD46 is a cellular receptor for human herpesvirus 6. *Cell* **99**:817-27.
119. **Satoh, T., J. Arai, T. Suenaga, J. Wang, A. Kogure, J. Uehori, N. Arase, I. Shiratori, S. Tanaka, Y. Kawaguchi, P. G. Spear, L. L. Lanier, and H. Arase.** 2008. PILRalpha is a herpes simplex virus-1 entry coreceptor that associates with glycoprotein B. *Cell* **132**:935-44.
120. **Shannon-Lowe, C. D., B. Neuhierl, G. Baldwin, A. B. Rickinson, and H. J. Delecluse.** 2006. Resting B cells as a transfer vehicle for Epstein-Barr virus infection of epithelial cells. *Proc Natl Acad Sci U S A* **103**:7065-70.
121. **Silva, A. L., J. Omerovic, T. S. Jardetzky, and R. Longnecker.** 2004. Mutational Analyses of Epstein-Barr Virus Glycoprotein 42 Reveal Functional Domains Not Involved in Receptor Binding But Required for Membrane Fusion. *Journal of Virology* **78**:5946-5956.
122. **Sodora, D. L., G. H. Cohen, M. I. Muggeridge, and R. J. Eisenberg.** 1991. Absence of asparagine-linked oligosaccharides from glycoprotein D of herpes simplex virus type 1 results in a structurally altered but biologically active protein. *J Virol* **65**:4424-31.
123. **Spear, P. G., and R. Longnecker.** 2003. Herpesvirus Entry: an Update. *Journal of Virology* **77**:10179-10185.
124. **Spear, P. G., S. Manoj, M. Yoon, C. R. Jogger, A. Zago, and D. Myscofski.** 2006. Different receptors binding to distinct interfaces on herpes simplex virus gD can trigger events leading to cell fusion and viral entry. *Virology* **344**:17-24.
125. **Speck, P., K. M. Haan, and R. Longnecker.** 2000. Epstein-Barr virus entry into cells. *Virology* **277**:1-5.
126. **Spriggs, M. K., R. J. Armitage, M. R. Comeau, L. Strockbine, T. Farrah, B. Macduff, D. Ulrich, M. R. Alderson, J. Mullberg, and J. I. Cohen.** 1996. *The*

- extracellular domain of the Epstein-Barr virus BZLF2 protein binds the HLA-DR beta chain and inhibits antigen presentation. *J Virol* **70**:5557-63.
127. **Steven, A. C., and P. G. Spear.** 2006. Biochemistry. Viral glycoproteins and an evolutionary conundrum. *Science* **313**:177-8.
 128. **Strnad, B. C., T. Schuster, R. Klein, R. F. Hopkins, 3rd, T. Witmer, R. H. Neubauer, and H. Rabin.** 1982. Production and characterization of monoclonal antibodies against the Epstein-Barr virus membrane antigen. *J Virol* **41**:258-64.
 129. **Subramanian, R. P., and R. J. Geraghty.** 2007. Herpes simplex virus type 1 mediates fusion through a hemifusion intermediate by sequential activity of glycoproteins D, H, L, and B. *Proc Natl Acad Sci U S A* **104**:2903-8.
 130. **Takada, K.** 2001. Role of Epstein-Barr virus in Burkitt's lymphoma. *Curr Top Microbiol Immunol* **258**:141-51.
 131. **Takada, K., K. Horinouchi, Y. Ono, T. Aya, T. Osato, M. Takahashi, and S. Hayasaka.** 1991. An Epstein-Barr virus-producer line Akata: establishment of the cell line and analysis of viral DNA. *Virus Genes* **5**:147-56.
 132. **Tanner, J., J. Weis, D. Fearon, Y. Whang, and E. Kieff.** 1987. Epstein-Barr virus gp350/220 binding to the B lymphocyte C3d receptor mediates adsorption, capping, and endocytosis. *Cell* **50**:203-13.
 133. **Turk, S. M., R. Jiang, L. S. Chesnokova, and L. M. Hutt-Fletcher.** 2006. Antibodies to gp350/220 enhance the ability of Epstein-Barr virus to infect epithelial cells. *J Virol* **80**:9628-33.
 134. **Urquiza, M., J. Suarez, R. Lopez, E. Vega, H. Patino, J. Garcia, M. A. Patarroyo, F. Guzman, and M. E. Patarroyo.** 2004. Identifying gp85-regions involved in Epstein-Barr virus binding to B-lymphocytes. *Biochem Biophys Res Commun* **319**:221-9.
 135. **Volpi, A.** 2004. Epstein-Barr virus and human herpesvirus type 8 infections of the central nervous system. *Herpes* **11 Suppl 2**:120A-127A.
 136. **Wang, X., D. Y. Huang, S. M. Huong, and E. S. Huang.** 2005. Integrin alphavbeta3 is a coreceptor for human cytomegalovirus. *Nat Med* **11**:515-21.
 137. **Wang, X., and L. M. Hutt-Fletcher.** 1998. Epstein-Barr virus lacking glycoprotein gp42 can bind to B cells but is not able to infect. *J Virol* **72**:158-63.
 138. **Wang, X., W. J. Kenyon, Q. Li, J. Mullberg, and L. M. Hutt-Fletcher.** 1998. Epstein-Barr virus uses different complexes of glycoproteins gH and gL to infect B lymphocytes and epithelial cells. *J Virol* **72**:5552-8.
 139. **Wei, W. I., and J. S. Sham.** 2005. Nasopharyngeal carcinoma. *Lancet* **365**:2041-54.

140. **Whetter, L. E., S. P. Day, E. A. Brown, O. Elroy-Stein, and S. M. Lemon.** 1994. Analysis of hepatitis A virus translation in a T7 polymerase-expressing cell line. *Arch Virol Suppl* **9**:291-298.
141. **White, J., and A. Helenius.** 1980. pH-dependent fusion between the Semliki Forest virus membrane and liposomes. *Proc Natl Acad Sci U S A* **77**:3273-7.
142. **Wild, C., J. W. Dubay, T. Greenwell, T. Baird, Jr., T. G. Oas, C. McDanal, E. Hunter, and T. Matthews.** 1994. Propensity for a leucine zipper-like domain of human immunodeficiency virus type 1 gp41 to form oligomers correlates with a role in virus-induced fusion rather than assembly of the glycoprotein complex. *Proc Natl Acad Sci U S A* **91**:12676-80.
143. **Wild, C. T., D. C. Shugars, T. K. Greenwell, C. B. McDanal, and T. J. Matthews.** 1994. Peptides corresponding to a predictive alpha-helical domain of human immunodeficiency virus type 1 gp41 are potent inhibitors of virus infection. *Proc Natl Acad Sci U S A* **91**:9770-4.
144. **Wiley, D. C., I. A. Wilson, and J. J. Skehel.** 1981. Structural identification of the antibody-binding sites of Hong Kong influenza haemagglutinin and their involvement in antigenic variation. *Nature* **289**:373-8.
145. **Wilson, I. A., J. J. Skehel, and D. C. Wiley.** 1981. Structure of the haemagglutinin membrane glycoprotein of influenza virus at 3 Å resolution. *Nature* **289**:366-73.
146. **Wu, L., C. M. Borza, and L. M. Hutt-Fletcher.** 2005. Mutations of Epstein-Barr virus gH that are differentially able to support fusion with B cells or epithelial cells. *J Virol* **79**:10923-30.
147. **Wu, L., and L. M. Hutt-Fletcher.** 2007. Point mutations in EBV gH that abrogate or differentially affect B cell and epithelial cell fusion. *Virology* **363**:148-55.
148. **Yang, L., and H. W. Huang.** 2002. Observation of a membrane fusion intermediate structure. *Science* **297**:1877-9.
149. **Yaswen, L. R., E. B. Stephens, L. C. Davenport, and L. M. Hutt-Fletcher.** 1993. Epstein-Barr virus glycoprotein gp85 associates with the BKRF2 gene product and is incompletely processed as a recombinant protein. *Virology* **195**:387-96.
150. **Zago, A., C. R. Jogger, and P. G. Spear.** 2004. Use of herpes simplex virus and pseudorabies virus chimeric glycoprotein D molecules to identify regions critical for membrane fusion. *Proc Natl Acad Sci U S A* **101**:17498-503.
151. **Zeng, J., J. Du, Y. Zhao, N. Palanisamy, and S. Wang.** 2007. Baculoviral vector-mediated transient and stable transgene expression in human embryonic stem cells. *Stem Cells* **25**:1055-61.

152. **Zhou, G., and B. Roizman.** 2007. Separation of receptor-binding and profusogenic domains of glycoprotein D of herpes simplex virus 1 into distinct interacting proteins. *Proc Natl Acad Sci U S A* **104**:4142-6.